

# **Effect of Marble Powder Waste as a Partial Replacement of Cement on Fresh and Mechanical Properties of Self Compacted Mortar**

**Marwan Mahmoud M. Bileid**

Submitted to the  
Institute of Graduate Studies and Research  
in partial fulfillment of the requirements for the degree of

Master of Science  
in  
Civil Engineering

Eastern Mediterranean University  
July 2023  
Gazimağusa, North Cyprus

Approval of the Institute of Graduate Studies and Research

---

Prof. Dr. Ali Hakan Ulusoy  
Director

I certify that this thesis satisfies all the requirements as a thesis for the degree of Master of Science in Civil Engineering.

---

Assoc. Prof. Dr. Eriş Uygur  
Chair, Department of Civil Engineering

We certify that we have read this thesis and that in our opinion it is fully adequate in scope and quality as a thesis for the degree of Master of Science in Civil Engineering.

---

Prof. Dr. Khaled Hamed Marar  
Supervisor

---

Examining Committee

1. Prof. Dr. Özgür Eren

2. Prof. Dr. Khaled Hamed Marar

3. Asst. Prof. Dr. Kezban Özlütaş

## ABSTRACT

Self-compacting concrete and mortar have revolutionized the construction sector but are more expensive to produce due to higher cement consumption and additives. To reduce the cost, cement can be replaced by CRMs. In this study, the main focus was to produce a high quality together with environmentally friendly self-compacting mortar. For this purpose, MD as CRM was employed at 0, 5, 10, 15, 20, and 30% fractions for both NSC and HSC series with w/c ratios of 0.50 and 0.38, respectively.

Fresh properties of SCM were evaluated by slump flow, flow rate, consistency retention, air content (%), and setting time. While the hardened properties of SCM were assessed by unit weight, compressive, splitting tensile, flexural strengths, water absorption, drying shrinkage, and heat degradation at (100 °C, 200 °C) which evaluated by the change in compressive strength, rebound number by Schmidt hammer, and UPV by pundit.

Observed data indicates that the spreading flow and the air content (%) were decreased with increasing the replacement level, while the flow rate  $T_{20}$ , and setting time were increased. The lowest spread flow, and air content (%) were found at a 30% replacement level. Similarly, the lowest prolonging in flow rate  $T_{20}$ , and setting time were found at a 5% replacement level compared to the control mix. Moreover, there was a decline in unit weight, strength values, and drying shrinkage. While there was an increase in water absorption when increasing the replacement level. The lowest decrease in unit weight, compressive, splitting, and flexural strengths compared to the control mix was at 5% MD for both NSCM and HSCM series. Likewise, the lowest

reduction in the drying shrinkage was found at a 15% replacement level for both NSCM and HSCM series. Furthermore, a satisfactory mortar quality with MD before and after heat exposure was demonstrated by Pundit test results. After exposure to the heat of 100 and 200 degree centigrade, a decrease in compressive strength, Schmidt hammer, and UPV were noted.

**Keywords:** Marble Dust (MD), Cement Replacement Materials (CRM), Normal Strength Self-Compacted Mortar (NSCM), High Strength Self-Compacted Mortar (HSCM), Workability, Mechanical Properties, Durability.

## ÖZ

Kendiliğinden yerleşen beton ve harç, inşaat sektöründe devrim yaratmış, ancak daha yüksek çimento tüketimi ve katkı maddeleri nedeniyle üretimi daha pahalı olmuştur. Öte yandan maliyeti düşürebilmenin yollarından birisi de çimentonun kullanımını azaltmak ve yerine ek malzeme kullanımı olabilmektedir. Bu çalışmanın ana odak noktası ise çevre dostu kendinden yerleşen harç ile birlikte yüksek kalitede bir ürün üretmektir. Bu sebeple kullanılan çimento %0, 5, 10, 15, 20 ve 30 oranlarında mermer tozu ile yer değiştirilerek normal ve de yüksek mukavemetli kendiliğinden yerleşen ve su/çimento oranı 0.5 ile 0.38 olan harçlar üretilmiştir.

Kendiliğinden yerleşen harçların sertleşmeden önceki özellikleri, yayılma akışı, akış hızı, tutarlılık koruması, hava içeriği (%), ve sertleşme süresi değerlendirilmiştir. Kendiliğinden yerleşen harçların sertleşmiş özellikleri ise birim ağırlık, basınç dayanımı, çekme dayanımı, eğilme dayanımı, su emme, kuruma çekmesi ve çeşitli sıcaklıklarda (100°C, 200°C) ısıl bozulma özellikleri değerlendirilmiştir. Bu değerlendirmeler, basınç dayanımındaki değişim, Schmidt çekiç ile geri tepme sayısı ve pundit ile ultrason geçiş hızı kullanılarak yapılmıştır.

Gözlemlenen veriler, değiştirme seviyesinin artmasıyla yayılma akışının ve hava içeriğinin (%) azaldığını, ancak akış hızı  $T_{20}$ 'nin ve sertleşme süresinin arttığını göstermektedir. En düşük yayılma akışı ve hava içeriği (%) değerleri, %30 değiştirme seviyesinde bulunmuştur. Benzer şekilde, kontrol karışımına kıyasla %5 değiştirme seviyesinde, akış hızı  $T_{20}$ 'nin ve sertleşme süresinin en az arttığı görülmüştür. Ayrıca birim ağırlık, dayanım değerleri ve kuruma çekmesinde bir azalma, değiştirme seviyesi

arttıkça su emme oranında ise bir artış meydana gelmiştir. Hem normal hem de yüksek mukavemetli kendiliğinden yerleşen harç serileri için kontrol karışımına kıyasla, birim ağırlık, basınç dayanımı, çekme dayanımı ve eğilme dayanımında en düşük azalma oranı %5 mermer tozu oranında kaydedilmiştir. Benzer şekilde, kuruma çekmesindeki en düşük azalma oranı normal hem de yüksek mukavemetli kendiliğinden yerleşen harç serileri için %15 değiştirme seviyesinde bulunmuştur. Ayrıca, Pundit test sonuçları, ısıya maruz kalma öncesi ve sonrasında mermer tozu ile tatmin edici bir harç kalitesini göstermiştir. Sıcaklıkları 100°C ve 200°C'ye maruz kalındığında ise, basınç dayanımında, Schmidt çekicinde ve ultrason darbe hızında bir azalma tespit edilmiştir.

**Anahtar Kelimeler:** Mermer Tozu, Çimento Yerine Kullanılan Malzemeler (CRM), Normal Dayanımlı Kendiliğinden Yerleşebilen Harç, Yüksek Dayanımlı Kendiliğinden Yerleşebilen Harç, İşlenebilirlik, Mekanik Özellikler, Dayanıklılık

# DEDICATION

To My Parents

## ACKNOWLEDGMENT

I would like to express special thanks to everybody who have been of support during my research study. I must say that the journey was full of challenges and without your support, guidance, and inspiration, I might not have successfully completed the project. I appreciate emotional, financial, and psychological supportive from my family and friends. I am grateful for the encouragement and prayers that you have been dedicating to me while carrying out this project. May Allah bless you abundantly!

I would never forget to express my gratitude to my supervisor Prof. Dr. Khaled Marar for his enthusiasm, insightful comments, guidance, and the patience he has been giving me while carrying out the project. The ideas, time, and practical advice he has consistently been offering me has been of great help in my study. Moreover, I would like to acknowledge his consistent following up on my project to ensure that I am implementing the required procedures and guidelines.

Finally, I want to say thank you for the College of engineering and especially the department of Civil engineering for the valuable support offered to me during the study. Thank you Mr. Ogün Kiliç for your support while carrying out the laboratory test for my project. To Eastern Mediterranean University, my gratitude can never be enough. Thank you for offering me an opportunity to exploit my talent from your institution and more so, offering access to my research material from the library. Thanks, Anas Bileid and Nasr Swei, for your invaluable help in the lab.

# TABLE OF CONTENTS

ABSTRACT.....	iii
ÖZ .....	v
DEDICATION .....	vii
ACKNOWLEDGMENT.....	viii
LIST OF TABLES .....	xiii
LIST OF FIGURES .....	xv
LIST OF SYMBOLS AND ABBREVIATIONS .....	xviii
1 INTRODUCTION .....	1
1.1 Study Overview and Issue Statement.....	1
1.2 Study Objectives.....	4
1.3 Scope of the Study.....	5
1.4 Outline of the Study .....	5
2 LITERATURE REVIEW.....	7
2.1 Outline .....	7
2.2 SCC Flowability .....	7
2.3 Self-Compacting Mortar.....	9
2.4 Evaluating SCC and SCM Workability.....	11
2.4.1 Slump Flow.....	12
2.4.2 V- Funnel Test .....	13
2.4.3 Workability and Viscosity Evaluation of SCM: A Review of Testing Methods in Previous Studies.....	14
2.5 Passing Ability Tests For SCC.....	16
2.6 Cement Replacement Materials.....	17

2.6.1 Micro Silica.....	17
2.6.2 Granulated Ground Blast Furnace Slag (GGBFS).....	18
2.6.3 Pulverized Fuel Ash (PFA).....	18
2.6.4 Rice Husk (RH) .....	19
2.7 Utilization of Cement Replacement Materials in Self-Compacting Mortar.....	19
2.8 Effects of Waste Marble Dust on Properties of SCC and SCM.....	22
2.8.1 Workability .....	22
2.8.2 Setting Time.....	23
2.8.3 Air Content and Unit Weight.....	24
2.8.4 Mechanical Properties.....	25
2.8.5 Water Absorption.....	27
2.8.6 Drying Shrinkage .....	28
2.8.7 Heat Resistance.....	29
2.9 Environmental and Economic Aspects.....	31
2.10 Summary .....	32
<b>3 RESEARCH METHODOLOGY .....</b>	<b>34</b>
3.1 Outline .....	34
3.2 Mixture Components .....	34
3.2.1 Cement.....	34
3.2.2 Marble Dust .....	35
3.2.3 Fine Aggregate.....	36
3.2.4 Mixing Water .....	37
3.2.5 Superplasticizers .....	37
3.3 Experimental Program.....	37
3.3.1 The Procedure of Mixing the Mortar .....	38

3.3.2 Trial Mixes.....	40
3.3.3 Quantities of Ingredients in the SCM’s Mix.....	41
3.3.4 Molding and Curing.....	41
3.4 Fresh Mortar Tests.....	43
3.4.1 Workability .....	43
3.4.2 Determination of Flow Rate .....	44
3.4.3 Air Content .....	45
3.4.4 Setting Time.....	46
3.5 Hardened Mortar Tests .....	47
3.5.1 Compressive Strength .....	47
3.5.2 Splitting Tensile Strength .....	48
3.5.3 Flexural Strength.....	49
3.5.4 Water Absorption.....	50
3.5.5 Drying Shrinkage .....	51
3.5.6 Heat Exposure Resistance at 100 and 200 Degrees Centigrade .....	52
3.5.7 Cracks Detection.....	53
3.5.8 Evaluation of the Specimen’s Hardness .....	54
3.5.9 Assessing Material Integrity with UPV .....	55
4 RESULTS AND DISCUSSION .....	57
4.1 Outline .....	57
4.2 Impact of MD on SCM's Workability .....	57
4.3 Impact of MD on SCM's Flow Rate .....	60
4.4 Impact of MD on SCM's Air Content .....	61
4.4.1 Air Content and Slump Flow Correlation.....	63
4.4.2 Air content and Flow Rate Correlation.....	64

4.5 Impact of MD on SCM's Setting Time.....	65
4.6 Impact of MD on SCM's Unit Weight.....	68
4.7 Impact of MD on SCM's Compressive Strength .....	69
4.8 Impact of MD on SCM's Splitting Tensile Strength of SCM.....	72
4.8.1 Splitting Tensile and Compressive Strengths Correlation.....	75
4.9 Effects of MD on Flexural Strength of SCM .....	76
4.9.1 Compressive Strength and Flexural Strengths Correlation.....	78
4.10 Impact of MD on SCM's Water Absorption.....	79
4.10.1 Compressive Strength and Water Absorption Correlation .....	82
4.11 Impact of MD on SCM's Heat Degradation (100 °C and 200 °C).....	83
4.11.1 Impact of MD on SCM's Compressive Strength After Heating .....	84
4.11.2 Impact of MD on SCM's on Schmidt Hammer After Heating .....	87
4.11.3 Effects of MD on UPV of SCM After Heating .....	89
4.11.4 Cracks Detection After Heating.....	92
4.12 Impact of MD on SCM's Drying Shrinkage.....	94
4.13 Economical Analysis for Using MD in Production of SCM.....	96
5 CONCLUSIONS AND GUIDANCE .....	99
5.1 Conclusion.....	99
5.2 Guidance.....	104
REFERENCES.....	105
APPENDIX.....	116

## LIST OF TABLES

Table 1: Cement physical and mechanical properties according to EN 196-6 and EN 196-1. ....	34
Table 2: Cement physical properties according to EN 196-3 .....	35
Table 3: Chemical properties of CEM II/B-S 42.5 N and marble dust.....	36
Table 4: Trial mixes of SCM .....	40
Table 5: SCM mix design. ....	41
Table 6: Flow rate consistency retention of SCM.....	61
Table 7: Air content loss for both NSCM and HSCM.....	63
Table 8: NSCM compressive strength loss .....	71
Table 9: HSCM compressive strength loss .....	72
Table 10: Splitting tensile strength results for NSCM series.....	74
Table 11: Splitting tensile strength results for HSCM series.....	74
Table 12: Flexural strength results for NSCM series.....	77
Table 13: Flexural strength results for HSCM series.....	78
Table 14: Effects of MD on water absorption and volume of permeable voids of NSCM .....	81
Table 15: Effects of MD on water absorption and volume of permeable voids of HSCM .....	82
Table 16: Compressive strength results of NSCM after heating.....	85
Table 17: Compressive strength results of HSCM after heating.....	87
Table 18: Compressive Strength and Schmidt hammer before and after heating relationship.....	89
Table 19: UPV results before and after heating at 20, 100, and 200 °C for NSCM..	90

Table 20: UPV results before and after heating at 20, 100, and 200 °C for HSCM..	91
Table 21: UPV and Compressive strength at different heating levels relationship ...	92
Table 22: Material unit price.....	97
Table 23: NSCM cost analysis.....	98
Table 24: HSCM cost analysis.....	98

## LIST OF FIGURES

Figure 1: Characteristics of material flow (Tattersall et al., 1983).....	9
Figure 2: Slump flow .....	12
Figure 3: Mini slump.....	13
Figure 4: V-funnel (Specification and Guidelines for Self-Compacting Concrete., 2002) .....	14
Figure 5: Mini v-funnel (Specification and Guidelines for Self-Compacting Concrete., 2002) .....	14
Figure 6: L-box, U-box, and J-ring apparatus.....	17
Figure 7: MD particle size distribution .....	35
Figure 8: Fine aggregate sieve analysis .....	37
Figure 9: SCM mixing procedure .....	38
Figure 10: Standard mini mixer .....	39
Figure 11: Concrete mixer with capacity of 0.25 cubic meter.....	39
Figure 12: Specimens in curing room .....	42
Figure 13: SCM specimens in water curing tank.....	43
Figure 14: Mini-slump flow (Specification and Guidelines for Self-Compacting Concrete., 2002).....	44
Figure 15: Testing of T <sub>20</sub> flow time .....	45
Figure 16: Air meter.....	46
Figure 17: Concrete and mortar penetrometer .....	46
Figure 18: Cuboid used in testing setting time .....	47
Figure 19: Hydraulic compression machine .....	48
Figure 20: Splitting tensile strength test.....	49

Figure 21: Flexural strength test .....	50
Figure 22: Boiled specimens for water absorption. ....	51
Figure 23: Measuring drying shrinkage .....	52
Figure 24: Testing specimens for elevated temperature .....	53
Figure 25: Stereo microscope .....	54
Figure 26: Schmidt hammer.....	55
Figure 27: Pundit Device .....	56
Figure 28: Effects of MD on NSCM relative slump .....	58
Figure 29: Effects of MD on HSCM relative slump .....	59
Figure 30: Effects of MD on NCM and HSCM slump flow.....	59
Figure 31: NSCM air content.....	62
Figure 32: HSCM air content.....	63
Figure 33: NSCM air content and slump flow relationship.....	64
Figure 34: HSCM air content and slump flow relationship.....	64
Figure 35: NSCM air content and flow rate relationship.....	65
Figure 36: HSCM air content and flow rate relationship.....	65
Figure 37: Setting time of NSCM .....	67
Figure 38: Setting time of HSCM .....	67
Figure 39: Effects of MD on unit weight of NSCM .....	68
Figure 40: Effects of MD on unit weight of HSCM .....	69
Figure 41: Compressive strength results for NSCM .....	71
Figure 42: Compressive strength results for HSCM .....	72
Figure 43: Effects of MD on splitting tensile strength of NSCM.....	73
Figure 44: Effects of MD on splitting tensile strength of HSCM.....	74
Figure 45: Splitting tensile and compressive strengths relationship for NSCM.....	75

Figure 46: Splitting tensile and compressive strengths relationship for HSCM.....	76
Figure 47: Effects of MD on flexural strength of NSCM.....	77
Figure 48: Effects of MD on flexural strength of HSCM.....	78
Figure 49: Compressive strength and flexural strength relationship for NSCM.....	79
Figure 50: Compressive strength and flexural strength relationship for HSCM.....	79
Figure 51: Effects of MD on water absorption of NSCM.....	81
Figure 52: Effects of MD on water absorption of HSCM.....	82
Figure 53: Compressive strength and water absorption relationship for NSCM.....	83
Figure 54: Compressive strength and water absorption relationship for HSCM.....	83
Figure 55: Effects of MD on compressive strength of NSCM after heating.....	85
Figure 56: Effects of MD on compressive strength of HSCM after heating.....	86
Figure 57: Effects of MD on rebound number of NSCM after heating.....	88
Figure 58: Effects of MD on rebound number of HSCM after heating.....	88
Figure 59: Results from the UPV described for the NSCM before and after heating at 20, 100, and 200 °C.....	90
Figure 60: Results from the UPV described for the HSCM before and after heating at 20, 100, and 200 °C.....	91
Figure 61: Stereo microscope image after heating to 200 °C: (a) HSCM20MD, (b) HSCM30MD, (c)HSCM30MD, (d)NSCM20MD, (e)NSCM30MD,.....	93
Figure 62: NSCM's drying shrinkage.....	96
Figure 63: HSCM's drying shrinkage.....	96

## LIST OF SYMBOLS AND ABBREVIATIONS

$\tau_0$	Yield Stress
$\mu$	Coefficient of Viscosity
$\dot{\gamma}$	Rate of Shear
CRM	Cement Replacement Materials
EFNARC	European Federation of National Associations Representing for Concrete
GGBFS	Granulated Ground Blast Furnace Slag
HSCM	High Strength Self Compacted Mortar
MD	Marble Dust
NSCM	Normal Strength Self-Compacted Mortar
SCC	Self-Compacted Concrete
SCM	Self-Compacted Mortar
SP	Superplasticizers
$T_{20}$	Time of Mortar Spread Flow to Reach 200mm
UPV	Ultrasonic Pulse Velocity
w/c	Water/Cement Ratio
WMD	Waste Marble Dust
$\Gamma_m$	Relative Slump
$\mu s$	Microsecond

# Chapter 1

## INTRODUCTION

### 1.1 Study Overview and Issue Statement

In the last 40 years, SCC has become a significantly new concrete technology. By improving concrete's workability and hence the building quality, the method was first developed by Japanese researchers in 1986 to boost concrete durability (Okamura & Ouchi., 2003), one of the concrete types is SCC that combines excellent stability with a high degree of flowability. These properties enable the concrete to completely level the applied formwork without the need for an external vibrator. SCC also needs to be able to travel through densely packed areas of reinforced concrete structures, which is a constant need (Okamura & Ouchi., 2003).

Although SCC is a new concrete technique, as was already noted, there are no standards defining its specifications. EFNARC, which is focused on specialized building chemicals and concrete systems, is responsible for publishing the only available guidelines (Specification and Guidelines for Self-Compacting Concrete., 2002). The workability evaluation of SCC is unstandardized, compared to conventional concrete, according to EFNARC, SCC in terms of workability should has ability to fill and compact, the ability to pass through reinforcement bars, and resistance to segregation.

The fresh SCM are mostly linked to the workability of fresh SCC. In actuality, the SCC design was created after a lengthy process of trial and error. However, SCM design takes considerably less time and money and makes it easier to reach a desired SCC. Therefore, it is crucial to research and balance SCM to reduce SCC phase trials. Due to its advantageous environmental effects and useful properties, using MD as a CRM in the production of SCM is warranted. It improves waste management by recycling a waste product, lessens the need for cement, and aids sustainability by recycling a waste product. It may also result in cost savings, promote research and innovation, and aid in the creation of more environmentally friendly building materials. To guarantee the best performance of the self-compacted mortar with inclusion of MD, proper testing and mix design are necessary.

Using a suitable mortar and restricting the dosage of coarse aggregate is a frequent approach to meet the self-compactibility. As a result, SCC may be tested using SCMs. (Domone and Jin., 1999). Evaluating the SCM's attributes is essential to SCC design (Specification and Guidelines for Self-Compacting Concrete., 2002). In addition, SCM's can be used as to fix structural components. Moreover, the utilization of both SCC and SCM is more costly than that of cement concretes or mortars due to higher cement content and the utilization of more costly chemical enhancers for maintaining the desired flowability of the mixture. Using CRMs is a practical technique to lower the cost of SCM while boosting durability.

Cement-based concrete and mortar are the most utilized building products worldwide. Because of its exceptional strength, cement is a frequently used building material. Yet, 5 to 8% (Lakreb et al., 2022) of all CO<sub>2</sub> emissions are attributable to its manufacturing. Cement manufacture is thus one of the significant causes of environmental issues.

A variety of post-consumer wastes and industrial byproducts were produced in recent years because of the growing worldwide output. These wastes must be recycled or reused to guarantee effective waste management. Using waste products in the formulation of cementitious materials is an intriguing strategy for producing more environmentally friendly and cost-effective cementitious materials while also ensuring lower CO<sub>2</sub> emissions.

To lower the cost and enhance the quality of cement, civil engineers are constantly looking for waste products that can be used as a mixing element. Each year there is a substantial amount of non-recyclable refuse produced, recycling waste also consumes energy and is detrimental to the environment. In addition, the ecosystem is greatly endangered by the accumulation and removal of rubbish in suburbs (Sakalkale et al., 2014).

One of the most significant components that is utilized to replace cement in concrete or mortar mixtures is waste marble dust. Since antiquity, marble has been primarily used for artistic functions and has been employed in construction. At processing plants, marble blocks are sawed and polished to create marble powder, which makes up around 25% of the total marble processed. As the largest marble exporter, India releases processing facilities for millions of tons of marble waste each year (Sakalkale et al., 2014). Marble residues from the soil, when discarded in the catchment area, impede groundwater permeability, and contribute to contamination. As a result, the environment would be protected from marble dumps if this waste marble were used in the construction sector (Dachowski and Kostrzewa., 2016).

## 1.2 Study Objectives

The following study assesses the utilization of MD as CRM to produce SCM. For this purpose, substitution of cement with MD was carried out at 0, 5, 10, 15, 20 and 30% of the cement weight to produce two different series of SCM mixes (normal and high strength). As a result, an environmentally friendly together with high quality self-compacted mortar will be created by using waste marble dust. Additionally, it is hypothesized that including this waste product into the manufacturing process of mortar would result in improvements to a variety of qualities of the mortar.

To evaluate the impact of MD on SCMs, experiments will be done as follows:

- Workability
- Flow rate and consistency retaining
- Air content
- Setting time
- Unit weight
- Compressive strength
- Splitting Tensile strength
- Flexural strength
- Water Absorption
- Drying shrinkage
- Heat resistance (Degradation) at 100 °C and 200 °C
- Non-destructive test (Schmidt hammer and pundit).

The aforementioned experiments are to be carried out in accordance with established professional protocols as outlined by the ASTM. The experiment results will be

evaluated, and a regression analysis will be conducted to demonstrate a relationship between high and normal strength self-compacted mortar containing MD.

### **1.3 Scope of the Study**

This study focuses on:

- Achieving the required workability suggested the EFNARC for production of SCM without bleeding and segregation.
- Evaluating fresh properties of SCM in the presence of MD as CRM.
- Evaluating the Mechanical and durability properties at different levels of replacement of cement by MD.
- Assessing the impact of MD as CRM when exposing to high temperature of 100 and 200 degree Celsius.
- Reducing the cost of SCM production. In addition to reducing the environmental impact caused by industrial waste material and cement production.
- Updating the existing literature, as well as fill the literature gaps since information about air content, water absorption, and heat resistance of SCM produced by MD as CRM wasn't found.

### **1.4 Outline of the Study**

The present thesis is organized in the following manner: The first chapter of this study centers on providing background of the research topic, presenting the problem statement, and outlining the study's objectives. Chapter 2 provides a thorough examination of the literature pertaining to the wide background on SCC and SCM, including their rheology control in accordance with various guidelines, the use of CRMs, and the influence of MD on the properties of SCC and SCM. Chapter 3 will provide an explanation of the experimental procedures and materials characteristics.

Chapter 4 presents an in-depth analysis of the outcomes and discussion of the results.

Chapter 5 provides a comprehensive analysis of the critical conclusions and recommendations.

## Chapter 2

### LITERATURE REVIEW

#### 2.1 Outline

Cement manufacture uses a lot of energy and emits a lot of CO<sub>2</sub>, moreover, the construction of robust concrete structures may potentially lead to significant expansion in the building sector. In order to mitigate energy consumption and minimize carbon dioxide emissions, this can be done by improving building quality and substituting waste materials for cement powder. (Nasr et al., 2019). SCC was created by Okamura in 1986 (Okamura and Ouchi., 2003) and can be compacted by its own weight without vibrating. SCC and SCM have minimal porosity, low permeability, an excellent microstructure, and appropriate mechanical qualities (Khaleel and Abdul Razak., 2012). To get economical and sustainable SCMs, the incorporation of supplementary materials in lieu of a portion of the cement content is deemed advantageous.

waste marble dust is a finely textured powder that results from the cutting and shaping of marble. Its main constituent is calcium carbonate, which is also found in materials such as limestone and chalk. The presence of other elements in the dust, such as silicon dioxide, aloxite, mineral oxides, differs depending on the composition of the marble that is being processed (Belaidi et al., 2012).

#### 2.2 SCC Flowability

The phenomenon commonly known as "flow" pertains to the instantaneous deformation of liquids and gases when subjected to minor shearing loads. Rheology,

as defined by (Ozawa et al.,1989), pertains to the scientific investigation of flow phenomena, encompassing the interplay between stress, strain, and their temporal derivatives. Broadly speaking, rheology pertains to substances whose flow properties are more intricate than those of an ideal elastic solid or a basic fluid (such as a gas or liquid) (Eley., 2019).

Flow characteristics are often determined with the use of shear stress-rate of shear plots (Figure 1). The coefficient of viscosity ( $\mu$ ) is calculated by dividing the shear stress by the shear rate for a Newtonian liquid. However, the rheology of newly poured mixture of concrete is commonly defined using the Bingham model. According to the Bingham model, the lowest stress required to commence flow is represented by a point where the flow curve and the stress axis intersect (Tattersall et al., 1983).

Bingham model reveals that the flow of freshly produced concrete is contingent upon surpassing an achievable stress level known as the yield stress ( $\tau_0$ ). As soon as the concrete begins to flow, shear stress rises linearly as the strain rate rises, this is identified as plastic viscosity. Consequently, as (Ozawa et al., 1989) mentioned both plastic viscosity and the yield stress are required in order for this model to accurately characterize the rheological characteristics of fresh concrete.

The rheology of newly produced concrete is assessed by device known as rheometer, that assesses the shear stress at different shear rates are utilized. However, the unique characteristics of fresh concrete mixture prevent the use of rheometers intended for clean fluids devoid of solid particles. The 5 rheological qualities of SCC that are offered on the market are therefore not agreed upon (NIST., 1999). Five rheometers were used in extensive research by NIST to test a variety of twelve concrete

compositions. In addition to having slumps varying from 90 to 235 mm, the mixtures also had a wide variety of yield stresses and plastic viscosities. Even for devices that directly provide yield stress and plastic viscosity in fundamental units, it was discovered that rheometers provided various values for the Bingham constants (NIST., 1999).

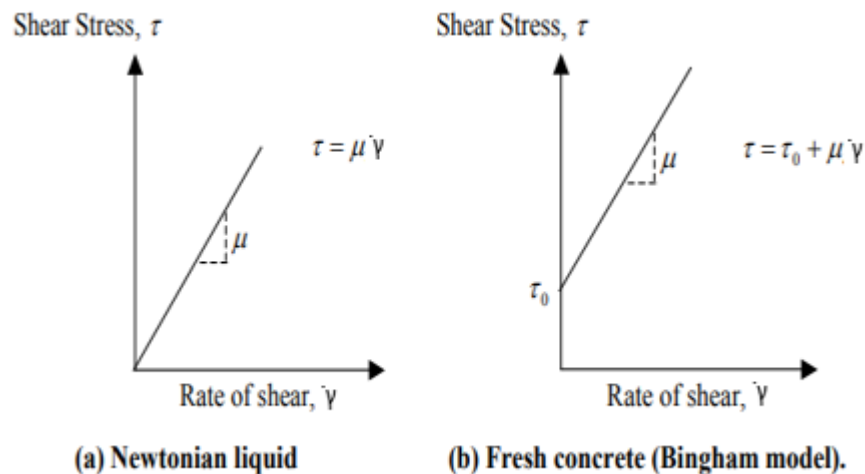


Figure 1: Characteristics of material flow (Tattersall et al., 1983).

### 2.3 Self-Compacting Mortar

Building structural retrofitting, rehabilitation, and restoration generally use SCM which is a component of (SCC). SCC can be delineated as mixture that compress into the specimens without segregation, even in the existence of complex steel bars, with consistency retention. (Specification and Guidelines for Self-Compacting Concrete., 2002). A newly developed advanced technology known as SCC that has advantages over traditional concrete considering practical and environmental factors. The mix proportion of SCC and SCM is largely reliant on the characteristics of the applied material, and substantial research has been conducted in many nations taking varied circumstances into consideration.

In order to get self-compactibility in SCMs, most mortar recipes call for a maximum of 40% sand by volume, superplasticizers (SP) to maintain the consistency of the SCM as previously employed (Okamura and Ozawa., 1995). However, according to previous studies, self compactibility of mortars were achieved when passed the sand limitation suggested by (Okamura and Ozawa., 1995).

According to study done by (Benabed et al., 2012) on SCMs with different types of sand, the self compactibility of were achieved by sand limit of 50%. Moreover, seashells used as sand substitution in study done by (Safi et al., 2015) on SCM, similarly the self compactibility were successfully achieved with sand to paste ratio of 0.58. Furthermore, (Şahmaran et al., 2006), and (Craeye et al., 2015) achieved the self compactibility of mortars at sand to paste ratio 0.59. Besides, self compactibility with higher sand to paste ratio of 0.63 were achieved by (Sri Rama Chand et al., 2016).

Superplasticizers and high powder content improve SCC mixture proportioning (Benabed et al., 2012). An efficient superplasticizer maintains consistency without increasing the amount of water in the SCM, which slightly alleviates the detrimental impacts of increased w/c ratio. Overly high admixture concentrations might delay setting and demolding. Both SCM and SCC applications should constantly optimize admixture dose.

The SCC mortar is used to reduce friction between the coarse aggregate and to help bind the aggregate together. Like concrete, it requires a low yield stress to allow for flow under its own weight, and a plastic viscosity high enough to avoid segregation during flow but low enough to allow for practical concreting. The proposed ranges for

SCM by (Domone and Jin., 1999) for the plastic viscosity and yield stress are 6 to 12 Pa.s and 20 to 50 Pa.s, respectively.

Poor workability of concrete or mortar can lead to various problems such as difficulty in placing and compacting the mix, resulting in more voids, lower mechanical strength, and durability (Mehdipour et al., 2013). The rise in yield stress and viscosity is more conspicuous during the quiescent state of the concrete mixture in contrast to its agitated state. The agitation of concrete results in the dispersion of flocculated cement particles, thereby enhancing its fluidity Z. Li, Taka-Aki Ohkubo, and Tanigawa (2004). (Felekoğlu et al., 2006) found that SCM exhibits viscous behavior at low mixing rotational speeds, but flowable behavior takes over at higher speeds. The elevated viscosity of the mixture at rest is disrupted during the agitation due to the shear thinning phenomenon, meaning the apparent viscosity reduces as the strain rate increases due to local shear or vibration aiding flow Cyr, Legrand, and Mouret (2000.). However, continual agitation may cause dynamic instability, which segregates and bleeds newly produced concrete or mortar. When transporting fresh mix in a truck mixer, vibration and agitation may promote particle segregation and sedimentation. Due to its pseudo-plasticity, a highly flowable mortar that is stable once cast may segregate during pumping or spreading into position, lowering its apparent viscosity.

## **2.4 Evaluating SCC and SCM Workability**

As previously mentioned, using a rheometer is not a practical or standardized method for evaluating the workability of SCC. Due to this limitation, Alternative methodologies are used for evaluating workability of SCC in a more practical manner. These alternative test methods offer several advantages, such as being cost-effective, less time-consuming, and easier to perform compared to using a rheometer. But it's

crucial to remember that there is no standard or organization that has standardized these actual test procedures. EFNARC has listed these methods, but they are described as descriptions and not definitive test procedures. This means that the methods are not uniformly recognized or regulated, and their results may vary depending on the user's interpretation.

In this section, a review will furnish concise explanations of practical testing techniques employed to evaluate the workability of SCC and SCM.

#### 2.4.1 Slump Flow

Measuring the flowability of SCC is commonly done through a test method known as slump flow. This method involves pouring the freshly mixed SCC into a slump cone and then measuring the diameter of the spread concrete on a horizontal plane. By doing so, the workability of the SCC can be determined.



Figure 2: Slump flow

By making a minor alteration to the slump cone apparatus, as depicted in Figure 3, it is possible to assess the characteristics of SCM through the employment of the slump flow test. EFNARC has described this modified cone, which has been utilized by other researchers, including (Safi et al. 2015) and (Horsakulthai, 2021).



Figure 3: Mini slump

### 2.4.2 V- Funnel Test

Measuring the flow rate of SCC is commonly done via test method known as v- funnel test. It entails the complete filling of a normal funnel with SCC, followed by the subsequent opening of the lower outlet to let the flow of the concrete through the funnel's V-shaped aperture. Subsequently, followed by time measurement when opening the cover to the point at which it's possible to see the concrete bucket from the top perspective. (Specification and Guidelines for Self-Compacting Concrete., 2002). This time measurement is an indicator of the SCC's viscosity and its ability to flow easily and uniformly, without segregating or blocking in the formwork. The V-Funnel test is a commonly employed method within the construction sector to verify the uniformity and excellence of SCC blends, and to optimize the proportion of ingredients for achieving the desired flow properties.

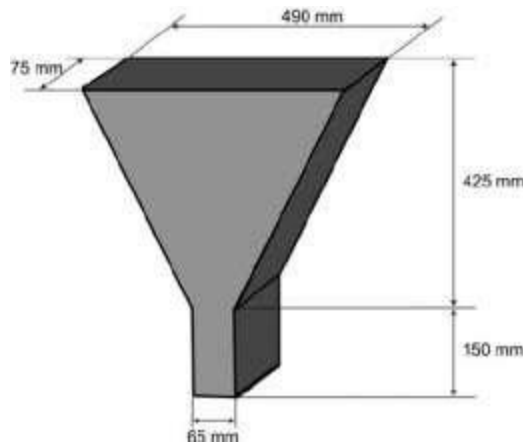


Figure 4: V-funnel (Specification and Guidelines for Self-Compacting Concrete., 2002)

With little change in size dimensions, this apparatus might be employed to evaluate the flow rate of SCM as shown in Figure 5. The aforementioned equipment has been employed by previous scholars, namely (Domone and Jin, 1999) and (Christianto, H. A,2004).

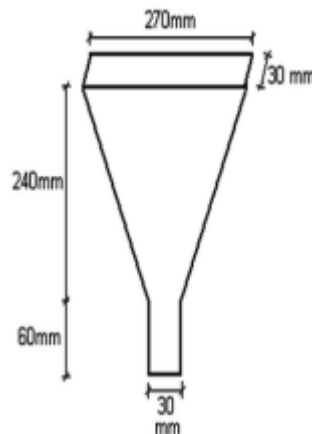


Figure 5: Mini v-funnel (Specification and Guidelines for Self-Compacting Concrete., 2002)

### 2.4.3 Workability and Viscosity Evaluation of SCM: A Review of Testing Methods in Previous Studies

Standardized testing methods for assessing the flowability of self-compacting mortar (SCM) do not currently exist. However, many studies on SCM utilize guidelines

established by EFNARC. These regulations recommend a spread flow of  $250 \pm 10$  mm and a V-funnel time of 7 to 11 seconds. The absence of a mini funnel in certain research endeavors has necessitated the sole utilization of the mini cone test as a means of evaluating the self-consolidating properties of the mortar.

The effects of seashells as sand replacements on SCM were investigated by (Safi et al., 2015), the workability of SCM was evaluated using mini slump having the same dimensions suggested by EFNARC, to ensure the self-compaction of mortar, the flow diameter was kept in range of 240 to 260mm.

(Horsakulthai., 2021) investigated the impact of recycled concrete powder on SCM. To evaluate the flow of SCM mini slump with diameter of  $250 \pm 10$ mm was tested following the guidelines suggested by EFNARC.

To ensure the flowability of SCM, mini slump flow test was done by (Khed et al., 2016) for producing SCM with both nano silica fume and fly ash as CRMs, spread flow diameter were evaluated according to EFNARC guidelines. Similar way of testing was also done by (Chu et al., 2022).

Both flow rate or viscosity and workability of SCM were checked by (Jawahar et al., 2013) using mini slump. The study followed EFNARC guidelines for evaluating the workability of SCM by mini slump, however, due to the unavailability of the mini v-funnel, viscosity of SCM was checked using mini cone. To assess the flow rate of SCM, flow time ( $T_{20}$ ) after releasing the cone until reaching 200mm was measured. This procedure is similar to slump flow for SCC. Similar way of testing also was done by (Libre et al., 2008) on evaluating the flow rate of high flowable mortars.

SCM cubes was exposed to different types of curing in study done by (Venkatesh et al., 2017), the workability of SCM was checked by Abram's cone of dimensions, top and bottom diameter 100 mm, and 200 mm with a height of 300 mm. EFNARC suggested that the flow diameter of SCC using Abram's cone with range of 650 to 800mm, which is same test was done on SCM in this study.

The flowability of SCM was evaluated using cone with dimensions of bottom diameter of 125 mm and a height of 63 mm (Molin Filho et al., 2019) . The relative flow time was calculated using an adaptation of (Okamura & Ouchi., 2003) methodology, and SCMs were predicted experimentally. According to (Edamatsu et al., 1999), the ultimate diameter should be 200–280 mm with relative flow area of 3 to 7, and the relative flow time should be from 1 to 2. To create SCC, (Takada and Walraven., 2001) suggested relative flow time and area values of 1.00 and 5.00, respectively. According to (Molin Filho et al., 2019) , larger relative flow area values result in mortars with more deformability, whereas lower relative flow time values are indicative of mortars with high viscosities.

The present study employed mini slump flow as a means of assessing the impact of MD as a substitute for cement, with varying proportions of 0%, 5%, 10%, 15%, 20%, and 30%, on the workability and flow rate of SCM analogous to (Jawahar et al., 2013) and (Libre et al., 2008). With the help of superplasticizers, the spread flow diameter was kept in the range suggested by EFNARC.

## **2.5 Passing Ability Tests For SCC**

Passing ability tests are commonly utilized to assess the flowability of SCC in scenarios where it needs to pass through tight spaces or obstacles, such as

reinforcement bars or narrow gaps, without requiring external compaction. The L-box, and J-ring tests are some of frequently used tests to assess SCC's passing ability as mentioned in EFNARC. Nonetheless, in this thesis refrains from employing said test procedures due to the absence of aggregates in SCMs, which are the main culprits behind reinforcement blockage.

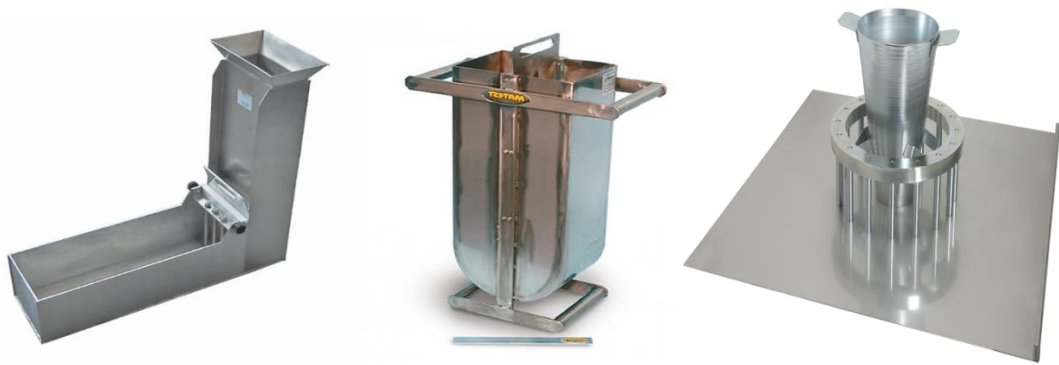


Figure 6: L-box, U-box, and J-ring apparatus

## 2.6 Cement Replacement Materials

Portland cement, a vital element of concrete, can be partially replaced with a variety of compounds known as cement replacement materials. These chemicals can be substances that exist naturally or industrial waste products that have been discovered to exhibit pozzolanic properties. Materials known as pozzolans react chemically with lime, which is the key aspect of Portland cement, to create compounds that harden and strengthen concrete. Some of the most popular CRM among all pozzolans are briefly mentioned below.

### 2.6.1 Micro Silica

The smoke that is produced by the furnace during the silicon synthesis process is collected and used as CRM. It is characterized as very tiny crystalline particles with a surface area of around  $20,000 \text{ m}^2/\text{kg}$ , which are far smaller than cement particles. Both the high fineness and considerable amount of silica in these particles make them

efficient pozzolanic material (King, D., 2012). The principal application of this substance is as a mineral supplement in concrete for the purpose of augmenting and optimizing its properties. Concrete that contains silica fume exhibits a comparatively elevated level of strength. The employment of silica fume, owing to its fine particle size and the advantageous pozzolanic reaction it induces, lead to in the producing denser and uniform structures within the matrix, which may enhance the durability factors.

### **2.6.2 Granulated Ground Blast Furnace Slag (GGBFS)**

As molten iron slag is quenched. It is characterized by a granular texture with minimal crystal formation. It exhibits a high degree of cementitious properties and undergoes hydration similar to that of Portland cement upon being ground to a fine cement consistency. Since the late 1950s, construction companies have incorporated GGBFS into their cement mixtures to enhance specific functionalities. GGBFS used as a raw material in cement manufacturing. Slag cement is another name for it, using (Vittalaih, Ravinder, and Vivek Kumar., 2020) GGBFS improves concrete's durability by reducing alkali-aggregate reactions and having a strong resistance to sulfate. Less chlorine diffusion and penetration can also lessen the probability of steel reinforcement corrosion.

### **2.6.3 Pulverized Fuel Ash (PFA)**

A powdery substance that is obtained from the gaseous byproducts of coal combustion for the generation of electrical power. PFA is a pozzolanic substance made up of aluminous and siliceous components that, when mixed with water, exhibit qualities similar to cement. It is characterized by its fine particles leading to increasing the unit weight of the concrete. As a result, chloride penetration is decreased and permeability

is lowered (Uysal, Yilmaz, and Ipek., 2012). Moreover, adding FA to the concrete mix increases strength and enhances resistance to sulfate attack.

#### **2.6.4 Rice Husk (RH)**

A residual substance generated by the incineration of RH. This ash has a very small porous structure and an 85–90% amorphous form composition, making it ideal for altering cement by pozzolanic reaction. Moreover, calcium hydroxide crystals from cement hydration react with amorphous silica in RH, this can improve the interlocking of the mortar mixture. As a result, larger densities and strengths may be created D. Samuel Abraham, Janaki Raman, and Aiswarya S (2018).

### **2.7 Utilization of Cement Replacement Materials in Self-Compacting Mortar**

Applying cement replacement materials in SCM resulting higher quality, and eco-friendly building materials, (Usman et al., 2018) studied the self-compacting pastes were made from wood waste that included both coarse and fine sawdust. The incorporation of sawdust into cementitious systems results in an elevated demand for water. Moreover, wet sawdust particles remain as inert material in mortar providing curing for internal matrix, as a result, the cement's hydration is aided by the curing agent, and the significant drying shrinkage is avoided. The integration of sawdust particles into SCM is impeded by the weakened strength during early stages due to the lower compressive strength and density of said particles. The advantages of employing Sawdust, however, may be observed in the decreased shrinkage, which enables a large decrease in microcracking brought on by shrinkage. Using cements with larger concentrations of di- and tri-calcium silicate can overcome the restriction of lower strength with Sawdust incorporation.

CRMs was used namely mica and feldspar for production of SCM by (Kohani Khoshkbijari et al., 2020). The study's results indicate that all SCM mixtures that contained mica and feldspar demonstrated satisfactory slump flow, with relative funnel velocity parameters falling within the acceptable range of EFNARC. The sorptivity coefficient was reduced and thermal durability was increased when mica and feldspar were used in place of cement.

The study conducted by Demirhan, Turk, and Ulugerger (2019) investigates the impact of substituting a significant amount of limestone dust with cement on the characteristics of SCMs. The findings indicated that the most important replacement level for limestone powder is 15%, after which performance attributes are impacted at varying rates. In terms of slump flow, SCMs with higher lime powder content demonstrated improved fresh characteristics. Moreover, the addition of limestone powder doesn't significantly affect mechanical properties. Furthermore, a drop in carbonation resistance observed in the samples containing CRMs as the limestone powder increases which is attributed to lower hydration rate. Besides, most supplemental ingredients, like limestone powder, reduce UPV when used.

Both pulverized fuel ash and two types of limestone dust were used as CRMs to produce SCM were investigated by (Felekoğlu et al., 2006). The flowability paste mixtures is characterized by pseudo-plasticity. The manifestation of viscous behavior is readily apparent under conditions of low rotational speeds, while flowable behavior predominates at higher rotational speeds. Attaining a more flowable consistency may necessitate elevated rotational rates. In comparison to plain cement paste, it was observed that all powders exhibited an increase in initial viscosity. However, the extent of this increase was found to be contingent upon the level of replacement of each CRM.

Furthermore, compressive strength showed that the two limestone fillers exhibited higher early strength enhancement compared to fly ash. However, after a period of 28 days, the mixtures that contained fly ash demonstrated a greater strength improvement due to the late pozzolanic reactions.

Incorporating Recycled Concrete powder (RCP) into self-compacting mortar by (Horsakulthai., 2021) was found to reduce electrical resistivity, increase porosity, and increase the coefficient of water absorption, according to this study. These findings imply that up to 20% is the ideal RCP replacement ratio, which has the least detrimental impact on compressive strength.

SCMs were produced by three types of CRMs by (Uk et al., 2009). The lowest flexural and compressive strengths were observed at 30% of limestone dust. Conversely, a 30% micro silica replacement level possessed the best strength values. Moreover, water absorption of the combinations that have no micro silica are greater than those of the reference mixture. Concluding that the separate use of limestone dust and fly ash was insufficient in effectively obstructing capillary pores compared to micro silica after 28 days.

Both micro silica and fly ash as binary and ternary mixes for producing SCMs were studied by (Benli., 2019). According to the study, increasing fly ash dose improved SCMs flow while decreasing segregation resistance. Moreover, mortars containing 10% fly ash possessed the best flexural strength value at the late age of 180 days. Besides, mortars containing 10% micro silica showed the best compressive strength improvement.

## **2.8 Effects of Waste Marble Dust on Properties of SCC and SCM**

Utilizing the WMD as a supplementary material in place of sand or cement in mixtures manufacturing enhances the material's physical and mechanical properties. An even denser structure can be produced by using WMD in the manufacturing of mortar. Due to its low cost, its usage in concrete and mortar as a cement substitute will be more cost-effective. WMD can be purchased from marble companies (Singh et al., 2017).

Marble is considered to be a crucial material in buildings, specifically for ornamental applications. Moreover, the waste dust of marble in question has been found to have detrimental impacts on various aspects of the ecosystem, including but not limited to the earth, water, soil, and health hazard. The disposal of fine marble manufacturing waste powders is a global environmental challenge (Alyamac and Ince., 2009). MD as CRM has direct effect on the properties of concretes, mortars, SCC, and SCM which will be discussed below.

### **2.8.1 Workability**

(Boukhelkhal et al., 2016) used the MD as CRM to produce SCC. The study entailed the preparation of SCC mixtures wherein different proportions of MD were utilized as a CRM. The results show that the workability of SCC is decreasing with increasing MD levels. The observed changes in the parameters were a decrease in slump flow and L-box ratio, and an increase in V-funnel time.

Three CRMs were used in the production of SCC namely marble dust, limestone dust, and fly ash by (Gesoglu et al., 2012). The findings indicate that MD as has lowered the workability of SCC. For instance, 20% MD as CRM resulted in prolongation of flow time by 13 seconds, and a reduction of 4% in slump diameter.

Both MD and granite dust was used as CRM to produce SCC by (Sadek et al., 2016). The study found that workability was reduced when rising the MD levels. Moreover, an increase in V-funnel time suggests a decrease in fluidity, causing difficulty in handling and placing the material.

The utilization of MD and GGBFS the production of SCM were evaluated by (Güneyisi et al., 2009). The study was on a binary Fractions of 5 to 20% of MD, 20 to 60% of GGBFS, and ternary mix of (MD and GGBFS) together. The outcomes indicated that MD showed the same adverse impacted on the workability in other words the slump diameter was reduced, and v-funnel time was slightly increased. However, the effect on the ternary mixes was somewhat lower.

(Khodabakhshian et al., 2018) assessed the feasibility of utilizing MD as a CRM, with varying ratios ranging from 5% to 20%. The study revealed that an increase in MD proportions was accompanied by a corresponding increase in the demand for superplasticizer.

The decrease in workability of concrete with increasing replacement level was observed by (Vardhan et al., 2009) when utilizing MD as a CRM in concrete, with replacement proportions ranging from 10 to 60% by weight. Due to angular morphology and amplified surface area of the MD, workability is reduced.

### **2.8.2 Setting Time**

Limestone dust, marble dust, and pulverized fuel ash was used to produce SCC in study done by (Gesoglu et al., 2012). 14 different mixes were done, which are binary mixes of limestone dust with fractions of 10, 20, 30% and MD with fractions of 5, 10, 20%. In addition to ternary mixes fixed 30% of pulverized fuel ash with the binary

mixes mentioned above. They concluded that increasing the amount of CRMs rises both setting times.

Binary and ternary mixes of MD and GGBFS used to produce SCM in study done by (Güneyisi et al., 2009). The study focused on a total of 19 mixes of binary fractions of 5, 10, 15, and 20% of MD, 20, 40, and 60% GGBFS, and a ternary mix of (MD and GGBFS). Results showed that both MD and GGBFS in SCM showed increments in both setting times.

Concrete was produced by partial replacement of cement by MD in study done by (Singh et al., 2017). The study involved different replacement fractions of MD, which were 0, 10, 15, 20, and 25%, with various water-to-binder ratios, results showed increment in both setting times of mortar. For instance, 25% MD extended the initial setting time by 33 minutes, while the final setting time prolonged by 61 minutes.

### **2.8.3 Air Content and Unit Weight**

The utilization of MD as CRM was investigated in conjunction with fly ash for SCC by (Topçu et al., 2009). The study involved seven distinct series, each consisting of a fixed 10% fly ash content and variable percentages of marble dust ranging from 5% to 55%. Air content was measured by an air meter and unit weight of the mixes were tested by constant volume bucket. The outcome of study sums that ternary mix of MD and pulverized fuel ash raised the air content and reduced the fresh unit weight of SCC.

A study was done on comparing limestone and marble dust as filler in SCC by (Alyousef et al., 2019), the fraction used was 20% cement replacement for both. Alyousef mentioned that the bulk of the grains in the marble dust filler are interposed between the cement grains as a result of its fineness, which eventually results in an

increase in compactness that lowers the air content. Finally, they concluded that MD compared with limestone dust and control mix slightly reduced the air content and increase the density, thus, increased unit weight.

(Grabiec et al., 2015) investigated the use of three different mineral additives to produce SCC. The mineral additives in the study were binary mixes of pulverized fuel ash, limestone dust, granite dust, and various ternary mixes of these three minerals. It was concluded that pulverized fuel ash showed the highest air content of 1.9% compared with 0.7% and 0.8% for limestone powder and granite powder. Moreover, incorporation of pulverized fuel ash with limestone powder and granite powder showed an enhancement in air content of SCC.

#### **2.8.4 Mechanical Properties**

SCC produced by MD and fly ash were investigated by (Topçu et al., 2009). Results sum that using MD as cement replacement has reduced both compressive and flexural strength, where 5 and 10% MD with fixed replacement of FA of 10% showed a slight reduction of 8% of compressive strength. Where for flexural strength almost same results of control mix at 5%MD.

Natural pozzolana and MD were used to produce SCC in study done by (Belaidi A., 2012). The researchers arrived at the conclusion that both CRMs into the concrete reduced compressive strength. Moreover, the results showed that Natural pozzolana as CRM has a positive impact on strength gains at late ages, specifically after 90 days. The binary mixes containing 5% Natural pozzolana and ternary systems containing 5% Natural pozzolana and 5% MD achieved their highest strength after a duration of 28 days.

SCC produced with use of MD as CRM by (Boukhelkhal et al., 2016). MD fractions were 5, 10, 15 and 20. Marble dust were sieved, and results showed that MD is finer than cement where 70% of MD particles is lower than 70  $\mu\text{m}$ . Besides, compressive test was tested on 3 periods of 3, 28, and 90 days. They concluded that MD as CRM reduced the compressive strength at early ages, however, almost same results were achieved by 5% MD on 28day.

Blends of silica fume, pulverized fuel ash, and MD was used as CRM to produce high strength SCC in study done by (Choudhary et al., 2020). The study was done on 5 different series of 16 mixes which are: control mix, binary mix for each supplementary material and three different ternary mixes of silica fume, pulverized fuel ash, and MD. Furthermore, compressive strength results showed that optimum replacement at 28days strength for binary mixes were 5% silica fume, 10%MD, and 15% pulverized fuel ash. For ternary mixes 15% silica fume +10%MD achieved the highest compressive strength by enhancing 25%, 15%, and 14% of 7,28, and 90days strength.

(Ergün., 2011) conducted a study that explored the utilization of MD as a CRM in SCC. The study also investigated the use of MD as CRM with varying levels of 5 to10%. Employing 5% MD to concrete mixture has enhanced the specimen's compressive strength, while, at 10% MD the strength reduced significantly, which can be attributed to a reduction in pozzolanic reactions. Moreover, (Khodabakhshian et al., 2018) reported that 5% MD has slightly improved the compressive strength, while increasing the CRM proportions lowered the compressive strength significantly.

(Güneyisi, Gesoğlu, and Özbay., 2009) also studied production of SCM using blends of both GGBFS and MD. Both compressive strength test and UPV test were used.

They concluded that the MD as binary mixes reduced the strength, for instance: 20% MD reduced 28-day strength by 22%. Moreover, ternary mixes of MD and GGBFS also showed a slight reduction in strength. However, optimum replacement of 40% of GGBFS was found. It was also noticeable that UPV values had a slight decrease for binary mixes of MD and increased for GGBFS.

### **2.8.5 Water Absorption**

(Raman et al., 2018) studied SCC'S mechanical and durability characteristics when using Rice hulls and MD as CRMs. Results showed that cooperation of Rice hulls with MD enhanced the mechanical properties of SCC due to Rice hulls containing silica which aid to get denser mixture. Thus, lower water absorption capacity was found in these ternary mixes.

High-strength SCC was produced by combination of three different CRMs, namely silica fume, fly ash, and MD in study done by (Choudhary et al., 2021). The study focused on five different series of 16 mixtures, including a control mix, a binary mix for each supplemental material, and three different ternary mixes of MD, silica fume, and pulverized fuel ash as mentioned before. They found that 10% exhibited almost the same absorption% and voids% as control mix, however, higher MD content rises both absorption and voids percentages. The highest absorption capacity and voids % were found in ternary mix (25% fly ash+30%MD) of 2.5% and 6% respectively.

(Boukhelkhal et al., 2018) also mentioned that MD as CRM influences the water absorption of SCC. To test water absorption capacity an ASTM C642 was followed. In addition to a water capillary absorption was done according to French standards, both tests were conducted on 28 days of curing. They determined that capillary (%) rose somewhat, and immersion absorption (%) slightly, when MD was partly replaced

for cement. Moreover, with a resulting coefficient of correlation of 0.9, they found that it strongly correlated to compressive strength.

### **2.8.6 Drying Shrinkage**

combination of pulverized fuel ash, silica fume, and MD was used as CRM to produce high strength SCC in study done by (Choudhary et al, 2021), drying shrinkage high strength SCC was assessed on five different series as mentioned before. They observed that higher drying shrinkage was found when silica fume is used, due to higher rate of hydration in the mixture contains silica fume. When MD is used drying shrinkage was lowered initially, compared with control mix 10% MD reduced the drying shrinkage at 180days by almost 18%. However, higher portions of MD 20 and 30% increased the drying shrinkage. Moreover, using fly ash as CRM reduced the dry shrinkage of high strength SCC where 35%FA exhibited the lowest drying shrinkage among the binary mixes at 180 days. Furthermore, the lowest drying shrinkage was found at (15% fly ash+10%MD) mix, due to lower content of lime in fly ash which reduces the hydration rate of cement in SCC mixes.

MD as CRM in mortars was investigated by (Li et al., 2018). The study was on different series with 4 different w/c ratios. Each w/c were examined with MD ratios of 0, 5, 10, 15, and 20%. Results showed that drying shrinkage rate was slightly reduced with lowering the water content, Li mentioned that lower drying shrinkage resulted from low water content mixtures is due to less water loss. However, increasing MD portions decreased drying shrinkage. Concluding that the drying shrinkage was always lowered when MD was used as CRM, and the decrease was greater at lower water content. For instance, lowering the w/c ratio from 0.55 to 0.40 resulted in decreasing the shrinkage by almost 8.50%.

An experimental study was done on a CRM on concrete by (Singh et al., 2017). MD replacement fractions were 0 to 25% with different water content. cement paste mortar was evaluated for drying shrinkage, results concluded that MD as CRM reduces the drying shrinkage of the mortar. For instance, 20%MD reduced the shrinkage from 1.31mm to 0.667mm.

Marble and brick dust were employed to produce SCM in study done by (Dalila et al., 2020), binary and ternary mixed was done to evaluate the drying shrinkage of SCM. They conclude that using brick dust or MD as cement replacement in binary mixes reduced the drying shrinkage.

### **2.8.7 Heat Resistance**

MD was substituted for cement by (Bayraktar et al., 2019) at level of 5 to 20%. The heated to temperatures of 150 to 900 °C for two hours were examined. Compressive strength data after 28 days revealed a decrease with MD addition. There was a minor strengthening in compression when air-cooled specimens were exposed to 150 °C, but when the temperature rose further, there was a decline in comparison to the reference mortar. Yet, samples that were cooled by the sprinkler method decreased as the temperature rose. Moreover, due to lower quantity of calcium hydroxide when using MD as CRM compared to pure PC cement, this phenomenon may be a contributing factor to the observed enhancement in strength up to a temperature of 150 °C. The microstructure analysis of mortar specimens exposed to elevated temperatures revealed that up to 300 °C, there was no discernible dispersion of aggregate, crack development, or void structure. However, above 300 °C, there was evidence of crack development between the aggregate grains of the binder.

In cement mortar, according to (Keleştemur et al., 2014), fine sand replaced by MD in amounts ranging from 20 to 50% by volume. The samples underwent exposure to 400 to 800 °C. The compressive strength has slightly lowered when exposed to temperature to 600 °C. However, above the mentioned temperature the effect was more significant. Moreover, the use of MD as an addition increased the resistance of mortars because the pores were reduced at high temperatures. Moreover, microcracks developed up to 800 °C after beginning to form at almost 400 °C. The development of microcracks may cause a decrease in compressive strength by adversely influencing the Interfacial Transition Zone. At 600 and 800 °C, the morphology of the specimens underwent significant alterations as a result of microcracks, an increase in voids and, consequently, porosity, the disintegration of calcium hydroxide, and damaged CSH bonds.

Moreover (Yamanel et al., 2019) utilized the MD for mortar production. The study was on 0, 5, 10, 15, and 20% cement replacement by MD. Mortar was tested for mechanical properties under Elevated temperature of 300, 600, and 900 °C. They have found that mortar with MD as CRM exhibited comparable compressive strength mortar up to 300 °C. However, when the temperature was increased up to 900 °C, significant reduction rates of almost 65% in the strength were found. Despite the loss in strength at higher temperatures, mixtures with MD still showed similar or better performance compared to control mix. Furthermore, a slight effect on the flexural strength of the material of mixes with MD after exposure to 300 °C was found. Mortars with 5% MD replacement also showed a slight loss of around 6% flexural strength. However, after exposing the specimens to higher temperatures, all mortars experienced significant strength loss, with reductions of around 80% when exposed to 900°C.

Nonetheless, mixtures with MD showed almost similar performance to the plain mix event when the heat exposure level was raised.

SCC made with different CRM at high temperatures was investigated by (Uysal., 2012) CRMs include limestone dust, MD, and blast dust. Lower weight loss is reported in SCC with polypropylene fibers and CRMs compared to SCC without polypropylene fibers. Greater reduction in UPV values when SCC mixes are subjected to high temperatures in SCC contains limestone dust. Moreover, MD showed slight decrement in compressive strength compared with limestone dust. All SCC specimens, no obvious spalling or cracks are seen at 200 and 400 °C, at 600 °C, minor fractures and spalling were seen. Furthermore, all specimens are seen to have noticeable cracks and spalling at 800 °C.

## **2.9 Environmental and Economic Aspects**

Due to the high cost of cement and the pollution it generated during production, which required energy resources like petrol and coal, scholars are thus working to use industrial waste to make cement concrete or mortar more affordable while also protecting the environment. As the building business develops, many materials are being researched as cement substitutes. The three most common industrial wastes, slag, micro silica, and MD are readily accessible and inexpensive (Shabbir et al., 2020). In addition to these materials, there are contaminants for the environment and many man-made risks. Therefore, employing them as cement substitutes would not only lower the cost of making concrete but also lower pollution.

Marble dust is the powdered waste product of the marble manufacturing. About 20 to 25 % of the marble that is mined is wasted during the shaping process, amounting to

millions of tons (Belaidi et al., 2012). Depending on the environment, the minerals or impurities present in the limestone during recrystallization, and other factors, the chemical conformation of marble will vary significantly. Due to its fineness the MD is used varying application in production of mortar or concrete, according to literature the MD can be used as CRM, filler material, and fine aggregate replacement. The main purpose of this study was to reduce both cost of production and environmental impact of using SCM, due the use of high cement content and chemical admixtures, where the most expensive component in the mixture is cement. MD is an inert material which doesn't interact with hydration products of cement, therefore, an expected inverse impact on both mechanical and durability factors of SCM specimens, in this study the cement was replaced with MD at various levels in order to evaluate the impact and concluding with selecting an optimum level of replacement for SCM production.

## **2.10 Summary**

SCMs are mortars that can fill formwork without vibrating and spread into a space without separating. Moreover, mortar forms the basis of different properties of self-compacted concrete, therefore, testing the properties of these mortars are essential for production of SCC, in fact testing the mortars required lower labor than the SCC. Furthermore, the production of both SCC and SCM is a bit expensive than conventional concrete or mortar, to reduce the cost several studies on replacing the cement with waste materials were done, in this study MD was selected as CRM for production of both NSCM and HSCM, due to the fact of North Cyprus has almost 39 marble factories according to Cyprus Turkish Chamber of Industry, where almost 25% of marble is wasted during shaping, meaning that tons of MD are wasted every year and when dumped in the catchment region, they reduce the permeability of the groundwater and increase pollution.

This study was done to evaluate the properties and fill literature gaps about using MD as CRM in the production of SCM. According to literature, using the MD as CRM to produce SCM has a significant impact on both fresh and hardened properties. Due to its smaller size, increasing the MD replacement level reduced the workability by (reducing slump diameter, and prolonging the flow time), and prolonging both setting times. While studies of air content for SCM weren't found, the studies found only on SCC confirm the reduction of air content when increasing the level of replacement. Moreover, because MD is a non-pozzolan material, mechanical properties and drying shrinkage were reduced. While information about the effects of water absorption and heat resistance wasn't valid, the studies were found only on SCC, where the mortar is the main component, so an expected rise in water absorption and lowering of resistance when exposed to heat similar to what is described in the literature.

## Chapter 3

### RESEARCH METHODOLOGY

#### 3.1 Outline

This chapter demonstrates the mixture component used and provides detailed explanations of the experimental procedures. Additionally, the chapter delves into the ASTM standards employed, as well as EFNARC's suggested methods for ensuring self-compacting mortar. Other methods used in conducting the experiments are also covered, and guidance on how to operate the relevant machines and apparatuses is included.

#### 3.2 Mixture Components

##### 3.2.1 Cement

The experiment employed cement type CEM II/B-S 42.5 N. Tables 1, 2, and 3 depict the cement characteristics.

Table 1: Cement physical and mechanical properties according to EN 196-6 and EN 196-1.

Cement Specific Gravity	Cement Specific Surface Area (cm <sup>2</sup> /g)	Cement sieve 90 μm retained (%)	Cement sieve 45 μm retained (%)	Cement Compressive Strength (MPa)		
				Day (2)	Day (7)	Day (28)
3.05	3632	0.19	4.72	28.7	40.2	52.30

Table 2: Cement physical properties according to EN 196-3

Water-cement ratio (%)	Cement Initial Setting Time (min)	Cement Le Chatelier Expansion (mm)
28.2	185	0.8

### 3.2.2 Marble Dust

The MD utilized in this study was procured from Oyo Granit Mermer located in North Cyprus. The methods of ASTM D854 and ASTM C29 were employed to ascertain the specific gravity and loose bulk density of MD. Results showed that the MD possessed a specific gravity of 2.62 and a loose bulk density of 955.7 kg/m<sup>3</sup>. Moreover, the size distribution of MD particles was evaluated through a hydrometer test based on ASTM D7928. From Figure 7, it's obvious that MD possess a size smaller than 65 μm. Furthermore, Table 3 presents the chemical composition of MD.

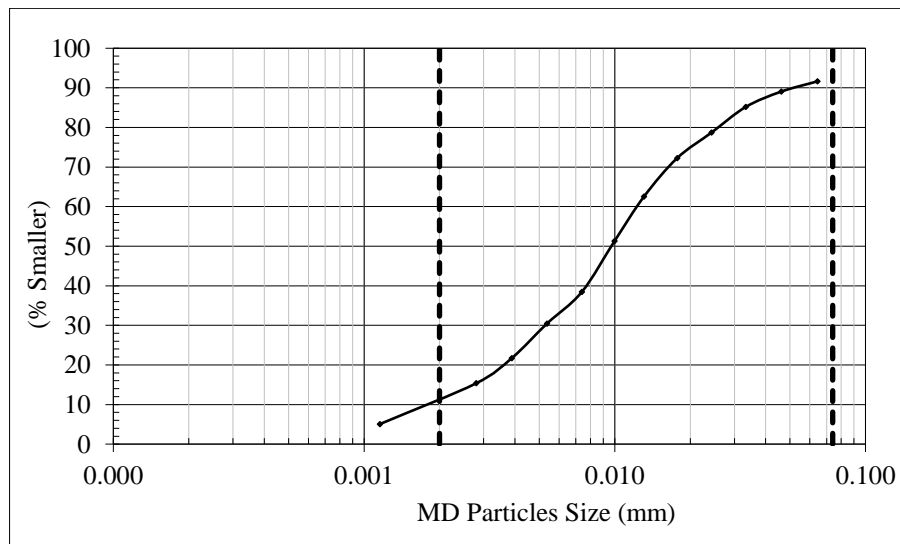


Figure 7: MD particle size distribution

Table 3: Chemical properties of CEM II/B-S 42.5 N and marble dust

Chemical Oxides	Cement (%)	MD (%)
CaO	56.62	47.46
SiO <sub>2</sub>	22.40	3.99
Al <sub>2</sub> O <sub>3</sub>	5.97	0.58
Fe <sub>2</sub> O <sub>3</sub>	3.39	0.00
MgO	3.19	3.64
SO <sub>3</sub>	2.94	0.31
CaO free	0.57	-
Cl	0.00	-
CO <sub>2</sub>	-	-
Na <sub>2</sub> O	-	-
SrO	-	-
P <sub>2</sub> O <sub>3</sub>	-	-
K <sub>2</sub> O	-	-
loss on ignition	2.93	42.67
Insoluble residue	0.53	-

### 3.2.3 Fine Aggregate

In this study, crushed limestone smaller than 5 mm in size was used. The aggregate underwent sieve analysis based on ASTM C136M-14, the particles size distribution is illustrated in Figure 8. The utilized fine particles possessed a specific gravity of 2.75, with water absorption of 1.38%. Additionally, both loose bulk density and compacted bulk density were determined to be 1712 kg/m<sup>3</sup> and 1927.2 kg/m<sup>3</sup>, using the ASTM C128-15 and ASTM C29 methods, respectively.

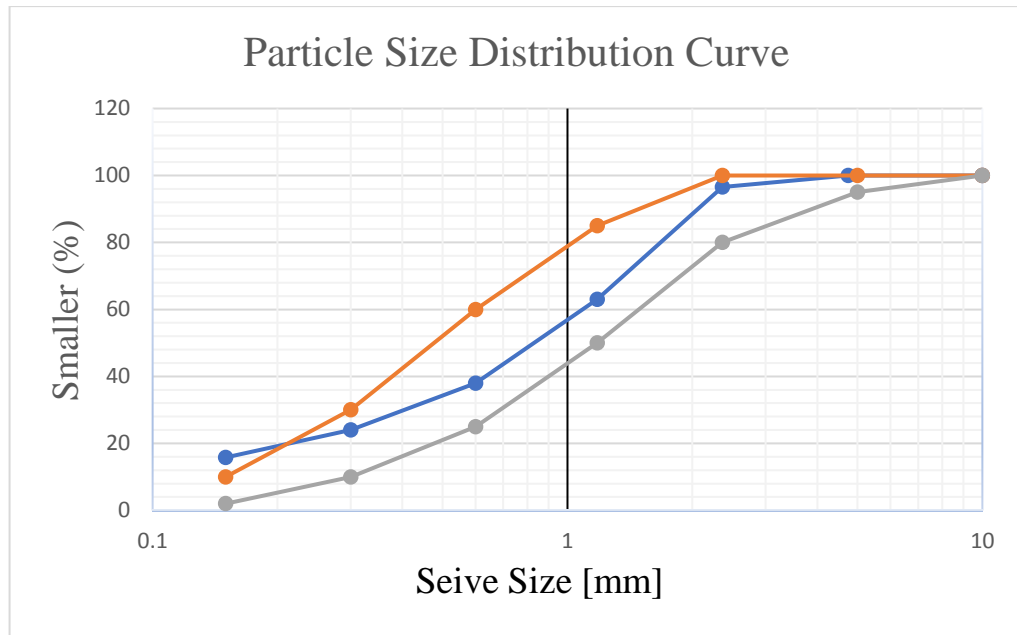


Figure 8: Fine aggregate sieve analysis

### 3.2.4 Mixing Water

Self-compacted mortar was mixed and cured using normal tap water.

### 3.2.5 Superplasticizers

The utilization of a Master Glenium 27 Admixture (EN 934-2:T3.1/3.2) for achieving flow diameter within a prescribed range of 240mm to 260mm in the SCM mixes.

## 3.3 Experimental Program

The aim of the study is to produce SCM by using MD as CRM. To achieve this objective, six distinct series were generated by substituting cement with MD in varying proportions of 0 to 30%. NSCM series was prepared with w/c ratio of 0.50, while the HSCM series was prepared with w/c ratio of 0.38. Moreover, Glenium 27 admixture was used to achieve the self compactibility of mortars. The fresh properties investigated are air content, both setting times, flow rate, and slump flow diameter. The hardened properties that were tested are compressive strength, splitting and flexural strengths, water absorption, Schmidt hammer, UPV, and cracks checked at elevated temperature, and drying shrinkage.

### 3.3.1 The Procedure of Mixing the Mortar

The methodology employed was akin to that described by (Christianto H. A., 2004) as illustrated in Figure 9. For trial mixes standard mini- mixer were used while for the studied SCM series a concrete mixer with a capacity of 0.25 cubic meters was used as shown in Figures 10 and 11.

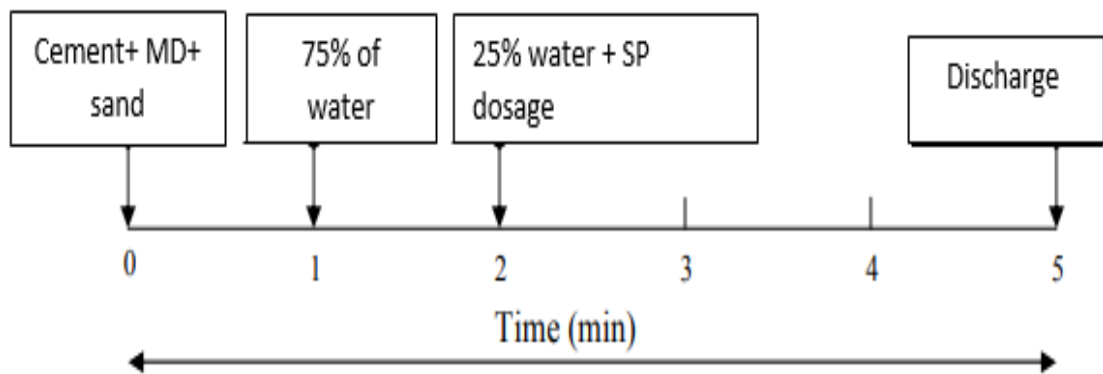


Figure 9: SCM mixing procedure



Figure 10: Standard mini mixer



Figure 11: Concrete mixer with capacity of 0.25 cubic meter

### 3.3.2 Trial Mixes

To achieve designed compressive strength for SCM several trials were done, firstly, mix proportions was done according to (BRE 331., 1988) standards. Then, to achieve the target strength while maintaining the slump, various w/c ratios were done with required superplasticizer dosage. Compressive strength of Each trial mix was determined using three 5cm cubes as well as workability was tested through mini slump. N3 and H3 were accepted in this study which have 89% and 79% of designed strength with flow diameter of 250 and 255 mm which are in range recommended by EFNARC as displayed in Table 4.

Table 4: Trial mixes of SCM

Trial no.	w/c	SP (%)	Mini slump flow (mm)	7 days compressive strength (MPa)	Percentage of designed strength (%)
N1	0.55	2	265	\	0.0
N1	0.55	1.75	255	24.6	66.5
N3	0.5	2	250	33.2	89.8
N4	0.47	2	240	36.5	98.7
H1	0.4	1	245	49.3	73.6
H2	0.38	1	245	\	0.0
H3	0.38	1.1	255	53.2	79.4
H4	0.35	1.25	235	\	0.0
H5	0.35	1.4	255	58.4	87.2
H6	0.33	1.4	250	65.4	97.6

### 3.3.3 Quantities of Ingredients in the SCM's Mix

The mix design of SCM was prepared according to (BRE 331., 1988) standard, by several trials as discussed before, and then, as shown in Table 5 two SCM series were chosen for high and normal strength SCM with characteristic compressive strengths at 28 days of 37 and 67 MPa, respectively.

Table 5: SCM mix design.

MIX NO	CEMENT	MARBLE DUST	WATER	FA	SP
NSCMOMD	500	-	250	1670	2%
NSCM5MD	475	25	250	1670	2%
NSCM10MD	450	50	250	1670	2%
NSCM15MD	425	75	250	1670	2%
NSCM20MD	400	100	250	1670	2%
NSCM30MD	350	150	250	1670	2%
HSCMOMD	658	-	250	1492	1.1%
HSCM5MD	625.1	32.9	250	1492	1.1%
HSCM10MD	592.2	65.8	250	1492	1.1%
HSCM15MD	559.3	98.7	250	1492	1.1%
HSCM20MD	526.4	131.6	250	1492	1.1%
HSCM30MD	460.6	197.4	250	1492	1.1%

### 3.3.4 Molding and Curing

Five distinct kinds of molds were produced for each SCM mix, including six cubes measuring 150 mm, one beam measuring (100 mm squared x 500 mm length) mm that was subsequently divided into five cubes measuring 100 mm, six cylinders measuring 100 mm x 200 mm, seven cubes measuring 100 mm, and eight beams measuring (40 mm squared x 160 mm length). First, the molds were cleaned and lubricated to make it easier to demold samples. Then, when self-compacting mortar was poured into the

specimens, it was no longer necessary to put the samples in the vibrating machine after the fresh mortar tests. Consequently, the molds were promptly poured with mortar and transferred to the curing chamber, where they were exposed to a temperature of 21 °C and a relative humidity of 99%. Subsequent to a period of twenty-four hours, after that the specimens were extracted from their molds.



Figure 12: Specimens in curing room



Figure 13: SCM specimens in water curing tank

### **3.4 Fresh Mortar Tests**

To determine the influence of various replacements of MD (0, 5, 10, 15, 20, and 30) % on the fresh properties of SCM, for both NSCM and HSCM series, mini-slump flow, flow rate, air content, and setting time were applied.

#### **3.4.1 Workability**

According to (Specification and Guidelines for Self-Compacting Concrete., 2002), using small cone as shown in Figure 14 the flow of SCM can be evaluated. For this test, a smooth plate with mortar in it is placed on top of the truncated cone mold, which is then raised upward. The mortar's final diameter is determined by averaging the measurements taken in two perpendicular directions.

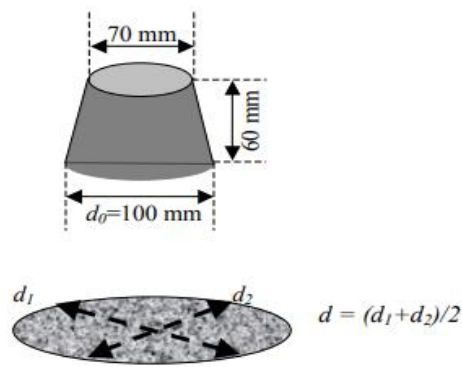


Figure 14: Mini-slump flow (Specification and Guidelines for Self-Compacting Concrete., 2002)

### 3.4.2 Determination of Flow Rate

Due to unavailability of the mini v-funnel suggested by EFNARC, the flow rate was evaluated using mini slump cone. Firstly, the plate was marked at 200mm diameter for both cross ponding dimensions as shown in Figure 15, then the cone was centered on the plate and filled with mortar. The cone was released, and the stopwatch was started simultaneously. The time ( $T_{20}$ ) was measured when the mortar flow reached diameter of 200mm, this test is similar for testing SCC. In addition, the time of the SCM remains in their properties “consistency retention” was evaluated using ( $T_{20}$ ) after 60 minutes after addition of water, The way of testing is similar to (Libre et al., 2008) and (Jawahar et al, 2013).



Figure 15: Testing of  $T_{20}$  flow time

### 3.4.3 Air Content

SCM air content has been measured using ASTM C231 / C231M. Firstly, the mold was cleaned, and the edges were greased using silicon grease, a fresh mortar was cast in the container in one layer without any compaction due to the self-compaction property of the mortar. Then the cover was well closed, the main valve was opened, and water was injected through water valves to ensure no air bubbles in the container, besides, the container was tapped to aid in releasing the air bubbles. Finally, the bleeding valve was closed and pumped using the hand pump until reaching the calibrated line. After that, the water valves were closed, the main valve was opened, and tapping the pressure gauge to get an accurate result. Reading was taken when the pointer stops moving.



Figure 16: Air meter

#### 3.4.4 Setting Time

The proctor penetrometer apparatus in Figure 17 was used to calculate the initial setting time and the progress of mortar hardness “final setting time”. This test process followed ASTM C403/C403M-99 guidelines. The SCM is poured into a 100 × 100 × 150 mm cuboid mould as shown in Figure 18 and kept at a temperature of 23 °C. The mortar's resistance to being penetrated by a standard needle is periodically measured.



Figure 17: Concrete and mortar penetrometer



Figure 18: Cuboid used in testing setting time

### **3.5 Hardened Mortar Tests**

The samples were put through a total of nine tests on their hardened state, including (compressive, flexural, and splitting tensile) strengths, water absorption, drying shrinkage, and heat degradation where its influence checked by, crack detection, UPV test, Schmidt hammer, and compressive strength.

#### **3.5.1 Compressive Strength**

The ASTM C39/C39M-18 standard was followed to evaluate the SCM's compressive strength. A compressive universal testing machine with a 3000 KN capability was used to test cubes of 150 mm and (100 mm used to check the compressive strength at elevated temperature).



Figure 19: Hydraulic compression machine

### **3.5.2 Splitting Tensile Strength**

The mixes' splitting tensile strength was assessed using 100x200 mm cylinders.

Besides, ASTM C496/C496M-17 was followed.



Figure 20: Splitting tensile strength test

### **3.5.3 Flexural Strength**

The beam specimens were prepared and evaluated, as illustrated in Figure 21 according to ASTM C348-21. For each mix, the flexural strength of three samples was evaluated for each testing age. Moreover, the testing machine has a maximum capacity of 15 KN.



Figure 21: Flexural strength test

### **3.5.4 Water Absorption**

In order to ascertain the water absorption capacity of the specimens, a total of three cubes measuring 100mm each were left in water tank for 28 days according to ASTM C642-13. Following the completion of the water curing process, the specimens were extracted from the tank and placed in an oven maintained at a temperature of  $100 \pm 5$  °C for a duration of approximately  $24 \pm 1$  hours, until a state of constant weight was achieved. The specimens were subsequently allowed to cool, and their weight was measured. Subsequently, the specimens were submerged in water for a duration of at least 48 hours, until two consecutive weight measurements exhibited a variance of less than 0.5%. Subsequently, the specimens were rendered devoid of moisture on their surface and their weight was measured. Subsequently, the specimens were placed within a receptacle and subjected to a boiling process lasting 300 minutes, followed

by a cooling period of 900 minutes. Finally, Surface dry weight was measured as well as the apparent mass in water.



Figure 22: Boiled specimens for water absorption.

### **3.5.5 Drying Shrinkage**

Drying shrinkage of SCM was done according to ASTM C596-18, the procedure was as follows: first, two beams of (40 squared x 160 mm length) for each mix were cut in half to have four specimens of (40 squared x 80 mm length). Then pins were stuck to the specimens by super glue and water cured for almost 72 hours. Later, the specimen was allowed to dry, and measurements were taken for 56 days.



Figure 23: Measuring drying shrinkage

### **3.5.6 Heat Exposure Resistance at 100 and 200 Degrees Centigrade**

Testing SCM specimens for the elevated temperature of 100 and 200 °C was done according to (Yamanel et al., 2019). Three 100mm cubes were subjected to a temperature increase of 5 °C per minute in an oven until the desired temperature was reached. The cubes were subsequently left in the oven for a duration of one hour. Following the exposure to heightened temperature, the oven was deactivated, and the cubes were permitted to undergo a cooling process within the oven until reaching ambient temperature. After cooling, specimens were subjected to a stereo microscope where cracks were detected. Then, UPV, Schmidt hammer, and compressive strength were applied.



Figure 24: Testing specimens for elevated temperature

### **3.5.7 Cracks Detection**

Following the cooling of SCM specimens to ambient temperature, a stereo microscope was used to detect the cracks as result of exposure to elevated temperatures. Firstly, the microscope lenses were calibrated using special calibration ruler at different levels, then cracks were detected and measured.



Figure 25: Stereo microscope

### **3.5.8 Evaluation of the Specimen's Hardness**

Mortar's hardness is evaluated using the Schmidt hammer test. ASTM C 805/C805M-18 is the standard that was employed in this experiment to measure the specimen's compressive strength. The 100 mm-cubic sample was used for the experiment after 28 days. First, after hitting the cubes' surface with the hammer, an average of ten results was determined. The numbers that are six units or more above the mean are disregarded. The bound number was then determined by averaging the remaining numbers.



Figure 26: Schmidt hammer.

### **3.5.9 Assessing Material Integrity with UPV**

This experiment followed ASTM C597-22 guidelines. For this experiment, 100mm-diameter cubes were employed. The calibration of the instrument was performed at the onset of the experiment. In order to optimize the outcomes, the transducers were lubricated with petroleum jelly and subsequently positioned at the center of every face of the mortar specimens, precisely opposite to each other. Subsequently, the duration of the travel was assessed and recorded. The device being used is illustrated in Figure 27.



Figure 27: Pundit Device

## **Chapter 4**

### **RESULTS AND DISCUSSION**

#### **4.1 Outline**

For an examination of how MD influences the performance and characteristics of SCM, this chapter presents experimental data for twelve different SCM combinations. The tests for workability, setting time, air content, compressive, flexural, and split tensile strengths, water absorption, drying shrinkage, and heat resistance were assessed using UPV, Schmidt hammers, compressive strength, and crack detection due to elevated temperatures. This chapter examines the results from these experiments, which are displayed in tabular format and illustrated in figures for better clarity and comprehension.

#### **4.2 Impact of MD on SCM's Workability**

According to the guidelines of EFNARC (Specification and Guidelines for Self-Compacting Concrete., 2002) workability of SCM is assessed by both mini-cone, and mini v-funnel with mentioned ranges. However, according to (Safi et al., 2015), (Horsakulthai., 2021), and (Chu et al., 2022). Using only the slump flow is sufficient to test the workability, as well as, achieving the self-compactibility.

The mini-slump test was utilized to assess the workability of SCM with various cement replacements by MD of 0%, 5%, 10%, 15%, 20%, and 30%. Relative slump results are shown in Figures 28, and 29 for normal and high-strength SCM.

It is obvious from Figures 28 and 29 that for normal and high-strength SCM increasing the MD portions reduced the relative slump values  $\Gamma_m$ . All twelve series were in the range suggested by EFNARC. However, only NSCM30 exhibited the lowest relative slump value, which was the lowest limit suggested by EFNARC. Similar findings on the effects of MD on SCM and SCC were found by (Güneyisi et al., 2009) and (Boukhelkhal et al., 2016). The observed decline in relative slump values is due to the MD smaller particle size in comparison to the cement led to a rise in the mixture's fineness. Therefore, it is probable that the requirement for water in the mixture will rise. Figure 30 depicts the average cross-pounding diameter values of the slump flow.

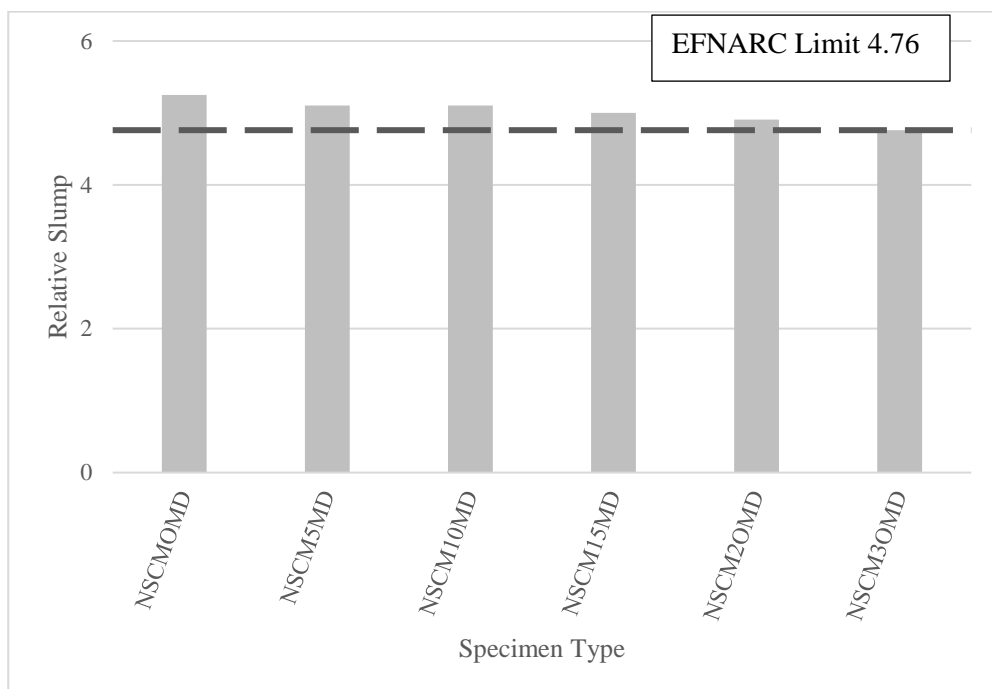


Figure 28: Effects of MD on NSCM relative slump

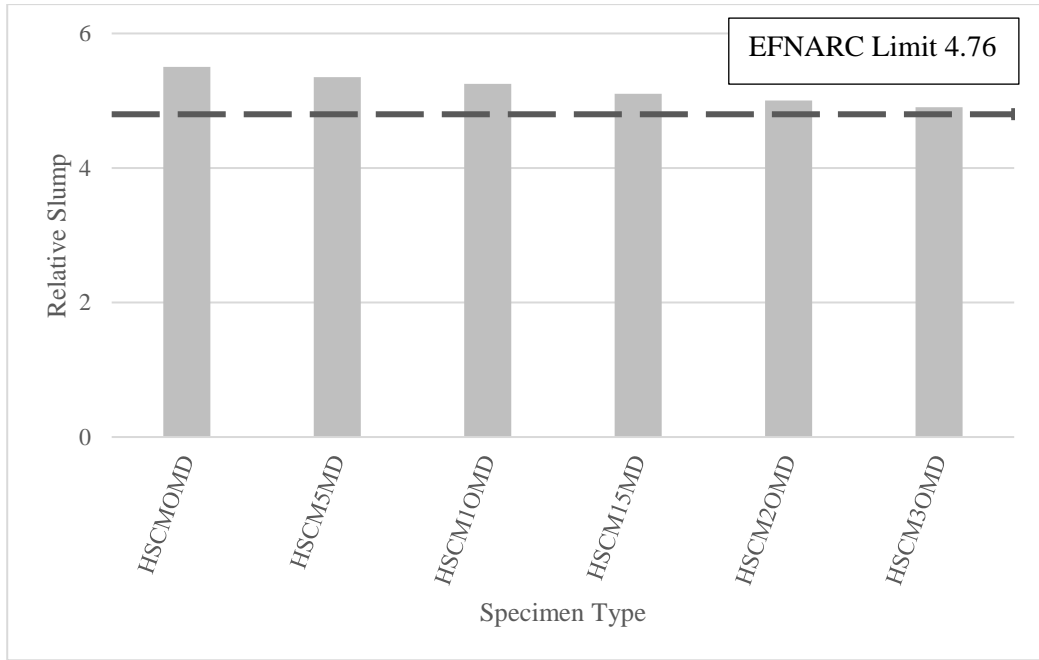


Figure 29: Effects of MD on HSCM relative slump

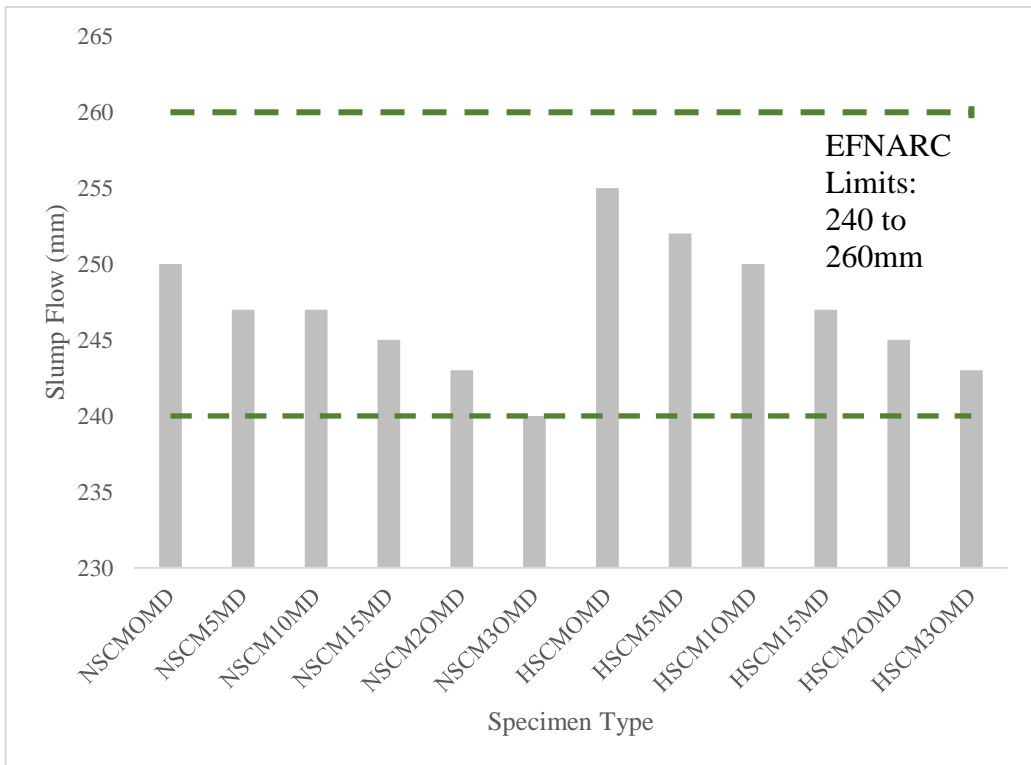


Figure 30: Effects of MD on NCM and HSCM slump flow

### **4.3 Impact of MD on SCM's Flow Rate**

The flow rate or the viscosity of the SCM was evaluated similar to (Libre et al., 2008) and (Jawahar et al., 2013). The flow time results of SCM are illustrated in Table 6.

The impact of mineral admixtures (MD) on flow rate appears to be consistent with that of slump flow, for both normal and high strength SCM series. The time  $T_{20}$  for the NSCM series ranges from 9.59 to 10.25 seconds. In comparison, HSCM series exhibited slightly lower flow times ranging from 8.62 to 9.11 seconds. This difference could be explained by HSCM series having a lower sand-to-paste ratio than the normal strength series. The increase in flow time for both series is a result of the MD's smaller particle size, which leads to increased water need in the mixture, subsequently reducing the flowability of the mix.

The consistency retention of the SCMs was evaluated by determining the  $T_{20}$  after 60 minutes. The findings presented in Table 6 revealed a marginal decrease in both slump flow and  $T_{20}$ . Despite this, almost all mixtures satisfied the slump flow requirements recommended by EFNARC, with the exception of NSCM30MD, which exhibited a flow of 238mm, below the lower limit. besides, no visual bleeding occurred for all mixes. The observed effect may be ascribed to an adequate dosage of superplasticizers, which prevents the segregation of mix.

Table 6: Flow rate consistency retention of SCM

MIX NO	Initial		After 60 min	
	Slump Flow (mm)	T <sub>20</sub> (sec)	Slump Flow (mm)	T <sub>20</sub> (sec)
NSCMOMD	250	9.59	248	9.47
NSCM5MD	247	9.73	247	9.61
NSCM10MD	247	9.81	245	9.63
NSCM15MD	245	9.89	244	9.7
NSCM20MD	243	10.2	242	10.07
NSCM30MD	240	10.25	238	10.13
HSCMOMD	255	8.62	254	8.51
HSCM5MD	252	8.76	252	8.69
HSCM10MD	250	8.87	248	8.79
HSCM15MD	247	8.96	246	8.89
HSCM20MD	245	9.07	242	8.91
HSCM30MD	243	9.11	240	9.01

#### 4.4 Impact of MD on SCM's Air Content

The amount of air in SCMs was evaluated by an air meter, which was tested for two series of high and normal strength SCM, with MD replacement fractions of 0, 5, 10, 15, 20, and 30%. The results of air content for both series are illustrated in Figures 31 and 32, in addition, air content losses for both series are demonstrated in Table 7.

Figure 31 shows the effects of MD on the NSCM, the air content values for MD replacement of 0%, 5%, 10%, 15%, 20%, and 30% by cement are 3.90, 3.00, 2.30, 2.15, 1.90, and 1.65%. Moreover, Figure 32 shows the results of HSCM which are 3.50, 2.80, 2.00, 1.75, 1.70, and 1.55%. Besides, according to Table 7, both NSCM and HSCM exhibited almost similar air content loss compared with the reference mix.

In concrete or mortar, adding more water might result in more air being incorporated into the mix since extra water tends to leave more spaces for air to fill. (Mora-Ortiz et al. 2021) found a decent linear relation between air content and water-to-binder ratio with values of  $R^2 = 0.93$  which is close to 1.0, the results of the correlation demonstrate that air content is increasing linearly with an increment of w/c ratio, similarly, in this study, NSCM with w/c ratio of 0.50 exhibited higher air content than HSCM with w/c of 0.38.

Due to its varied particle size, marble slurry contributes to the provision of a denser and more compact mix. This is demonstrated by the reduction in (%) air content for both series, which demonstrated a declining trend. Similar to (Singh et al., 2017) for the air content of concrete, the MD's smaller particle size increased the mix's surface area and decreased the amount of room available for air bubbles to develop and solidify. This was ascribed to the marble dust's finer particle size.

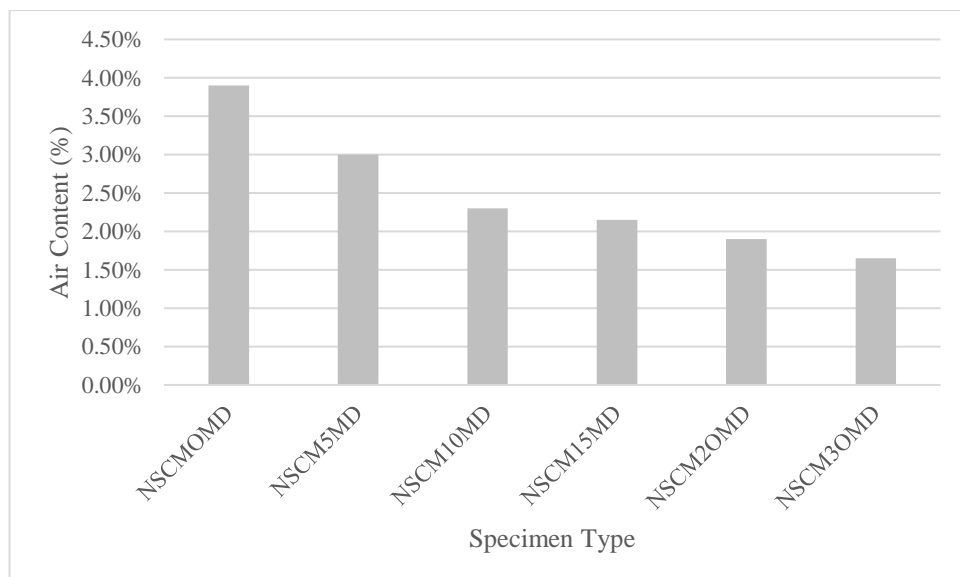


Figure 31: NSCM air content

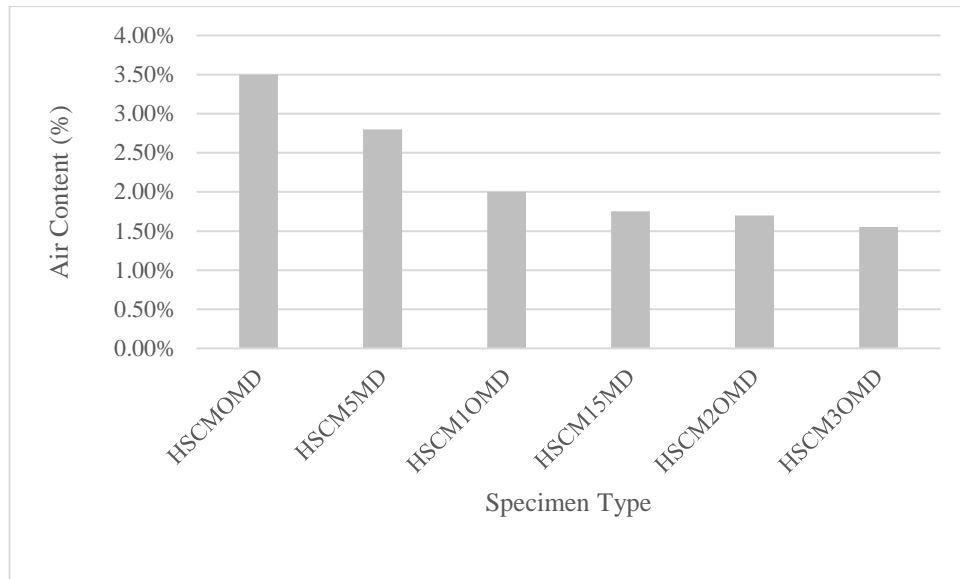


Figure 32: HSCM air content

Table 7: Air content loss for both NSCM and HSCM

Mix No	Air Content (%)	Air Content Loss (%)
NSCMOMD	3.90%	0.0
NSCM5MD	3%	-23.1
NSCM10MD	2.30%	-41.0
NSCM15MD	2.15%	-44.9
NSCM20MD	1.90%	-51.3
NSCM30MD	1.65%	-57.7
HSCMOMD	3.50%	0.0
HSCM5MD	3%	-20.0
HSCM10MD	2.00%	-42.9
HSCM15MD	2%	-50.0
HSCM20MD	1.70%	-51.4
HSCM30MD	1.55%	-55.7

#### 4.4.1 Air Content and Slump Flow Correlation

Regression analysis using a linear regression factor was utilized to find a correlation between the air content and slump flow of both SCM series. Figures 33 and 34

illustrate the relationship between Air content and slump flow for NSCM and HSCM.

Both Figures showed that the flow diameter rises with increasing air content values.

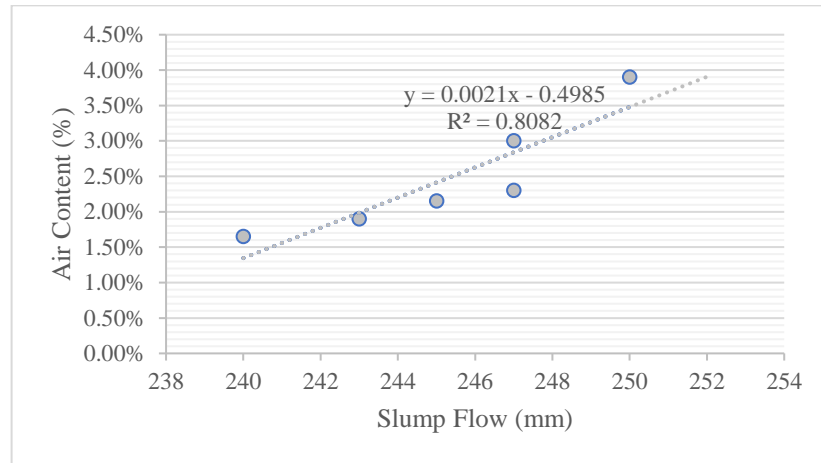


Figure 33: NSCM air content and slump flow relationship

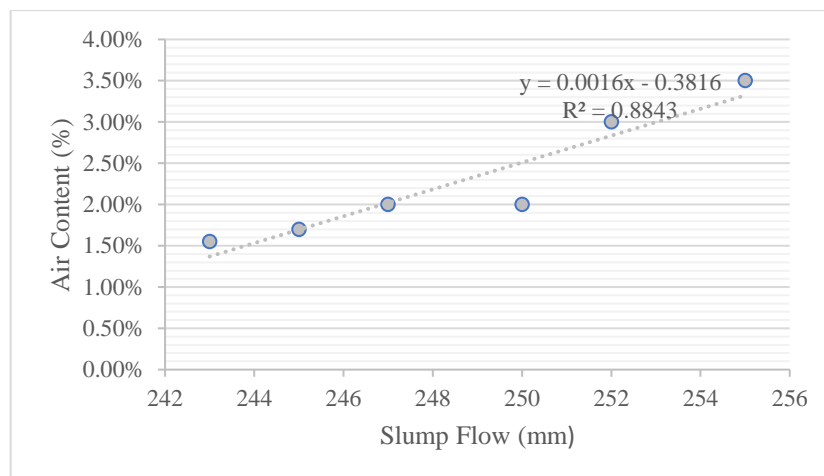


Figure 34: HSCM air content and slump flow relationship

#### 4.4.2 Air content and Flow Rate Correlation

Regression analysis using a linear regression factor was utilized to find a correlation between the air content and flow rate of both SCM series. Figures 35 and 36 displays the linear correlation between air content and flow rate ( $T_{20}$ ) for normal and high strength SCM. As seen from the Figures both normal and high SCM exhibited strong relation, HSCM showed stronger correlation with regression coefficient  $R^2$  of 0.93

comparing to NSCM with regression coefficient  $R^2$  of 0.79. To sum up, increasing the air content of SCM leads to the flow time ( $T_{20}$ ) to decrease.

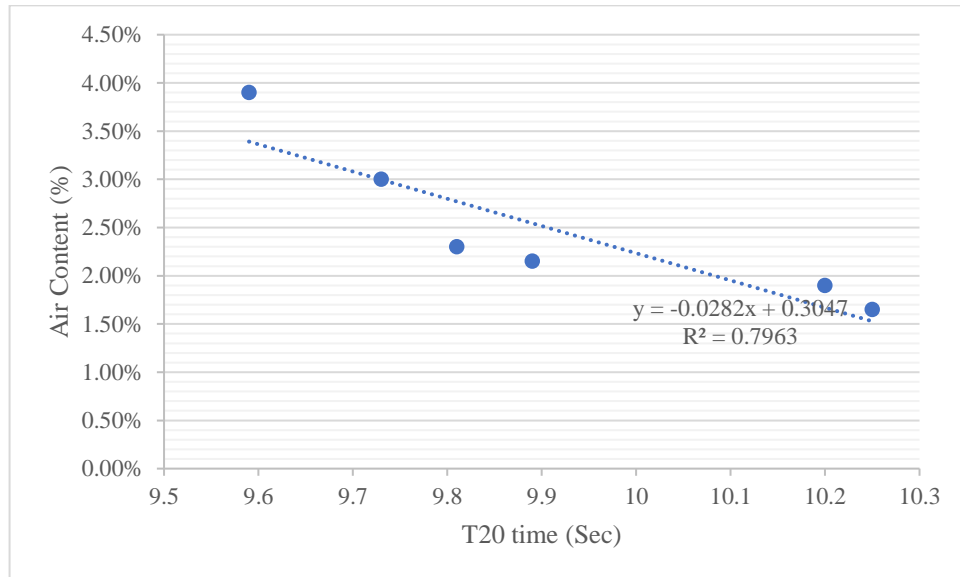


Figure 35: NSCM air content and flow rate relationship

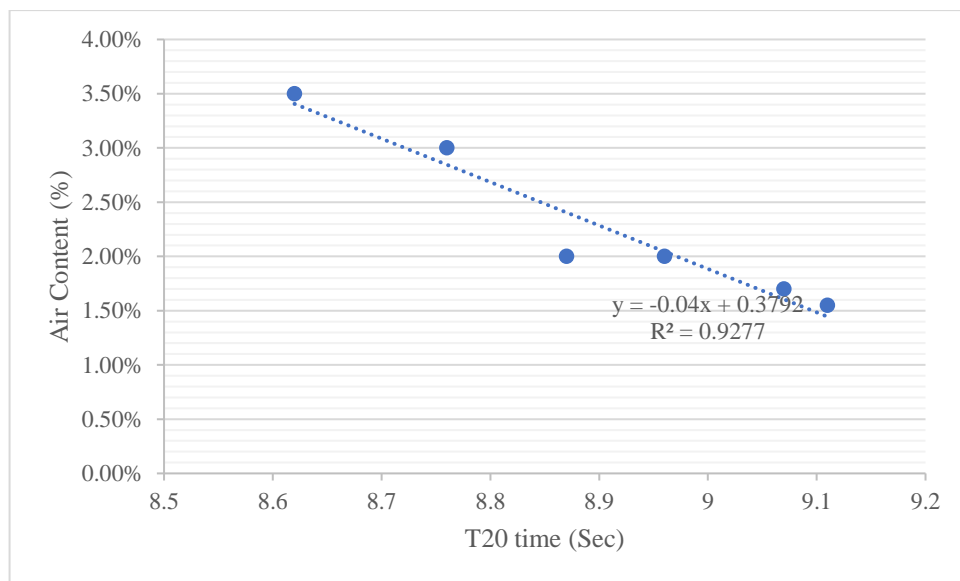


Figure 36: HSCM air content and flow rate relationship

#### 4.5 Impact of MD on SCM's Setting Time

Both setting times for normal and high-strength SCM are illustrated in Figures 37 and 38, respectively. As seen from Figure 37, the initial setting times of normal strength

SCM with MD replacement of 0%, 5%, 10%, 15%, 20%, and 30% by cement are 439, 443, 472, 495, 555, and 615 minutes, respectively. Moreover, the final setting times for these replacement percentages are 771, 786, 806, 841, 895, and 954 minutes, respectively.

Figure 38 presents the both setting times of HSCM series. The initial setting times for MD replacement of 0%, 5%, 10%, 15%, 20%, and 30% by cement are 388, 395, 414, 451, 478, and 532 minutes, respectively. In addition, the final setting times for these replacement percentages are 685, 695, 737, 781, 807, and 866 minutes, respectively.

The replacements of cement by marble powder have increased both setting times for all SCM mixes. For NSCM series, the initial setting time was prolonged by 3%, 8%, 13%, 26.5%, and 40%, while the final setting time was prolonged by 2%, 5%, 9%, 16%, and 23.75%. Similarly, for high strength SCM mixes, the initial setting time was extended by 1.80, 6.70, 16.24, 23.20, and 37.11%, while the final setting time was extended by 1.46, 7.59, 14.01, 17.81, and 26.42%. Similar results were found by (Gesoglu et al., 2012) while testing setting time for SCC.

The prolongation of the setting times can be attributed to the reduced dimensions of the MD particles, which causes the SCM to have a higher water demand. The escalated requirement for water is due to minute marble powder particles that occupy the empty spaces within the mortar mixture, which affects the flowability and workability of the mixture, and causing it to take longer to set and harden. Moreover, as observed from the results that HSCM series exhibit lower setting times than the NSCM series, This can be attributed to lower the water amount in the cement, which has been shown to

accelerate the process of cement hydration. Additionally, a decrease in the amount of superplasticizer used may have also contributed to this effect.

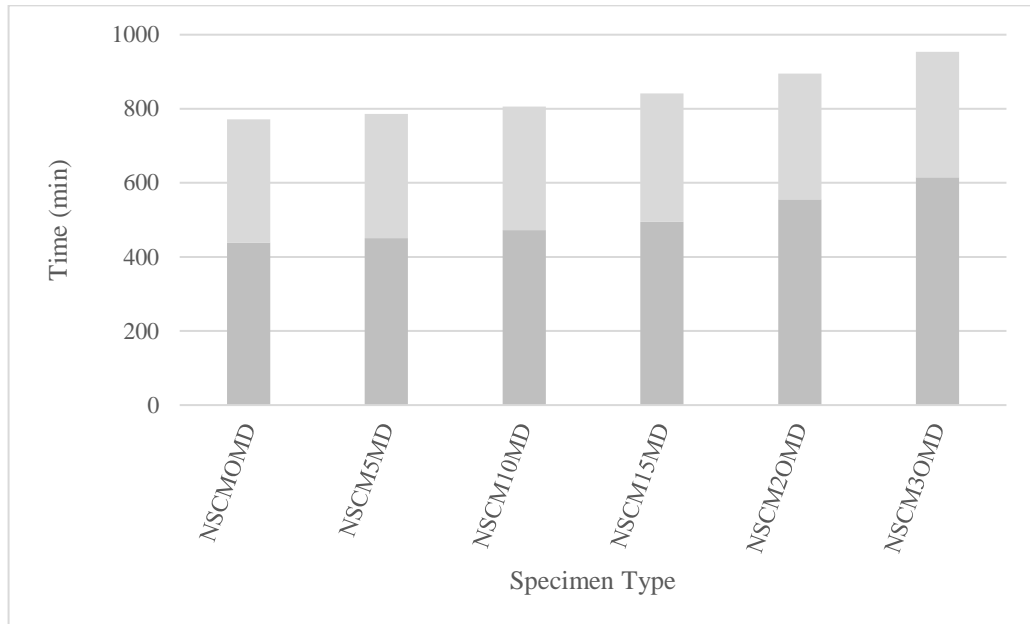


Figure 37: Setting time of NSCM

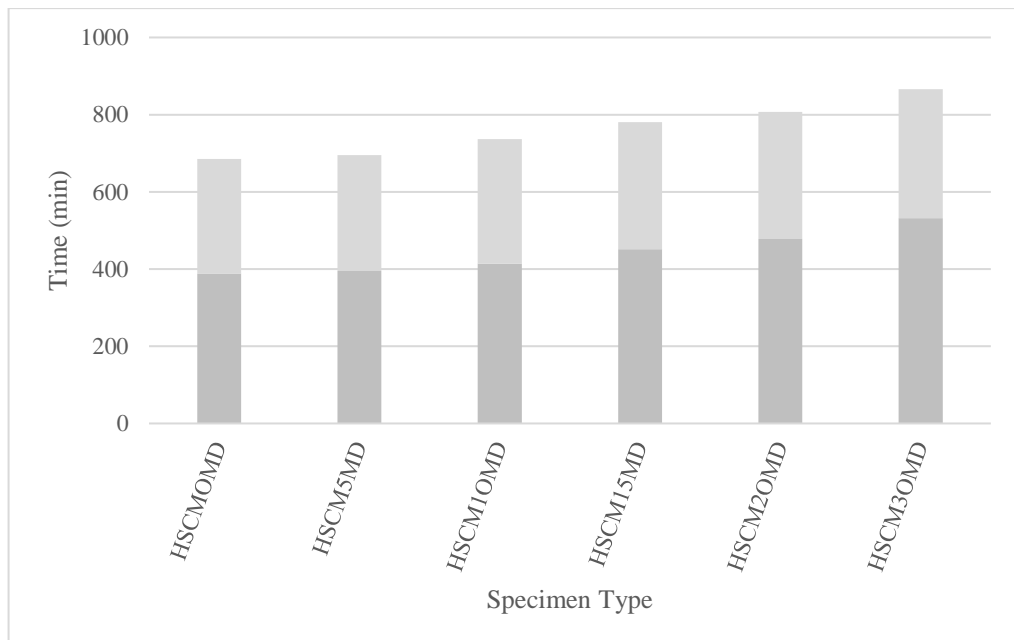


Figure 38: Setting time of HSCM

#### 4.6 Impact of MD on SCM's Unit Weight

The unit weight of SCM was tested for both 7 and 28 curing days, the test was done on (150mm) cubes, when testing the cubes for compressive strength, the cubes were first surface dried by a towel, then the by electronic balance with accuracy of 0.001g, the weight of cubes were measured. The unit weight of each cube was determined by dividing its weight by its volume. The effects of MD on both NSCM and HSCM series are illustrated in Figures 39 and 40.

As can be observed that increasing the MD portions for both NSCM and HSCM series, the unit weight of the SCM tends to decrease, as result of lower specific gravity of the MD. Similar to (Rashwan et al., 2020) in testing concrete unit weight, the finding confirms that increasing the MD portions, reduces the unit weight at both 7 and 28 days. Likewise, the findings are in the same context with study done by (Xi et al., 2019) on the cement mortar, the density were slightly reduced with increasing MD portions, for instance, 10% MD reduced the density from 2152 to 2068 kg/m<sup>3</sup>.

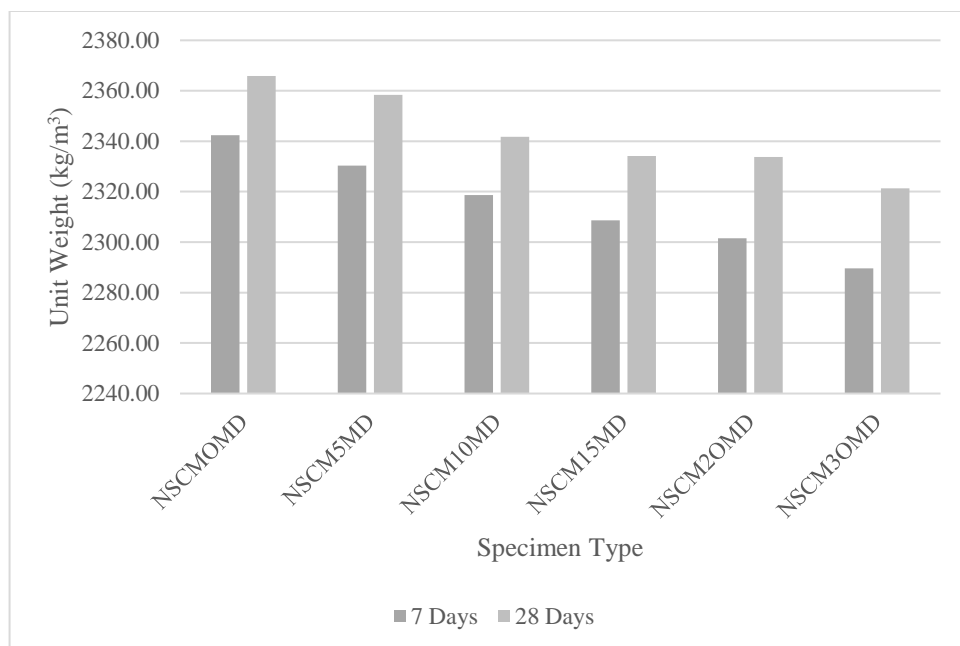


Figure 39: Effects of MD on unit weight of NSCM

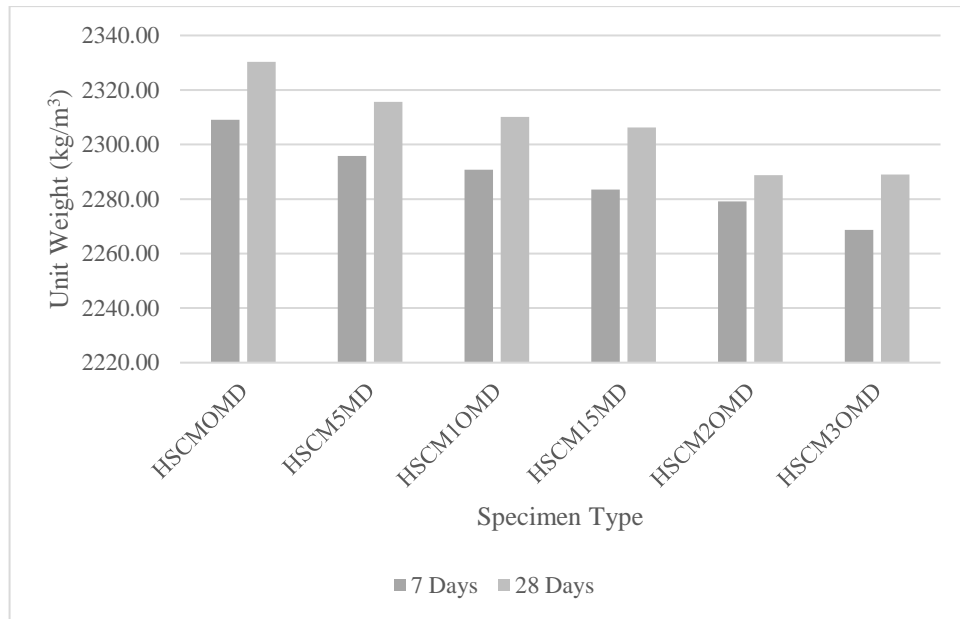


Figure 40: Effects of MD on unit weight of HSCM

#### 4.7 Impact of MD on SCM's Compressive Strength

The key variables that determine the compressive strength of mixture are the mix design, w/c, and aggregate qualities (type, size, shape, grading, and surface texture). The designed compressive strength in this study was 37, and 67 MPa for normal and high-strength SCM. The effects of MD on NSCM and HSCM are illustrated in Figures 41 and 42, respectively.

From Figure 41, as shown 28 days characteristic compressive strength was achieved successfully after the trials, increasing the MD portions in NSCM series decreased the compressive strength significantly, especially at early testing age. Late (28 and 56 days) compressive strength degradation has decreased, compressive strength losses of NSCM in percentages are illustrated in Table 8.

Similarly, from Figure 42 for the HSCM, the 28 days characteristic compressive strength was also almost achieved. The control mix showed a 66.2 MPa which is close

to the designed strength. Using MD as CRM in HSCM has similar impact as NSCM. Increasing the MD portions led to higher reduction in compressive strength results. The SCM samples latter age strength at 28 and 56 days up to 10% MD is less reduced. This can be explained by balancing the strength loss due to replacing the cement with non-pozzolanic material by filling effect of MD particles. However, beyond the 10%, the 28- and 56-days' compressive strengths compared with control mixtures start to decrease drastically when raising the MD portions. This is due to the Cement Substitution by non-pozzolanic dust, leading to the attenuation of  $C_3S$  and  $C_2S$ , the primary contributors to strength enhancement. Compressive strength losses of HSCM in percentages are illustrated in Table 9.

Founding results are similar to study results done by (Güneyisi et al., 2009), since using MD as CRM with ranging portions of 5 to 20%. Results showed an inverse relationship was observed between increasing MD portions and compressive strength reduction. This could be explained by the reduction in cementing materials "dilution". Given that marble powder is primarily composed of  $CaCO_3$ , the dilution of the pozzolanic processes may also be to blame for the mortars containing MD losing their compressive strength.

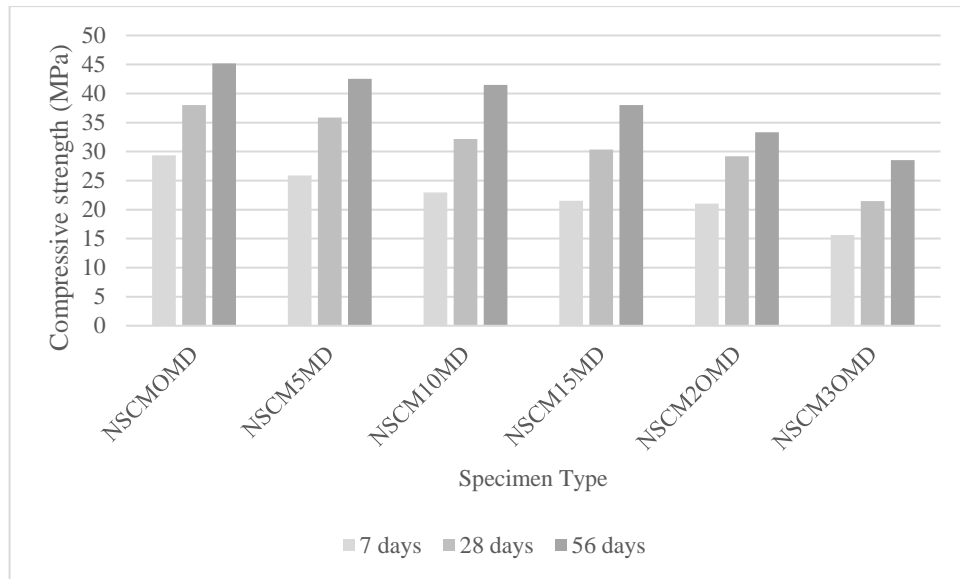


Figure 41: Compressive strength results for NSCM

Table 8: NSCM compressive strength loss

Mix No	Results at 7 Days	Reduction (%)	Results at 28 Days	Reduction (%)	Results at 56 Days	Reduction (%)
NSCM0MD	29.3	0.0	38.0	0.00	45.2	0.0
NSCM5MD	25.9	-11.6	35.9	-5.53	42.5	-5.9
NSCM10MD	23.0	-21.7	32.2	-15.26	41.5	-8.2
NSCM15MD	21.6	-26.5	30.4	-20.00	38.0	-15.9
NSCM20MD	21.0	-28.3	29.2	-23.16	33.3	-26.3
NSCM30MD	15.6	-46.8	21.5	-43.42	28.5	-36.9

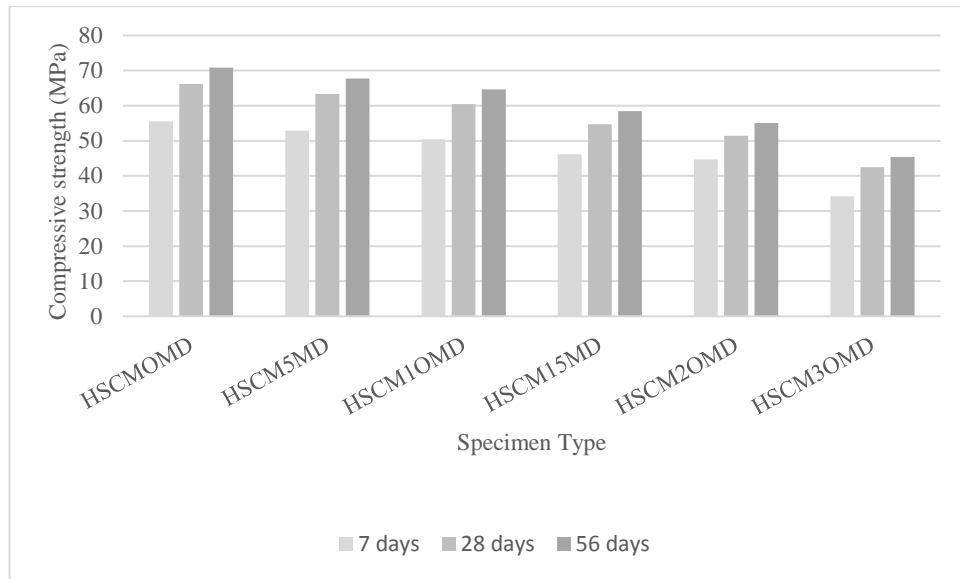


Figure 42: Compressive strength results for HSCM

Table 9: HSCM compressive strength loss

Mix No	Results at 7 Days	Reduction (%)	Results at 28 Days	Reduction (%)	Results at 56 Days	Reduction (%)
HSCMOMD	55.5	0.0	66.2	0.00	70.8	0.0
HSCM5MD	52.8	-4.8	63.3	-4.38	67.8	-4.3
HSCM10MD	50.4	-9.2	60.4	-8.76	64.6	-8.7
HSCM15MD	46.1	-16.9	54.7	-17.37	58.5	-17.4
HSCM20MD	44.7	-19.5	51.4	-22.36	55.0	-22.2
HSCM30MD	34.2	-38.4	42.5	-35.80	45.4	-35.8

#### 4.8 Impact of MD on SCM's Splitting Tensile Strength of SCM

To evaluate how MD affects SCM splitting tensile strength, an average of three cylindrical specimens for each testing period with dimensions of 200 x 100 mm, were tested for the NSCM and HSCM series on 7 and 28 days, respectively.

Figures 43 and 44 show the effects of MD on NSCM and HSCM series, while Tables 10 and 11 indicate the percentage reduction in tensile strength. As illustrated in Figures, both series exhibited almost similar declining trend as compressive strength,

at 5% MD showed insignificant change in tensile strength of both series, the losses in tensile strength for NSCM and HSCM series were 11.66 and 7.77% at 7 days, while on lateral ages (28 day) the losses tends to decrease to 8.1 and 3.3% this could be attributed to balancing the strength loss due to replacing the cementing materials with MD which consists of calcite by the micro filler effect of marble dust. Beyond 5 % strength losses tend to increase with increasing MD portions. The findings are in line with a study on the impact of MD on SCC by (Boukhelkhal et al., 2016), who suggested that an ideal replacement level for MD cement would be 5%. They discovered that 5% substitution showed almost similar strength values compared with control SCC.

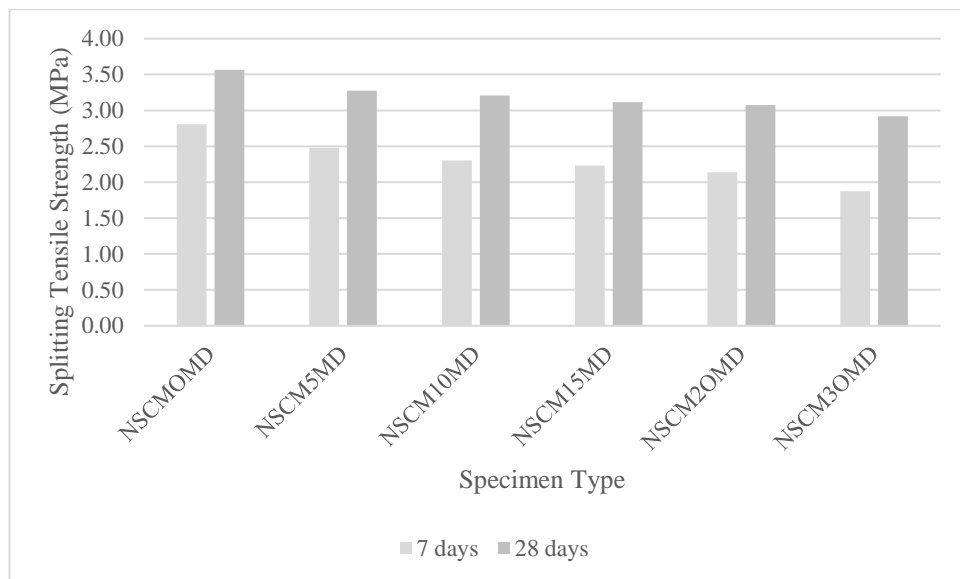


Figure 43: Effects of MD on splitting tensile strength of NSCM

Table 10: Splitting tensile strength results for NSCM series

Mix No	Splitting tensile strength (MPa) At 7 days	Loss (%)	Splitting tensile strength (MPa) At 28 days	Loss (%)
NSCMOMD	2.81	0.00	3.56	0.00
NSCM5MD	2.48	-11.66	3.27	-8.09
NSCM10MD	2.31	-17.83	3.21	-9.89
NSCM15MD	2.23	-20.41	3.11	-12.60
NSCM20MD	2.14	-23.73	3.07	-13.69
NSCM30MD	1.88	-33.16	2.92	-18.09

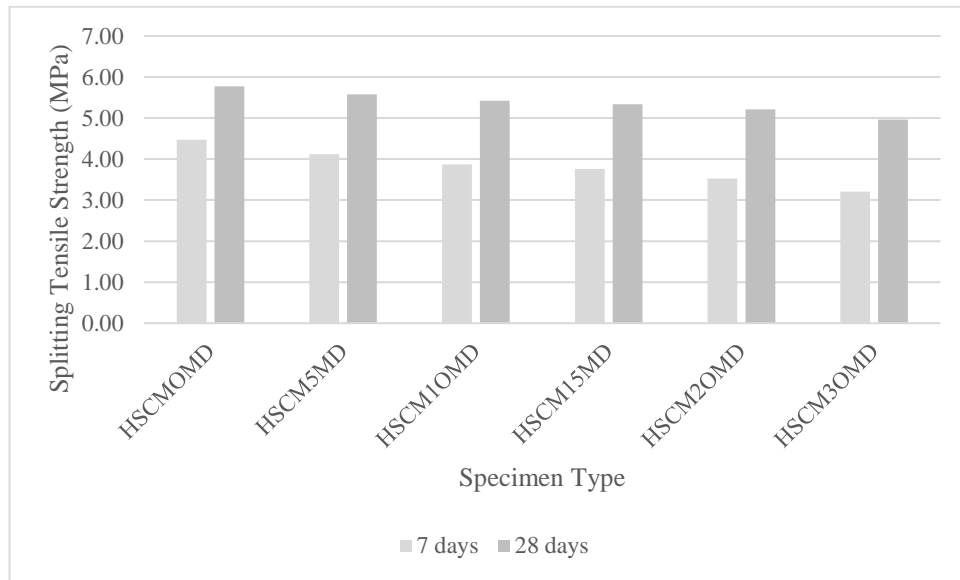


Figure 44: Effects of MD on splitting tensile strength of HSCM

Table 11: Splitting tensile strength results for HSCM series

Mix No	Splitting tensile strength (MPa) At 7 days	Loss (%)	Splitting tensile strength (MPa) At 28 days	Loss (%)
HSCMOMD	4.47	0.00	5.77	0.00
HSCM5MD	4.12	-7.77	5.58	-3.29
HSCM10MD	3.87	-13.36	5.42	-6.07
HSCM15MD	3.76	-15.83	5.34	-7.45
HSCM20MD	3.53	-20.98	5.21	-9.71
HSCM30MD	3.21	-28.14	4.96	-14.04

#### 4.8.1 Splitting Tensile and Compressive Strengths Correlation

Splitting tensile and compressive strengths were correlated using the linear regression coefficient  $R^2$ . The less dispersion there is, the closer the value of  $R^2$  is to 1.00. Figures 45 and 46 demonstrate linear relationship between the types of strength for normal NSCM and HSCM on 28 days. Both SCM series showed high regression coefficient  $R^2$  of 0.86 and 0.96. Analysis revealed that both Strengths values of SCM found to be directly proportional.

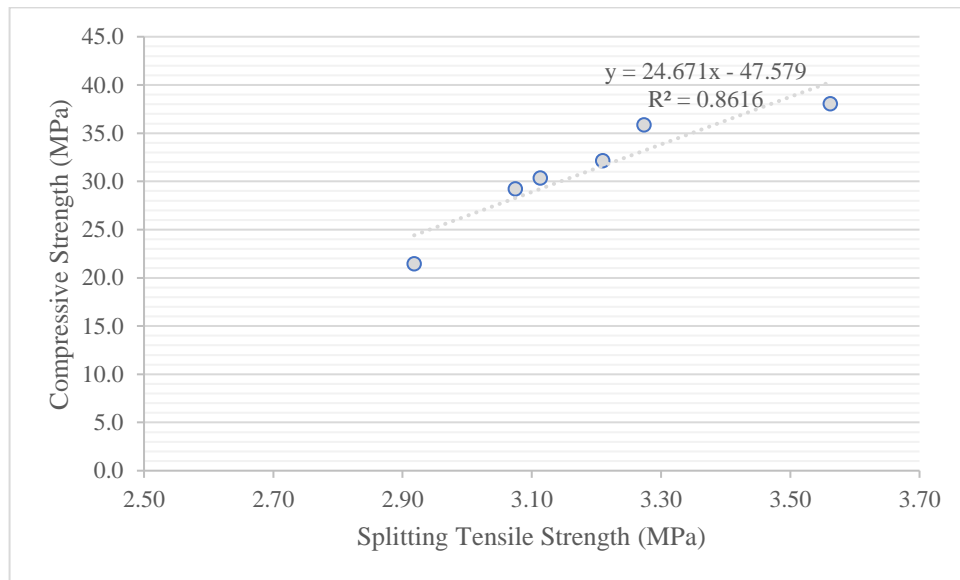


Figure 45: Splitting tensile and compressive strengths relationship for NSCM

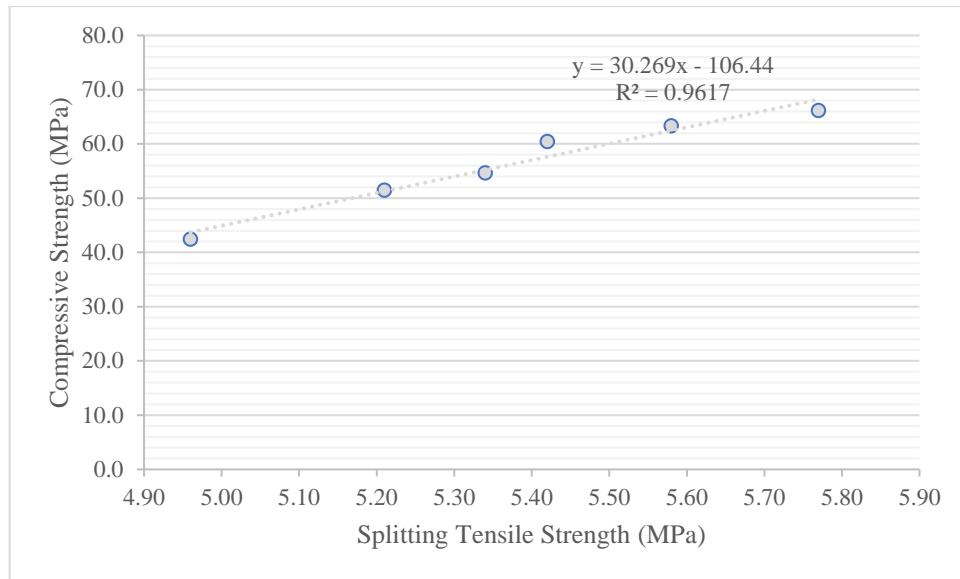


Figure 46: Splitting tensile and compressive strengths relationship for HSCM

#### 4.9 Effects of MD on Flexural Strength of SCM

An average of 3 beams measuring 40x 40x160 mm for each testing period were employed to test the splitting tensile strength of NSCM and HSCM series on 7 and 28 days.

Both Figures 47 and 48 demonstrate flexural strength results. Besides, the effects of MD on both series are explained by the loss in percentages in Tables 12 and 13 for both testing periods of 7 and 28 days. Similar to compressive and tensile strengths, the lowest reduction in flexural strength was noticed in 5% replacement of cement by MD in both normal and high strength SCM series. The reduction of flexural for 5% MD of both series were 4.45 and 3.30 % at 7 days, while in lateral ages 28 days the reduction has decreased to 2.20 and 1.38% for normal and high strength SCM series. Moreover, replacing the cement with 10% MD showed slight reduction compared to 5%MD, the reduction percentages were 2.75 and 6.83% for NSCM and HSCM series. Further increase in MD has inverse impact on the flexural strength values. The reduction in flexural could be attributed in strength loss due to MD doesn't exhibit pozzolanic

reaction. Results were similar to study done by (Topçu et al., 2009) on SCC, flexural strength results for replacement of cement by 5% MD were almost same.

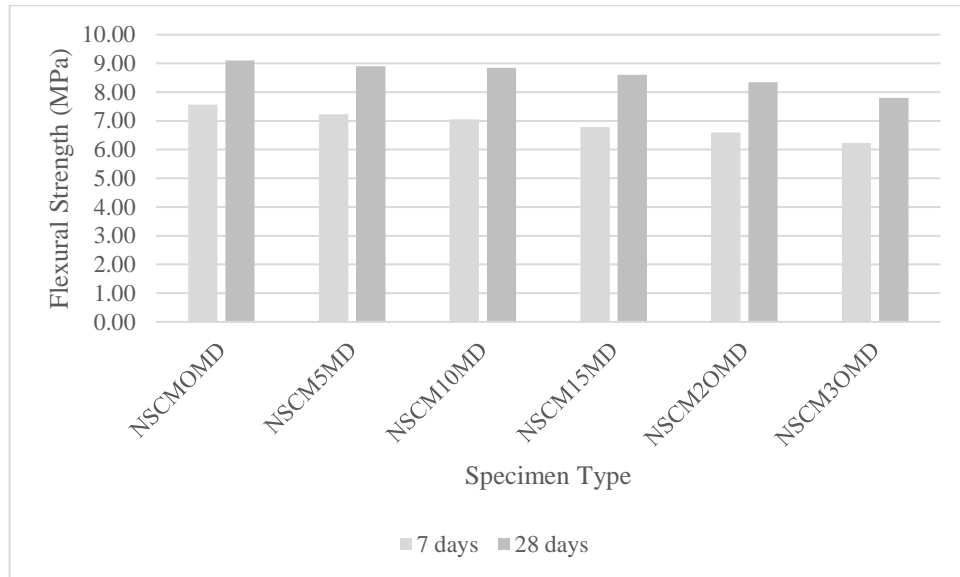


Figure 47: Effects of MD on flexural strength of NSCM

Table 12: Flexural strength results for NSCM series

Mix No.	7 days flexural strength (MPa)	Loss (%)	28 days flexural strength (MPa)	Loss (%)
NSCM0MD	7.57	0.00	9.10	0.00
NSCM5MD	7.23	-4.45	8.90	-2.20
NSCM10MD	7.05	-6.83	8.85	-2.75
NSCM15MD	6.78	-10.40	8.60	-5.49
NSCM20MD	6.59	-12.91	8.35	-8.24
NSCM30MD	6.23	-17.67	7.80	-14.29

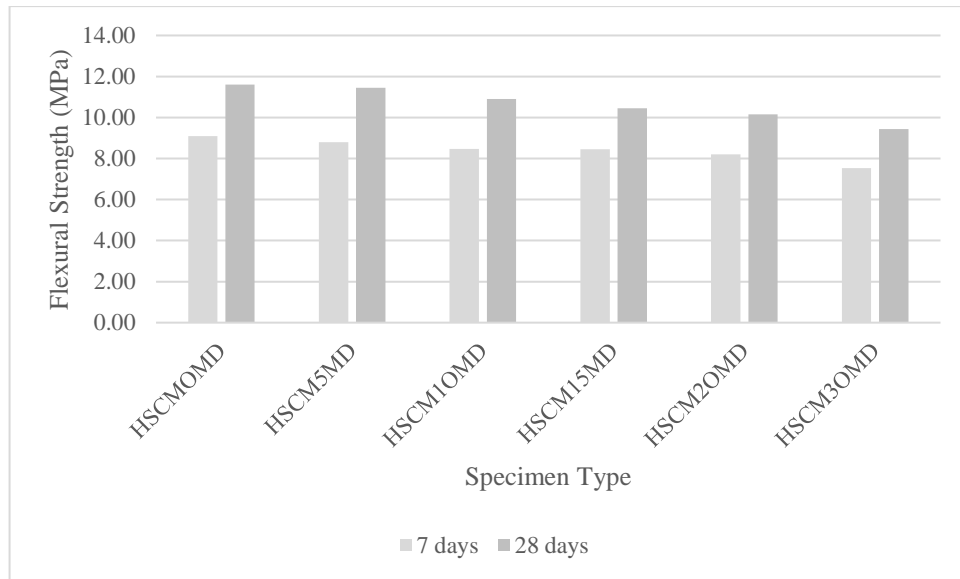


Figure 48: Effects of MD on flexural strength of HSCM

Table 13: Flexural strength results for HSCM series

Mix No.	7 days flexural strength (MPa)	Loss (%)	28 days flexural strength (MPa)	Loss (%)
HSCMOMD	9.10	0.00	11.61	0.00
HSCM5MD	8.80	-3.30	11.45	-1.38
HSCM10MD	8.47	-6.96	10.91	-6.03
HSCM15MD	8.45	-7.14	10.45	-9.99
HSCM20MD	8.20	-9.89	10.15	-12.58
HSCM30MD	7.53	-17.25	9.43	-18.78

#### 4.9.1 Compressive Strength and Flexural Strengths Correlation

Flexural and compressive strengths were correlated using linear regression coefficient  $R^2$ . Both strength values for NSCM and HSCM series are shown to be linearly related in Figures 49 and 50 for a duration of 28 days. The high regression coefficient  $R^2$  of 0.95 and 0.98 was seen in both SCM series. Analysis revealed that both Strengths values of SCM found to be directly proportional.

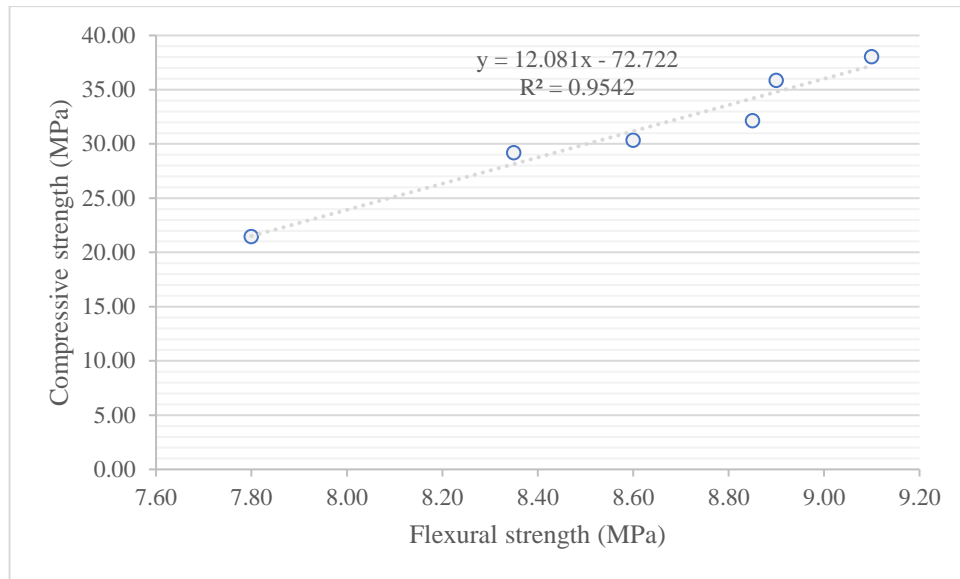


Figure 49: Compressive strength and flexural strength relationship for NSCM

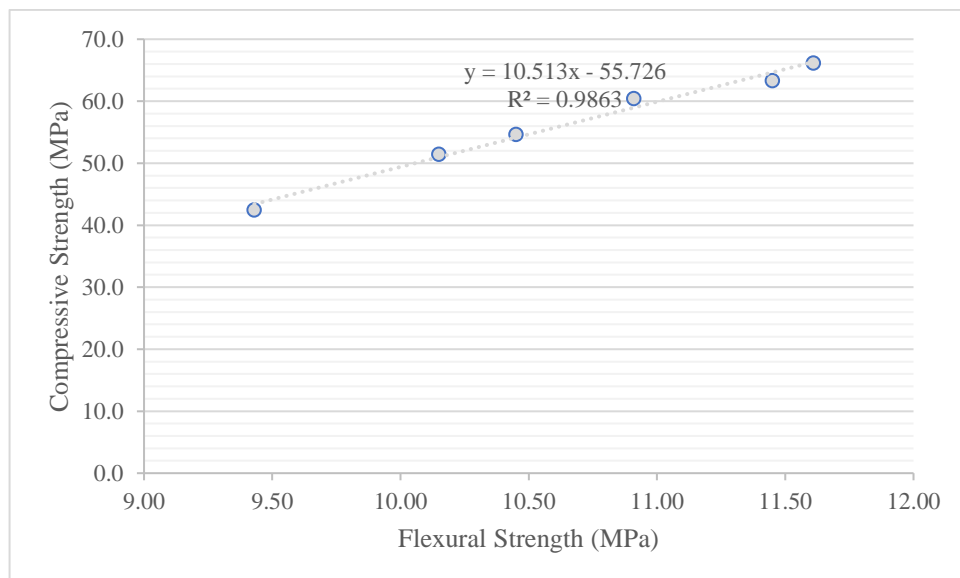


Figure 50: Compressive strength and flexural strength relationship for HSCM

#### 4.10 Impact of MD on SCM's Water Absorption

The pore structure of mortars has a considerable impact on their durability. Water absorption by immersion can be used to examine this characteristic. In accordance with ASTM C642-13, mortar cubic samples measuring 100 mm underwent water absorption tests. To do this, once the mortar samples had cured for 28 days, then following the standard the experimental procedure was done.

Figures 51 and 52 show how the water absorption by immersion before and after boiling varies for NSCM and HSCM mixes, Tables 14 and 15 show the results of absorption in percentage before and after boiling, and the volume of permeable voids are presented in numbers.

The observed data clearly show that increasing the MD increases water absorption. Replacement of cement by MD with portion of 5% showed slight increment in water absorption before boiling, more slight increment was noticed after boiling of the specimens. Likewise, 10% MD for both NSCM and HSCM series showed a bit higher water absorption than 5% MD and increased after boiling. Further increase in MD portions led the SCM specimens to have higher water absorption. As can be seen denser mixture was noticed for HSCM, in other words, lower water absorption values were found. This due to lower w/c ratio in the HSCM series as compared to the NSCM series, where higher w/c ratio results in a decrease in the ratio of gel volume to interstitial space, leading to an increase in porosity and a corresponding reduction in the strength of the mortar (Wongkeo et al., 2014).

After boiling the specimens, the increase in water absorption was sounded more in mixtures with portions greater than 10%, this could be attributed to lower quality SCM specimens, where replacing the cement with non-cementing material caused lower strength specimens, in addition to, lower C-S-H gel produced by hydration of cement. Thus, increasing the porosity of SCM specimens. This can be explained by the volume of permeable voids in Tables 14 and 15. Similarly, up to 10% MD the reduction in the voids was insignificant, beyond 10% the voids (%) tend to increase convergently with increasing the MD portions.

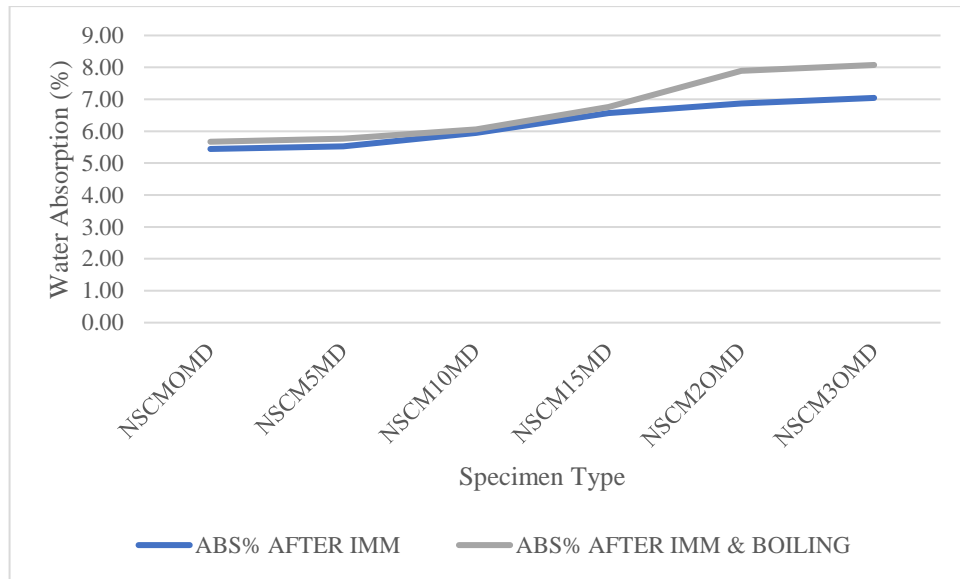


Figure 51: Effects of MD on water absorption of NSCM

Table 14: Effects of MD on water absorption and volume of permeable voids of NSCM

Mix No.	Absorption of SCM (%) After Immersion	Absorption of SCM (%) After Immersion and Boiling	Volume (%) of Permeable Voids
NSCM0MD	5.44	5.67	9.77
NSCM5MD	5.53	5.77	9.93
NSCM10MD	5.95	6.05	10.08
NSCM15MD	6.57	6.76	11.24
NSCM20MD	6.87	7.89	11.34
NSCM30MD	7.04	8.07	13.06

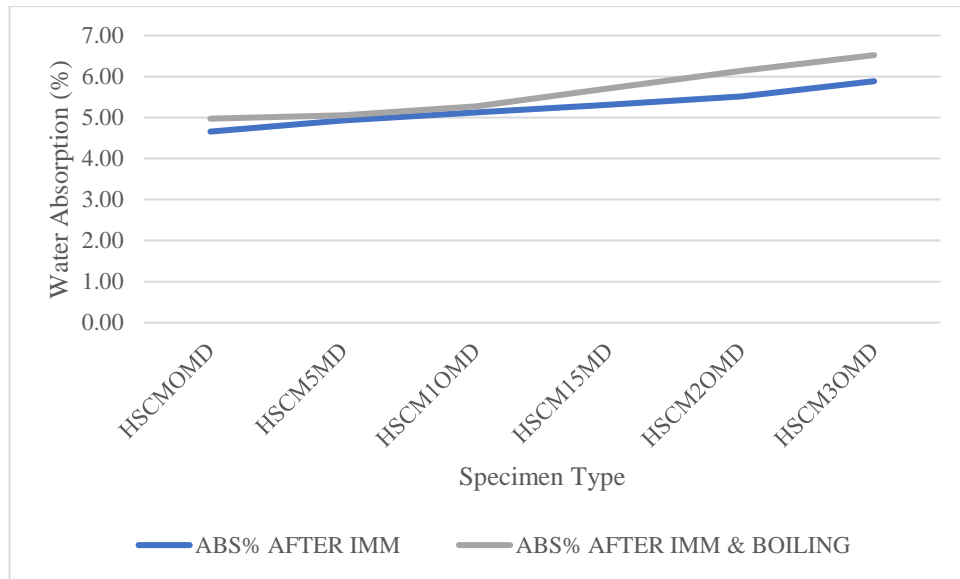


Figure 52: Effects of MD on water absorption of HSCM

Table 15: Effects of MD on water absorption and volume of permeable voids of HSCM

Mix No.	Absorption of SCM (%) After Immersion	Absorption of SCM (%) After Immersion and Boiling	Volume (%) of Permeable Voids
HSCM0MD	4.66	4.97	10.54
HSCM5MD	4.93	5.05	11.55
HSCM10MD	5.12	5.27	11.82
HSCM15MD	5.31	5.71	12.76
HSCM20MD	5.51	6.14	13.74
HSCM30MD	5.89	6.52	15.60

#### 4.10.1 Compressive Strength and Water Absorption Correlation

The linear regression type was utilized to evaluate the regression coefficient  $R^2$ . Figures 53 and 54 depict a declining trend for both NSCM and HSCM over a 28-day period. The high regression coefficient  $R^2$  of 0.96 and 0.91 was seen in normal and high strength SCM series. Analysis revealed that decreasing water absorption (%) tends to increase compressive strength of SCM.

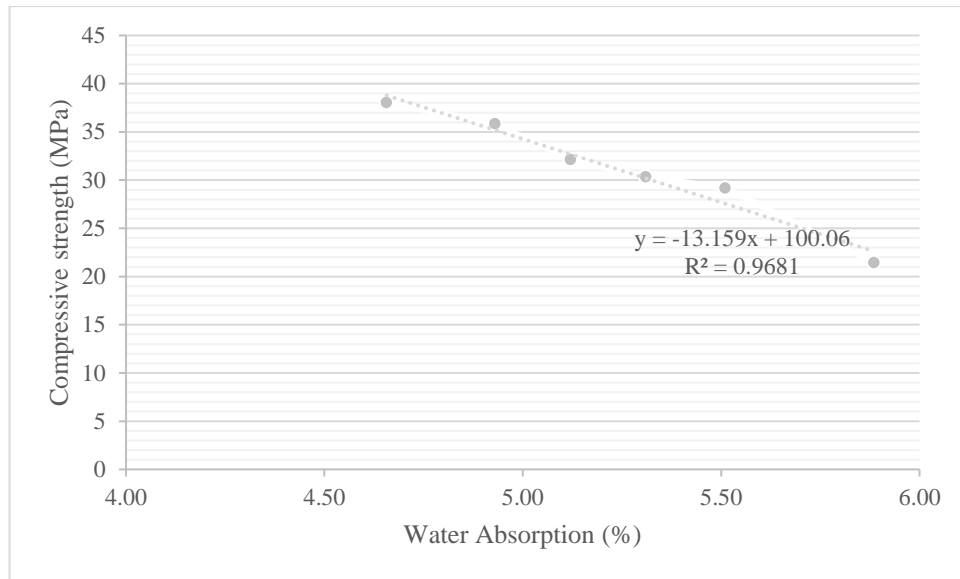


Figure 53: Compressive strength and water absorption relationship for NSCM

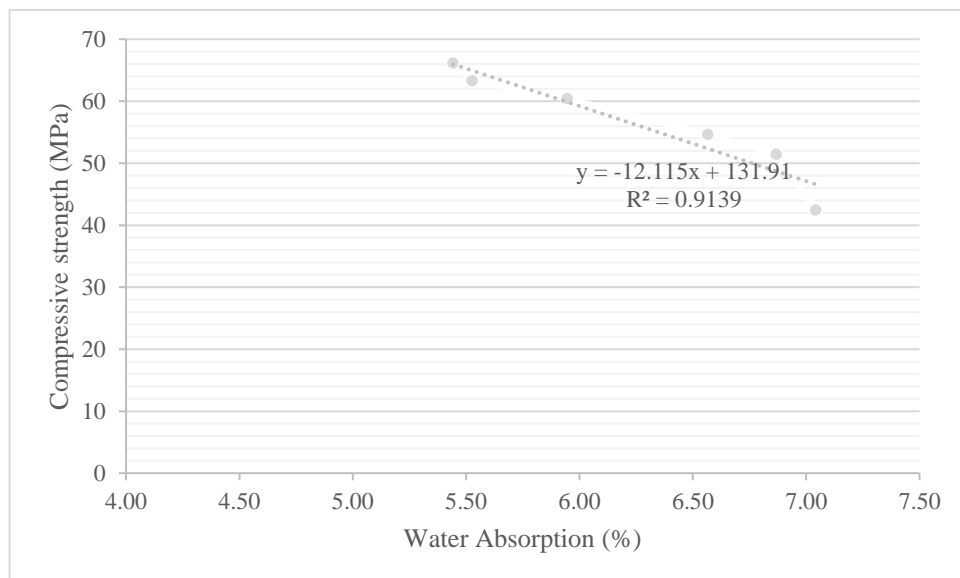


Figure 54: Compressive strength and water absorption relationship for HSCM

#### 4.11 Impact of MD on SCM's Heat Degradation (100 °C and 200 °C)

The study involved utilizing the mean value of three cubes measuring 100 mm to evaluate the effect of MD on NSCM and HSCM series under elevated temperatures. Both destructive and non-destructive tests, including the Compressive Strength Test, Schmidt Hammer, UPV Test, and Cracks Detection by Microscope, were carried out.

#### **4.11.1 Impact of MD on SCM's Compressive Strength After Heating**

To evaluate the compressive strength of SCM, an average of three 100 mm cubes for each heating pattern 100 and 200 °C were used, in addition to 150mm cubes were used to evaluate the strength at 20 °C. The effects of MD of NSCM and HSCM on compressive strength after heating are illustrated in Figures 55 and 56, besides, Tables 16 and 17 demonstrates the strength results and change due to heating of specimens.

The NSCM analysis results, as depicted in Figure 55 and Table 16, indicate a significant reduction in compressive strength as the MD portion and heating temperature increase. Control mix (0% MD) showed the lowest decrease in compressive strength at 100 °C approximately 3.00%, likewise, increased the heating temperature to 200 °C reduced the strength by almost 6.8%. in the presence of MD, the mixture denoted as NSCM5MD exhibited the least decrease in compressive strength, with reductions of approximately 8.1% and 21.5% observed at temperatures of 100 °C and 200 °C, respectively. Increasing the MD portion to 10% led to double the loss in compressive strength to 16.7% at 100 °C, and considerable increase in reduction at 200 °C to almost 28.5%. Up 15 % the compressive strength reduction in percentage at 100 °C was almost similar to the reduction at 20 °C, in other words they exhibited similar pattern. Moreover, as shown from Figure 55 increasing the MD portions beyond 15%, The correlation between the increase in heating temperature and the reduction in compressive strength was more pronounced.

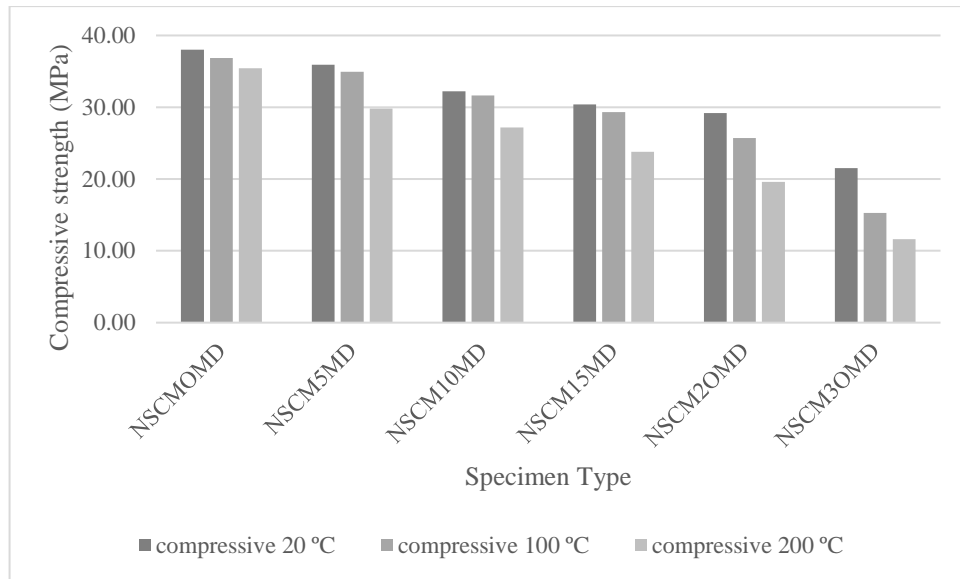


Figure 55: Effects of MD on compressive strength of NSCM after heating

Table 16: Compressive strength results of NSCM after heating

Mix No	Compressive strength at 20°C (MPa)	Strength Loss (%)	Compressive strength at 100°C (MPa)	Strength Loss (%)	Compressive strength at 200°C (MPa)	Strength Loss (%)
NSCM0MD	38	0	36.86	-3	35.43	-6.76
NSCM5MD	35.9	-5.53	34.93	-8.08	29.83	-21.49
NSCM10MD	32.2	-15.26	31.66	-16.69	27.17	-28.51
NSCM15MD	30.4	-20	29.34	-22.79	23.78	-37.43
NSCM20MD	29.2	-23.16	25.7	-32.38	19.59	-48.44
NSCM30MD	21.5	-43.42	15.27	-59.83	11.63	-69.39

Similarly, HSCM series from Figure 56 and Table 17, reference mix exhibited the lowest reduction, the reductions were 1.50% and 4.20% when subjected to temperatures of 100°C and 200°C, respectively. In the presence of MD, Specifically, the HSCM5MD mixture exhibited the lowest reduction in compressive strength at both 100 and 200 °C, with reductions of approximately 6.2% and 17.9%, respectively. The reduction values in percentage in HSCM seem to be lower than the NSCM series, this can be attributed to a lower w/c ratio, which results in higher strengthen cementing

gel. Furthermore, increasing the replacement portion to 10% also slight reduction compared with 5% MD, the reduction values were approximately 12.8% and 24.3% at 100 and 200 °C. Up to 10% MD at 100 °C the reduction values were showing almost similar reduction trend as at 20 °C, while beyond 10% MD, the reduction is significant. For instance, comparing 10 and 15% MD mixes, HSCM10MD exhibited a reduction of almost 8.8 and 12.8 % at 20 and 100 °C, the percentage of the reduction slightly increased, while HSCM15MD mixture showed a reduction percentage of 17.4 and 30.4% at 20 and 100 °C. The decrease in strength was more sounded in the presence of MD, this can be attributed to lower CSH gel produced. In fact, the presence of MD which mainly component of calcite in the SCM mixture did not show any pozzolanic reaction. Moreover, it can be connected to the thermal expansion of the SCM specimens, which causes internal stresses and dimensional change of the SCM cubes. Furthermore, the highest reduction in compressive strength were found at 200 °C, for instance, NSCM3OMD and HSCM3OMD compressive strengths were lowered by almost 69.4 and 63 % compared to control mix at 20 °C. This can be explained by burning of CSH gel as mentioned in (Aydin 2018).

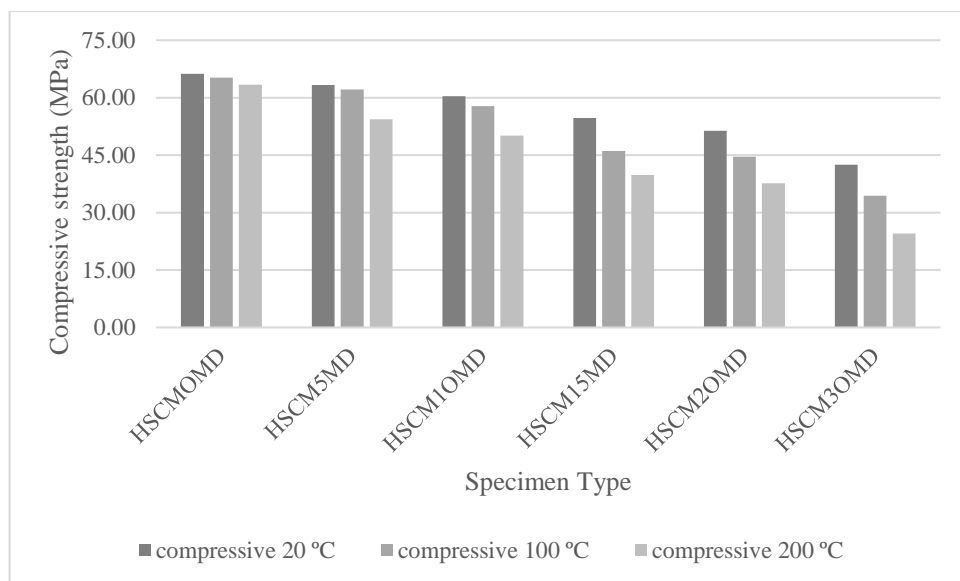


Figure 56: Effects of MD on compressive strength of HSCM after heating

Table 17: Compressive strength results of HSCM after heating

Mix No	Compressive strength at 20°C (MPa)	Strength Loss (%)	Compressive strength at 100°C (MPa)	Strength Loss (%)	Compressive strength at 200°C (MPa)	Strength Loss (%)
HSCM0MD	66.20	0.00	65.21	-1.50	63.42	-4.20
HSCM5MD	63.30	-4.38	62.10	-6.19	54.37	-17.86
HSCM10MD	60.40	-8.76	57.76	-12.75	50.13	-24.27
HSCM15MD	54.70	-17.37	46.11	-30.35	39.79	-39.89
HSCM20MD	51.40	-22.36	44.60	-32.63	37.65	-43.13
HSCM30MD	42.50	-35.80	34.42	-48.01	24.51	-62.98

The results found is similar to study done by (Bayraktar et al., 2019) on cement mortar, MD was substituted for cement in proportions of 5, 10, 15, and 20%, and mortars were heated to increased temperatures for two hours. Compressive strength data showed a decrease with MD addition. Microstructure analysis showed that fracture formation was undetectable up to 300 °C.

#### 4.11.2 Impact of MD on SCM's on Schmidt Hummer After Heating

The arbitrary Schmidt hammer scale has a range of 10-100. Multiple surface hits were made, and the average was computed, to ensure the accuracy of our test results and to eliminate inaccuracies. Figures 57 and 58 display the rebound number values for NSCM and HSCM before and after heating to 100 and 200 °C.

As can be observed that from Figure 57 the rebound number was ranging from 23.43 to 17.80 with increasing MD portions at 20 °C, increasing the temperature to 100 °C reduced the range to (21.70 - 15.80). Furthermore, at 200 °C there was significant reduction, the range of rebound number was (18.97 - 14.11). Likewise, from Figure 58

higher surface hardness was noticed in HSCM series, the rang of rebound number was (38.45 - 31.54) at 20 °C. Further increase in temperature and MD has significant reduction on the rebound number of HSCM. for instance, HSCM30MD at 200 °C reduced the rebound number to 21.52.

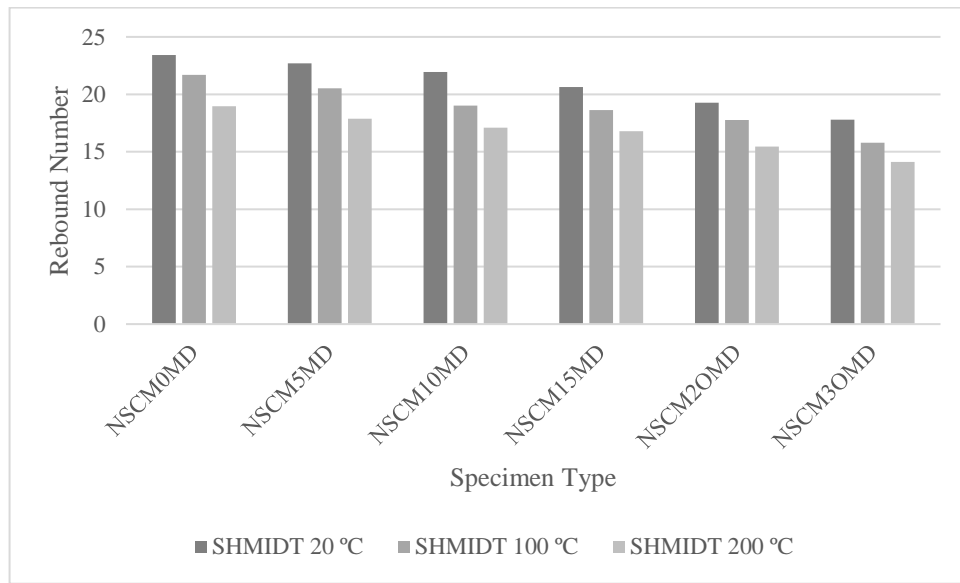


Figure 57: Effects of MD on rebound number of NSCM after heating

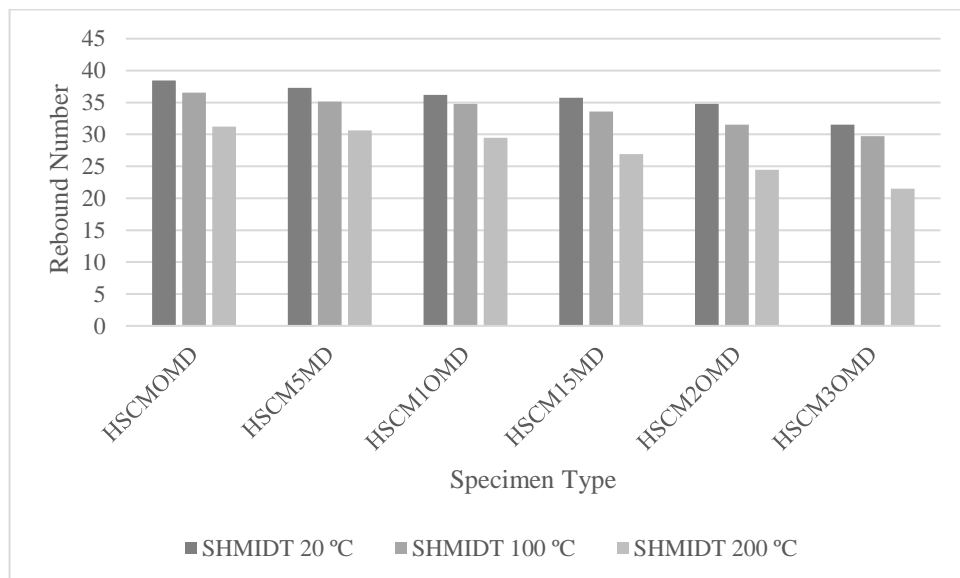


Figure 58: Effects of MD on rebound number of HSCM after heating

#### 4.11.2.1 Compressive Strength and Schmidt Hammer Before and After Heating Correlation

Table 18 demonstrates correlations between rebound number and compressive strength for both series of SCM data before and after heating. Compressive strength by the compression machine and surface hardness by Schmidt Hammer were found to have a strong correlation. The regression coefficient results for both NSCM and HSCM ranged from 0.91 to 0.96, concluding that increasing the compressive strength led to better surface hardness, thus higher rebound number.

Table 18: Compressive Strength and Schmidt hammer before and after heating relationship

Mix Series.	Regression Type	at 20 °C Equation	R <sup>2</sup>	Equation When 100 °C Heating	R <sup>2</sup>	Equation When 200 °C Heating	R <sup>2</sup>
NSCM	Linear	Y = 2.6158x - 23.641	0.9375	Y = 4.5499x - 100.92	0.9378	Y = 4.7799x - 55.333	0.9132
HSCM		Y = 3.585x - 71.498	0.9633	Y = 4.5571x - 101.17	0.9299	Y = 3.5189x - 51.321	0.9441

#### 4.11.3 Effects of MD on UPV of SCM After Heating

The UPV method involves sending a sound wave through a specimen, such as mortar, to identify and categorize cracks. Figure 59 and Table 19 present the duration, measured in microseconds, of the propagation of sonic waves through the specimens subjected to NSCM, both prior to and subsequent to heating. The outcomes pertaining to HSCM are presented in Table 20 and Figure 60.

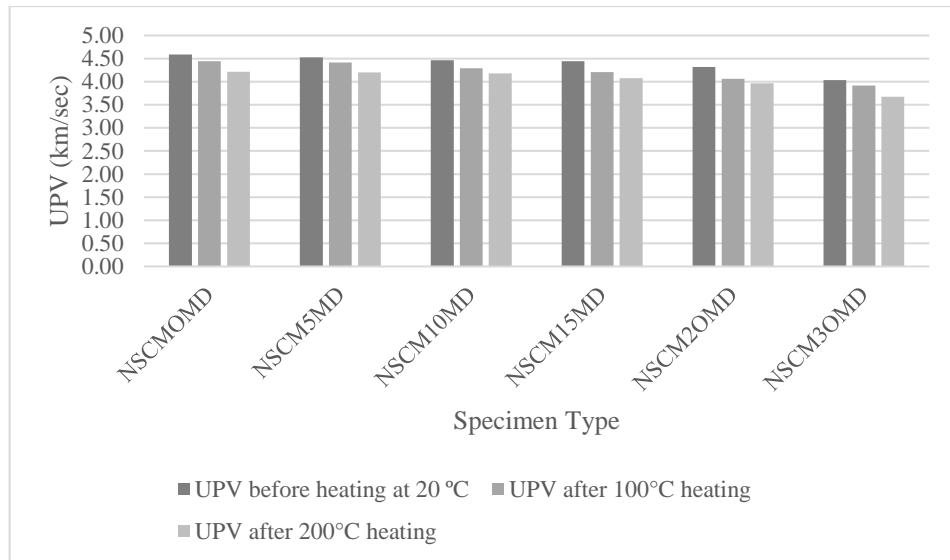


Figure 59: Results from the UPV described for the NSCM before and after heating at 20, 100, and 200 °C

Table 19: UPV results before and after heating at 20, 100, and 200 °C for NSCM

Mix No	UPV at 20 °C (μs)	km/ sec	UPV at 100°C (μs)	km/ sec	UPV at 200°C (μs)	km/ sec
NSCM0MD	21.80	4.59	22.50	4.44	23.73	4.21
NSCM5MD	22.11	4.52	22.65	4.42	23.80	4.20
NSCM10MD	22.40	4.46	23.32	4.29	23.91	4.18
NSCM15MD	22.51	4.44	23.78	4.21	24.55	4.07
NSCM20MD	23.15	4.32	24.61	4.06	25.21	3.97
NSCM30MD	24.81	4.03	25.53	3.92	27.23	3.67

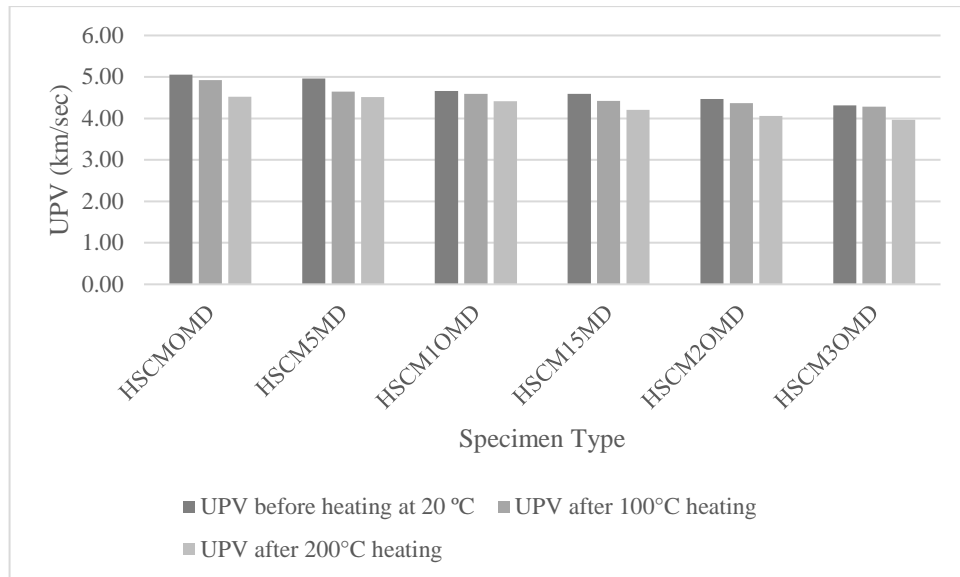


Figure 60: Results from the UPV described for the HSCM before and after heating at 20, 100, and 200 °C

Table 20: UPV results before and after heating at 20, 100, and 200 °C for HSCM

Mix No	UPV at 20 °C (μs)	km/ sec	UPV at 100°C (μs)	km/ sec	UPV at 200°C (μs)	km/ sec
HSCM0MD	19.78	5.06	20.31	4.92	22.11	4.52
HSCM5MD	20.15	4.96	21.53	4.64	22.14	4.52
HSCM10MD	21.45	4.66	21.78	4.59	22.64	4.42
HSCM15MD	21.78	4.59	22.63	4.42	23.78	4.21
HSCM20MD	22.39	4.47	22.91	4.36	24.63	4.06
HSCM30MD	23.17	4.32	23.34	4.28	25.23	3.96

The data shown in Tables 19 and 20 for NSCM and HSCM demonstrate that as the amount of heat exposure rises, it takes longer for the sound to travel through the mortar. Consequently, due to the alteration in volume of the specimen in which microscopic fractures have formed, as well as the moisture escaped as a consequence of the small fractures that remained, are both caused by heat exposure and have an influence on the quality of the mortar. The velocity drop can be connected to the decline in SCM's compressive strength specimens. These results are similar to the study (Uysal., 2012) on the SCC, where increasing the MD portions from 10 to 30 % at both 20 and 200 °C

decrease the pulse velocity values, whereas 10% MD showed a slight reduction in velocity before heating, and reduced almost 27% at 200 °C, likewise, further increase in heating temperature to 800 °C reduced the velocity significantly to almost 80%.

#### 4.11.3.1 Correlations for UPV and Compressive Strength at Different Heating Levels

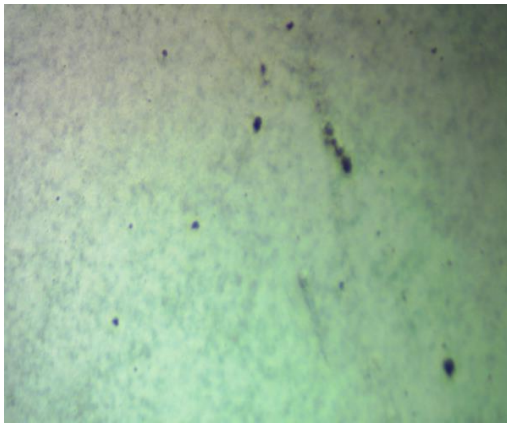
Tables 21 demonstrate correlations between UPV and compressive strength for both series of SCM data before and after heating. compressive strength by the compression machine and UPV by pundit were found to have a strong correlation. The regression coefficient for both NSCM and HSCM before and after heating results were in range of (0.85-0.95).

Table 21: UPV and Compressive strength at different heating levels relationship

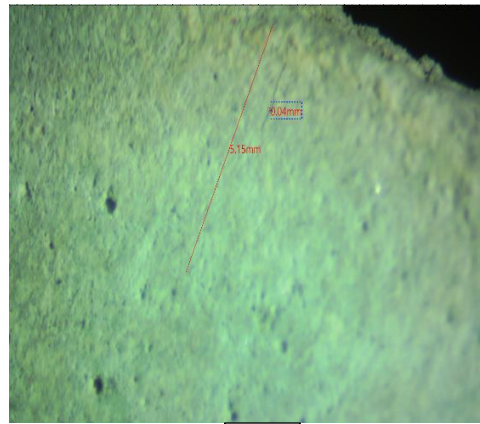
Mix No	Regression Type	Equation at 20 °C	R <sup>2</sup>	Equation at 100°C	R <sup>2</sup>	Equation at 200 °C	R <sup>2</sup>
NSCM	Linear	Y = 0.0335x + 3.3476	0.95	Y = 0.0167x + 3.3574	0.9501	Y = 0.0236x + 3.4689	0.8931
HSCM		Y = 0.0309x + 2.9307	0.9006	Y = 0.0183x + 3.5912	0.8697	Y = 0.0139x + 3.4237	0.8559

#### 4.11.4 Cracks Detection After Heating

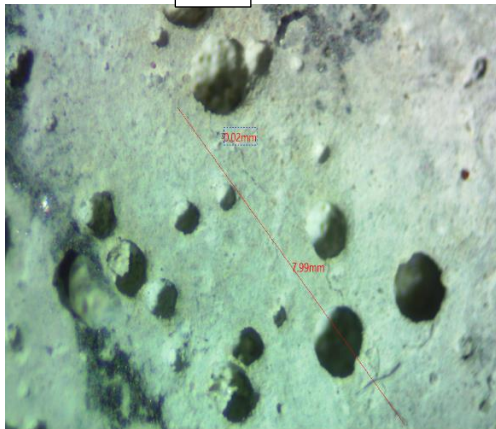
The cracks in the cubes were detected by using a stereo microscope after SCM specimens were permitted to reach the surrounding temperature. Prior to fracture detection and measurement, the microscope lenses were calibrated using a specific calibration ruler at various levels.



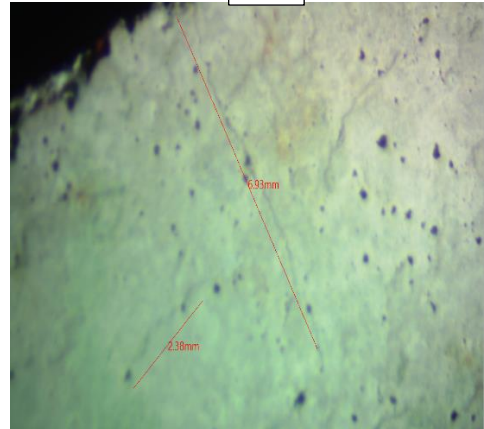
(a)



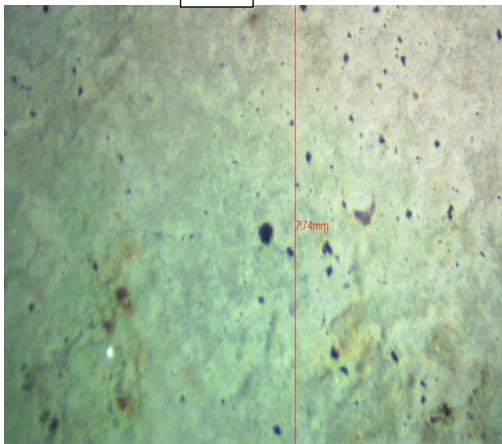
(b)



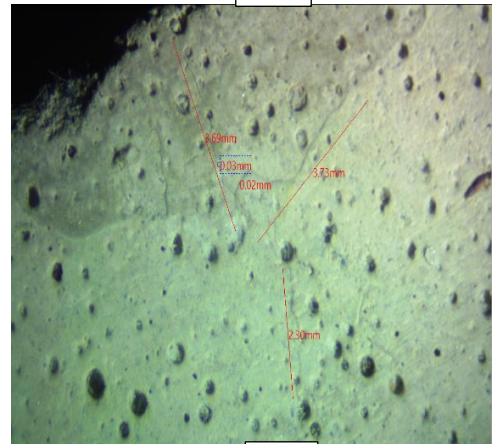
(c)



(d)



(e)



(f)

Figure 61: Stereo microscope image after heating to 200 °C: (a) HSCM20MD, (b) HSCM30MD, (c)HSCM30MD, (d)NSCM20MD, (e)NSCM30MD, (f) NSCM30MD

As can be observed from Figure 61 cracks were detected only after heating the specimens to 200 °C, where Figure 61 (a), (b), (c) refers to HSCM series with replacement portion of 20, and 30% MD. Moreover, Figure 61 (d), (e), (f) refers to NSCM series with replacement portion of 20, and 30% MD. From Figure 61 (a) there were no detected cracks for HSCM20MD, however, increasing the MD portion to 30% in Figure 61(b), and (c) showed a linear crack at the side of the cube near to the surface, the cracks lengths were 5.15 mm and 7.99 mm, while they had approximate width of 0.04 and 0.02 mm. Furthermore, starting from 20% MD in NSCM cracks were detected in Figure 61 (d), (e), (f), higher linear cracks lengths were detected in NSCM series than the high strength. This can be explained by lower w/c ratio for HSCM series. From Figure 61 (d) NSCM20MD two vertical and horizontal cracks were detected with lengths of 6.93 and 2.83 mm. In addition, in Figure 61 (e) showed higher crack length for NSCM30MD specimens of 7.74 mm, Figure 61 (f) also showed multi-dimensional cracks were detected in NSCM30MD. Concluding that increasing the cement replacement by MD portion has reduction effect the strength of both SCM series at both before and after heating, furthermore, strength reduction was more sounded when increasing heating temperature to 200 °C due to the occurrence of thermal cracks.

#### **4.12 Impact of MD on SCM's Drying Shrinkage**

The drying shrinkage test for both NSCM and HSCM series were applied according to ASTM 596-18. Furthermore, an average of 4 readings were taken for each mix. where the readings were taken at 4, 8, 14,21,28, 35, and 56 days for each beam.

The results of both NSCM and HSCM series are displayed in Figures 62 and 63, as can be observed that with increasing time periods, all SCM drying shrinkage were

increased. This is induced by cement hydration, as shrinkage is a function of cement hydration. However, compared to a control NSCM and HSCM, in the presence of MD Shrinkage values decreased significantly. Increasing the MD replacement level showed higher reduction in drying shrinkage of SCM. Marble powder is considered an inert substance, and the value of shrinkage depends on the hydration rate of the cement. In cases where shrinkage is restricted, internal tensile stress in the internal SCM matrix will occur, which results in fractures (Yamanel et al., 2019).

The drying shrinkage results for both NSCM and HSCM in Figures 62 and 63 shows that HSCM series with lower water content showed higher shrinkage values than the NSCM, reduced porosity in mortar is achieved by lowering the water content in the HSCM mix; as a result, cured mortar will have reduced shrinkage due to evaporation. Conversely, the increased density of the mortar hindered its ability to absorb additional water during the evaporation process, thereby affecting the degree of shrinkage. This maybe the case took place within the HSCM series.

(Li et al, 2018) studies the effects of MD as a CRM. The study was done on various w/c ratio on the ultimate drying shrinkage of mortar were evaluated. The findings confirm that lowering w/c with various MD replacement fractions exhibited lower ultimate shrinkage strain. However, counter to this study results, the decrease in ultimate shrinkage was more noticeable in lower w/c ratios, A reduction in the ultimate shrinkage strain was observed when the w/c was lowered by 0.15, resulting in a 40.0% and 50% decrease, respectively, after 180 days with a 20% increase in MD.

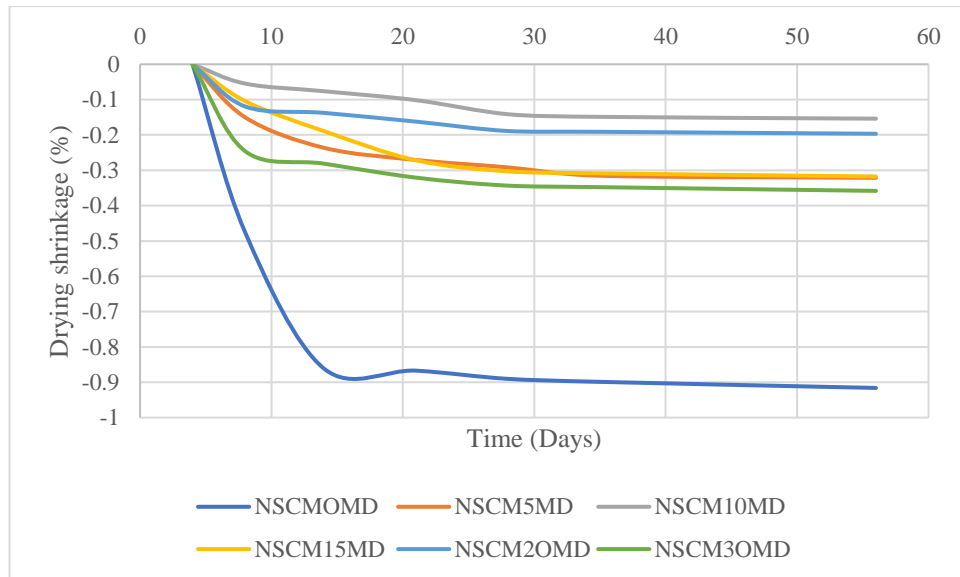


Figure 62: NSCM's drying shrinkage

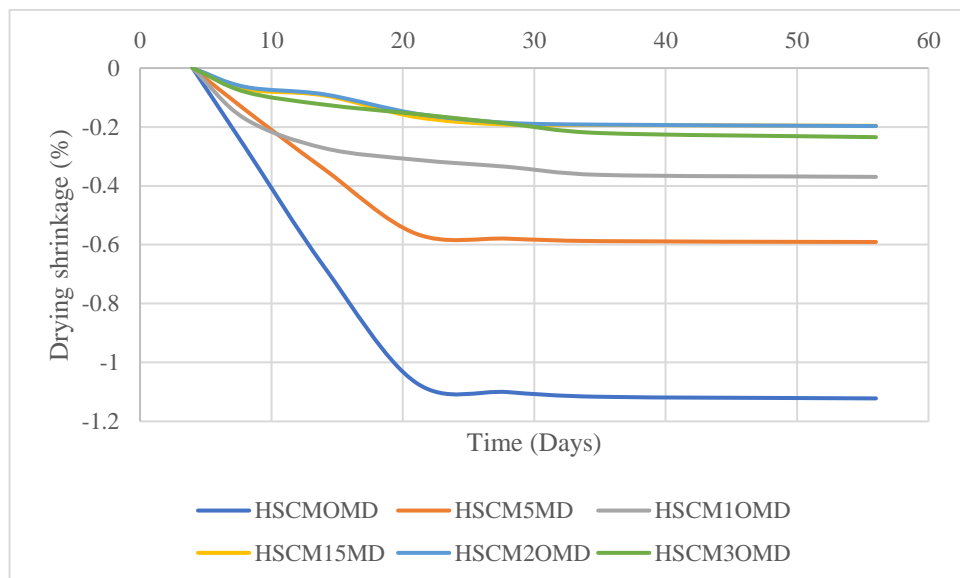


Figure 63: HSCM's drying shrinkage

### 4.13 Economical Analysis for Using MD in Production of SCM

In addition to the smaller size of MD particles, it is a non-pozzolan material. According to the experiment results, the SCM is inversely affected by the increase in CRM level. Economic analysis is done in order to support the harmful impact of marble dust as a CRM. As mentioned in the literature, according to the Cyprus Turkish Chamber of Industry, North Cyprus has almost 39 marble factories, noting that the marble dust

production depends on market demand and the production capacity of each factory. The MD in this study was gathered from Oyo Granit Mermer. In the period of three weeks, the collected dust was almost 53 kg (dry), for an average of 920 kg per year. In North Cyprus, there are 39 marble factories. So, an average of 35 to 40 tons are wasted every year.

As noticed from the results, the optimum replacement levels for both NSCM and HSCM were at 15% and 10% replacement levels, respectively. Where these mixtures were within the range limit of ensuring the self-compactibility of mortars and the other inverse effects weren't severe, as well as the designed compressive strengths almost or were achieved for both series at the given replacement on 56 days. In order to evaluate the benefits of using the MD as a CRM in production of SCMs, the materials prices and currency exchange rate were taken according to the Famagusta, North Cyprus market in July 2023.

Table 22: Material unit price

Material	Unit Price	Exchange Rate	Equivalent to TL
Cement	168 TL/ 50kg	1 TL	168 TL/ 50kg
MD	0 TL	1 TL	0 TL
Fine Aggregate	19.24 £/ 1000kg	34.64 TL	667 TL/ 1000kg
Water	15 TL/ 1000 kg	1 TL	168 TL/ 50kg
Glenium 27	700 \$/ 1000kg	26.87 TL	18,810 TL/ 1000kg

Table 23: NSCM cost analysis

Material	NSCM0MD		NSCM5MD		NSCM10MD		NSCM15MD	
	Quantity (Kg)	Price	Quantity (Kg)	Price	Quantity (Kg)	Price	Quantity (Kg)	Price
Cement	500	1,680 TL	475	1,596 TL	450	1,512 TL	425	1,428 TL
MD	0	0 TL	25	0 TL	50	0 TL	75	0 TL
Fine Aggregate	1670	1,114 TL	1670	1,114 TL	1670	1,114 TL	1670	1,114 TL
Water	250	3.75 TL	250	3.75 TL	250	3.75 TL	250	3.75 TL
Glinuim 27	10	188.1 TL	10	188.1 TL	10	188.1 TL	10	188.1 TL
Total	2,985.85 TL		2,901.85 TL		2,817.85 TL		2,733.85 TL	

Table 24: HSCM cost analysis

Material	HSCM0MD		HSCM5MD		HSCM10MD	
	Quantity (Kg)	Price	Quantity (Kg)	Price	Quantity (Kg)	Price
Cement	658	2,211 TL	625.1	2,100 TL	592.2	1,990 TL
MD	0	0 TL	32.9	0 TL	65.8	0 TL
Fine Aggregate	1492	995 TL	1492	995 TL	1492	995 TL
Water	250	3.75 TL	250	3.75 TL	250	3.75 TL
Glinuim 27	7.238	136 TL	7.238	136 TL	7.238	136 TL
Total	3,345.75 TL		3,234.75 TL		3,124.75 TL	

According to the cost analysis for both SCM series as shown in Tables 23 and 24, replacing the cement with MD reduced the cost of SCM production, almost 9% of the total cost was reduced when using 15% MD in the production of NSCM, while the reduction was 7% for HSCM at 10% MD replacement level. Concluding that using MD as CRM aids in production of economical SCM

## Chapter 5

### CONCLUSIONS AND GUIDANCE

#### 5.1 Conclusion

The primary research goal is to generate a SCM that is environmentally sustainable. To achieve this, cement was substituted with varying proportions of MD, specifically 0%, 5%, 10%, 15%, 20%, and 30%. The designed compressive strength for NSCM and HSCM was 37 and 67Mpa, respectively, at the 28 days. Fresh SCMs were evaluated by workability test, flow rate and consistency retention, air content, and setting time. While the hardened properties were evaluated by unit weight, (compressive, splitting tensile, and flexural strengths), water absorption, drying shrinkage, and heat degradation at (100 and 200 °C) which evaluated by cracks detection, compressive strength, in addition to, two non-destructive tests which are Schmidt hammer, and UPV test and following conclusion have been drawn:

1. The workability of both NSCM and HSCM was assessed according to EFNARC by using mini slump flow. Increasing the cement replacement portions from 0 to 30% by MD has an adverse impact on the flow of both SCM series, for instance, the slump flow was dropped from 250 and 255mm to 247 and 250mm when cement was replaced by 10% of MD for both NSCM and HSCM. Similarly, the findings of this investigation were consistent with prior research.
2. Because of the unavailability of a mini v-funnel, the flow rate of SCM was evaluated by the ( $T_{20}$ ) similar to previous studies. Similarly, both NSCM and

HSCM were adversely impacted by increasing the MD portions. Moreover, the time ( $T_{20}$ ) was also measured after 60 minutes to assess the flow consistency retention, the results showed that almost similar flow time was measured, and no visual bleeding was observed for all mixes.

3. A noteworthy decrease was observed in the air content of both NSCM and HSCM series. The air content (%) values for NSCM ranges from 3.90 to 1.65%, while HSCM ranges from 3.50 to 1.55% when increasing the MD portions from 0 to 30%. Almost similar air content loss was noticed for both NSCM and HSCM series.
4. Using regression coefficient  $R^2$  between air content of both NSCM and HSCM series, slump flow, and flow rate. Air content of SCM found to have a strong correlation with slump flow where the regression coefficient  $R^2$  values were 0.80 and 0.88 for NSCM and HSCM. Similarly, strong correlation found between Air content and flow rate of both NSCM and HSCM with regression coefficient of 0.90 and 0.80.
5. Prolonging in both initial and final setting time for both SCM series was found with the presence of MD. HSCM with lower w/c ratio, and lower SP dosage found to have shorter settings than the NSCM series. Moreover, replacing the cement with 5% of MD has a slight prolong effect on both NSCM and HSCM mixes, the prolonging percentage for the initial setting was 3 and 0.25%, while the final setting was prolonged by 2 and 2.6% for both NSCM and HSCM series. Up to 15% MD the prolonging time doesn't exceed a 15% increment for both series. However, beyond 15% MD, both setting times were significantly affected.

6. Replacement of cement by lower specific gravity MD particles has slightly reduced the unit weight at 7 and 28 days of both NSCM and HSCM series, and the highest reduction in unit weight of SCM was noticed at 30% replacement level for both series.
7. After several trials, the designed compressive strength was achieved successfully. However, In the presence of the MD, the compressive strength experiences a notable reduction as the replacement level increases. Due replacing the cement with non-pozzolanic material, the lowest reduction in compressive strength was noticed at 5% replacement level for both series at all testing periods. It can be concluded that an optimum replacement at 28 days is 5%. On the other hand, at lateral ages 56 days, mixture NSCM15MD attained intended compressive strength. While for HSCM series the only mixture achieved intended compressive strength is HSCM5MD. This is due to balancing the strength loss caused by the filler effect of MD particles.
8. Analogous to the compressive strength, the minimum reduction in the splitting tensile strength was observed in 5% MD for both series. Likewise, at 10% the loss is almost convergent for both NSCM and HSCM series. The splitting tensile strength exhibits a deliberate decrease upon increasing the MD portions beyond 10%. Additionally, it was observed that the splitting tensile strength exhibited a substantial correlation with the compressive strength. The NSCM and HSCM series displayed regression coefficients of 0.86 and 0.96, respectively.
9. Comparable to the compressive strength, the flexural strength exhibited the minimum reduction in strength at 5% MD for both series. The study reveals that the flexural strength losses exhibit a range of 0 to 14.29% and 18.78% for

NSCM and HSCM series, respectively, upon elevating the MD portion from 0 to 30%. Similarly, it was observed that the flexural strength exhibited a robust relationship with the compressive strength, with a regression coefficient of 0.95 and 0.98 for the NSCM and HSCM series, respectively.

10. The NSCM series demonstrated elevated water absorption in comparison to the HSCM series, due to higher water content. This resulted in a decrease in the gel-to-space ratio, raise porosity, and a reduction in the strength of the mortar. Moreover, MD replacement increases SCM series water absorption. The increase varies from 5.44 and 4.66% to 7.04 and 5.89 for both NSCM and HSCM series. Likewise, the absorption after boiling and volume of permeable voids were higher when the MD portion was raised. Additionally, in NSCM and HSCM series, high regression coefficient  $R^2$  with compressive strength of 0.96 and 0.91 was observed.

11. The effects of heat exposure on both NSCM and HSCM series were evaluated on 100mm cubes for compressive strength, Schmidt hammer, UPV, and cracks detections by using stereo microscope. Finalizing the conclusion of findings before and after subjecting the specimens to heat in the following points:

A. Compressive strength significantly decreased when the MD level and heating temperature increased. According to NSCM analysis at 100 °C, the control mixture exhibited a modest decline, but increasing the heating temperature to 200 °C decreased strength by 6.8%. The lowest decline was noticed at a 5% replacement level. Moreover, the loss was doubled at 100 °C and the decrease was enhanced by 28.5% at 200 °C when the MD portion was raised to 10%. beyond 10% compressive

strength was significantly affected by increasing the heating temperature.

- B. Similar to compressive strength, the rebound number reduced with increasing both MD and heating temperature, At the 5% MD replacement level for both series, the average rebound number was almost essentially identical to the control mix. As replacement level increases, both NSCM and HSCM mixes rebound somewhat less. Likewise, when increasing the temperature from 20 °C to 200 °C higher reduction in rebound number was noticed, the reduction was more sounded while increasing the replacement level. As expected, strong regression coefficients were found at 0.91 and 0.94.
- C. According to UPV data, both NSCM and HSCM suffered following heating. However, in NSCM and HSCM, the UPV remained above 3.67 km/s and 3.96 km/s, respectively, indicating that the good mortar quality is still retained even after heating. Additionally, at all heating levels, UPV and compressive strength results were highly correlated.
- D. Minor cracks could be only detected after 200 °C heating exposure for both NSCM and HSCM. Besides, the cracks were detected only at the side close to the surface of the specimen for NSCM at replacement levels of 20 and 30%, while the cracks were detected just in HSCM series at a replacement level of 30%.

12. The drying shrinkage of both NSCM and HSCM series were affected with increasing the replacement level, higher drying shrinkage was noticed for HSCM control mix than the NSCM with higher w/c ratio, however, the reduction in drying shrinkage the was higher for NSCM when increasing the

MD level to 30% the reduction was 0.89 and 0.56% compared to both NSCM and HSCM control mixes.

13. Utilizing MD in the production of SCM reduces industrial waste materials and their impact on the environment. Economical and eco-friendly SCM was successfully produced by using the MD as CRM, where the cost of production for the NSCM and HSCM series was reduced by almost 9% and 7%, respectively.

## **5.2 Guidance**

It is suggested that future study concentrate on:

- Compare the rheological tests suggested by EFNARC for SCC on SCM.
- To observe the effects of MD on the hardened properties, long-term mechanical tests on SCM beyond 56 days should be made.
- Investigate the heat exposure for both flexural and splitting tensile strength of SCM.
- Investigate the durability properties of MD as cement replacement on SCM
- Study the effects of MD as filler material on characteristics of SCM. So that there will be no replacing of cementing material with non-pozzolanic material.
- study the effects of MD blended with SF as CRM on SCM, due to high pozzolanic activity of SF which will improve the setting and the mechanical properties.

## REFERENCES

- Alyamaç, K. E., & Ince, R. (2009). A preliminary concrete mix design for SCC with marble powders. *Construction and building Materials*, 23(3), 1201-1210.
- Alyousef, R., Benjeddou, O., Soussi, C., Khadimallah, M. A., & Mustafa Mohamed, A. (2019). Effects of incorporation of marble powder obtained by recycling waste sludge and limestone powder on rheology, compressive strength, and durability of self-compacting concrete. *Advances in Materials Science and Engineering*, 1–15.
- Aydin, E. (2019). Effects of elevated temperature for the marble cement paste products for better sustainable construction. *Politeknik Dergisi*, 22(2), 259-267.
- Bayraktar, O. Y., Saglam-Citoglu, G., Belgin, C. M., & Cetin, M. (2019). Investigation of the mechanical properties of marble dust and silica fume substituted portland cement samples under high temperature effect. *Fresenius Environmental Bulletin*, 28(5), 3865-3875.
- Belaidi, A. S. E., Azzouz, L., Kadri, E., & Kenai, S. (2012). Effect of natural pozzolana and marble powder on the properties of self-compacting concrete. *Construction and Building Materials*, 31, 251–257.
- Benabed, B., Kadri, E.-H., Azzouz, L., & Kenai, S. (2012). Properties of self-compacting mortar made with various types of sand. *Cement and Concrete Composites*, 34(10), 1167–1173.

- Benli, A. (2019). Mechanical and durability properties of self-compacting mortars containing binary and ternary mixes of fly ash and silica fume. *Structural Concrete*, 20(3), 1096–1108.
- Boucherit, D., Debiebt, F., Kenai, S., Khalfaoui, M. A., & Chellali, S. (2020). Experimental Study on Marble and Brick Powders as Partial Replacement of Cement in Self-compacting Mortar. *Current Materials Science: Formerly: Recent Patents on Materials Science*, 13(1), 45-57.
- Boukhelkhal, A., Azzouz, L., Belaïdi, A. S. E., & Benabed, B. (2016). Effects of marble powder as a partial replacement of cement on some engineering properties of self-compacting concrete. *Journal of adhesion science and Technology*, 30(22), 2405-2419.
- Boukhelkhal, A., Azzouz, L., Belaïdi, A. S., & Benabed, B. (2016). Effects of marble powder as a partial replacement of cement on some engineering properties of self-compacting concrete. *Journal of Adhesion Science and Technology*, 30(22), 2405–2419.
- Boukhelkhal, A., Azzouz, L., Benchaa, B., & Belaidi, A. S. (2018). Strength and durability of low-impact environmental self-compacting concrete incorporating waste marble powder. *Journal of Building Materials and Structures*, 4(2), 31–41.
- Choudhary, R., Gupta, R., & Nagar, R. (2020). Impact on fresh, mechanical, and microstructural properties of high strength self-compacting concrete by marble

cutting slurry waste, fly ash, and silica fume. *Construction and Building Materials*, 239, 117888.

Choudhary, R., Gupta, R., Alomayri, T., Jain, A., & Nagar, R. (2021). Permeation, corrosion, and drying shrinkage assessment of self-compacting high strength concrete comprising waste marble slurry and fly ash, with silica fume. *Structures*, 33, 971–985.

Christianto, H. A. (2004). Effect of chemical and mineral admixtures on the fresh properties of self-compacting mortars (Master's thesis, Middle East Technical University).

Chu, H., Shi, W., Wang, Q., Gao, L., & Wang, D. (2022). Feasibility of manufacturing self-compacting mortar with high elastic modulus by  $Al_2O_3$  micro powder: A preliminary study. *Construction and Building Materials*, 340, 127736.

Craeye, B., De Schutter, G., Vuye, C., & Gerardy, I. (2015). Cement-waste interactions: Hardening self-compacting mortar exposed to gamma radiation. *Progress in Nuclear Energy*, 83, 212–219.

Cyr, M., Legrand, C., & Mouret, M. (2000). Study of the shear thickening effect of superplasticizers on the rheological behaviour of cement pastes containing or not mineral additives. *Cement and Concrete Research*, 30(9), 1477–1483.

Dachowski, R., & Kostrzewa, P. (2016). The use of waste materials in the construction industry. *Procedia Engineering*, 161, 754–758.

- Demirhan, S., Turk, K., & Ulugerger, K. (2019). Fresh and hardened properties of self-consolidating Portland limestone cement mortars: Effect of high-volume limestone powder replaced by Cement. *Construction and Building Materials*, *196*, 115–125.
- Domone, P. J., & JIN, J. (1999). Properties of mortar for self-compacting concrete. In *Self-compacting concrete (Stockholm, 13-14 September 1999)* (pp. 109-120)
- Edamatsu, Y., Nishida, N., & Ouchi, M. (1999). A rational mix-design method for self-compacting concrete considering interaction between coarse aggregate and mortar particles. In *Self-compacting concrete (Stockholm, 13-14 September 1999)* (pp. 309-320).
- Eley, R. R. (2019). Applied Rheology and architectural coating performance. *Journal of Coatings Technology and Research*, *16*(2), 263–305.
- Ergün, A. (2011). Effects of the usage of diatomite and waste marble powder as partial replacement of cement on the mechanical properties of concrete. *Construction and Building Materials*, *25*(2), 806-812.
- Felekoğlu, B., Tosun, K., Baradan, B., Altun, A., & Uyulgan, B. (2006). The effect of fly ash and limestone fillers on the viscosity and compressive strength of self-compacting repair mortars. *Cement and Concrete Research*, *36*(9), 1719–1726.
- Gesoğlu, M., Güneyisi, E., Kocabağ, M. E., Bayram, V., & Mermerdaş, K. (2012). Fresh and hardened characteristics of self-compacting concretes made with

combined use of marble powder, limestone filler, and Fly Ash. *Construction and Building Materials*, 37, 160–170.

Grabiec, A., Zawal, D., & Kostrzewski, W. (2015). Effect of waste mineral additives on flow stability over time in self-compacting concrete mixes with low clinker content. *Journal of Ecological Engineering*, 16, 206–214.

Güneyisi, E., Gesoğlu, M., & Özbay, E. (2009). Effects of marble powder and slag on the properties of self-compacting mortars. *Materials and Structures*, 42(6), 813–826.

Guru, J. J., Sashidhar, C., Ramana, R. I., & Annie, P. J. (2013). Optimization of superplasticiser and viscosity modifying agent in self compacting mortar.

Horsakulthai, V. (2021). Effect of recycled concrete powder on strength, electrical resistivity, and water absorption of self-compacting mortars. *Case Studies in Construction Materials*, 15, e00725.

Journal of Research of the National Institute of Standards and Technology (NIST), “Measurement of the Rheological Properties of High-Performance Concrete”, *State of the Art Report*, Volume 104, Number 5, September– October 1999

Keleştemur, O., Arıcı, E., Yıldız, S., & Gökçer, B. (2014). Performance evaluation of cement mortars containing marble dust and glass fiber exposed to high temperature by using Taguchi method. *Construction and Building Materials*, 60, 17-24.

- Khaleel, O. R., & Abdul Razak, H. (2012). The effect of powder type on the setting time and self compactability of Mortar. *Construction and Building Materials*, 36, 20–26.
- Khed, V. C., Mohammed, B. S., & Nuruddin, M. F. (2016). Effects of nano-silica modified self-compacted, high volume fly ash mortar on slump flow and compressive strength. *Madridge Journal of Nanotechnology & Nanoscience*, 1(1), 9–12.
- Khodabakhshian, A., De Brito, J., Ghalehnovi, M., & Shamsabadi, E. A. (2018). Mechanical, environmental and economic performance of structural concrete containing silica fume and marble industry waste powder. *Construction and Building Materials*, 169, 237-251.
- King, D. (2012, August). The effect of silica fume on the properties of concrete as defined in concrete society report 74, cementitious materials. In *37th Conference on our world in concrete and structures, Singapore* (pp. 29-31).
- Kohani Khoshkbijari, R., Fard Samimi, M., Mohammadi, F., & Talebitaher, P. (2020). Effects of mica and feldspar as partial cement replacement on the rheological, mechanical and thermal durability of self-compacting mortars. *Construction and Building Materials*, 263, 120149.
- Lakreb, N., Şen, U., Beddiar, A., Zitoune, R., Nobre, C., Gomes, M. G., & Pereira, H. (2022). Properties of eco-friendly mortars produced by partial cement

replacement with waste cork particles: a feasibility study. *Biomass Conversion and Biorefinery*, 1-11.

Li, L. G., Huang, Z. H., Tan, Y. P., Kwan, A. K. H., & Liu, F. (2018). Use of marble dust as paste replacement for recycling waste and improving durability and dimensional stability of mortar. *Construction and Building Materials*, 166, 423–432.

Li, Z., Ohkubo, T., & Tanigawa, Y. (2004). Theoretical analysis of time-dependence and thixotropy of fluidity for high fluidity concrete. *Journal of Materials in Civil Engineering*, 16(3), 247–256.

Mehdipour, I., Razzaghi, M. S., Amini, K., & Shekarchi, M. (2013). Effect of mineral admixtures on fluidity and stability of self-consolidating mortar subjected to prolonged mixing time. *Construction and Building Materials*, 40, 1029–1037.

Molin Filho, R. G., Longhi, D. A., de Souza, R. C., Ferrer, M. M., Vanderlei, R. D., Paraíso, P. R., & Jorge, L. M. (2018). Self-compacting mortar with sugarcane bagasse ash: Development of a sustainable alternative for Brazilian Civil Construction. *Environment, Development and Sustainability*, 21(5), 2125–2143.

Mora-Ortiz, R. S., Del Angel-Meraz, E., Díaz, S. A., Magaña-Hernández, F., Munguía-Balvanera, E., Pantoja Castro, M. A., Alavez-Ramírez, J., & Alejandro Quiroga, L. (2021). Effect of pre-wetting recycled mortar aggregate on the mechanical properties of masonry mortar. *Materials*, 14(6), 1547.

- Nasr, D., Behforouz, B., Borujeni, P. R., Borujeni, S. A., & Zehtab, B. (2019). Effect of nano-silica on mechanical properties and durability of self-compacting mortar containing natural zeolite: Experimental investigations and Artificial Neural Network modeling. *Construction and Building Materials*, 229, 116888.
- Okamura, H., & Ouchi, M. (2003). Self-compacting concrete. *Journal of advanced concrete technology*, 1(1), 5-15.
- Okamura, H., OZAWA, K., & Ouchi, M. (1995). Self-compacting high-performance concrete. *콘크리트학회지*, 7(5), 33-41.
- Publications. EFNARC. <https://efnarc.org/publications>
- Rashwan, M. A., Al - Basiony, T. M., Mashaly, A. O., & Khalil, M. M. (2020). Behaviour of fresh and hardened concrete incorporating marble and granite sludge as cement replacement. *Journal of Building Engineering*, 32, 101697.
- Sadek, D. M., El-Attar, M. M., & Ali, H. A. (2016). Reusing of marble and granite powders in self-compacting concrete for sustainable development. *Journal of Cleaner Production*, 121, 19–32.
- Safi, B., Saidi, M., Daoui, A., Bellal, A., Mechekak, A., & Toumi, K. (2015). The use of seashells as a fine aggregate (by sand substitution) in self-compacting mortar (SCM). *Construction and Building Materials*, 78, 430–438.

- Sakalkale, A. D., Dhawale, G. D., & Kedar, R. S. (2014). Experimental study on use of waste marble dust in concrete. *Int. J. Eng. Res. Appl*, 4(10), 44-50.
- Shabbir, F., Ahmad, A., Arshid, U., Tahir, F., & Malik, A. A. (2020). Effect of Partial CRM with Marble Powder, Silica Fume and Ground Granulated Blast Furnace Slag on Concrete. *Technical Journal*, 25(03), 11-18.
- Shekarchi, M., Libre, N. A., Mehdipour, I., Sangtarashha, A., & Shafieefar, A. (2008). Shrinkage of highly flowable mortar reinforced with polypropylene fibre. *In The 3 rd International Conference–ACF/VCA* (pp. 210-216).
- Singh, M., Srivastava, A., & Bhunia, D. (2017). An investigation on effect of partial replacement of cement by waste marble slurry. *Construction and Building Materials*, 134, 471–488.
- Sri Rama Chand, M., Swamy Naga Ratna Giri, P., Rathish Kumar, P., Rajesh Kumar, G., & Raveena, C. (2016). Effect of self curing chemicals in self compacting mortars. *Construction and Building Materials*, 107, 356–364.
- Şahmaran, M., Christianto, H. A., & Yaman, İ. Ö. (2006). The effect of chemical admixtures and mineral additives on the properties of self-compacting mortars. *Cement and Concrete Composites*, 28(5), 432–440.
- Takada, K., & Walraven, J. C. (2001). Influence of mixing efficiency on the properties of flowable cement pastes. *In international symposium on self-compacting concrete* (pp. 545-554). COMS engineering corporation.

- Tattersall, G. H., & Banfill, P. F. (1983). *The rheology of fresh concrete* (No. Monograph).
- Topçu, İ. B., Bilir, T., & Uygunoğlu, T. (2009). Effect of waste marble dust content as filler on properties of self-compacting concrete. *Construction and Building Materials*, 23(5), 1947–1953.
- Türkel, S., & Altuntaş, Y. (2009). The effect of limestone powder, fly ash and silica fume on the properties of self-compacting repair mortars. *Sadhana*, 34(2), 331–343.
- Usman, M., Khan, A. Y., Farooq, S. H., Hanif, A., Tang, S., Khushnood, R. A., & Rizwan, S. A. (2018). Eco-friendly self-compacting cement pastes incorporating wood waste as cement replacement: A feasibility study. *Journal of Cleaner Production*, 190, 679–688.
- Uysal, M. (2012). Self-compacting concrete incorporating filler additives: Performance at high temperatures. *Construction and Building Materials*, 26(1), 701–706.
- Uysal, M., Yilmaz, K., & Ipek, M. (2012). The effect of mineral admixtures on mechanical properties, chloride ion permeability and impermeability of self-compacting concrete. *Construction and Building Materials*, 27(1), 263–270.
- Venkatesh, G. J., Vivek, S. S., & Dhinakaran, G. (2017). Study on compressive strength of self-compacting mortar cubes under normal & Electric Oven Curing

methods. *IOP Conference Series: Earth and Environmental Science*, 80, 012002.

Vittalaih, A., Ravinder, R., & Kumar, C. V. (2020). Study on effect of strength and durability parameters and performance of self-compacting concrete replacement with GGBS at different dosages. *E3S Web of Conferences*, 184, 01106.

Wongkeo, W., Thongsanitgarn, P., Ngamjarrojana, A., & Chaipanich, A. (2014). Compressive strength and chloride resistance of self-compacting concrete containing high level fly ash and silica fume. *Materials & Design*, 64, 261–269.

Xi, Y., Anastasiou, E., Karozou, A., & Silvestri, S. (2019). Fresh and hardened properties of cement mortars using marble sludge fines and cement sludge fines. *Construction and Building Materials*, 220, 142–148.

Yamanel, K., Durak, U., İlkentapa, S., İsa Atabey, İ., Karahan, O., & Duran Atiş, C. (2019). Influence of waste marble powder as a replacement of cement on the properties of mortar. *Revista de La Construcción*, 18(2), 290–300.

Zhang, S. P., & Zong, L. (2014). Evaluation of relationship between water absorption and durability of concrete materials. *Advances in Materials Science and Engineering*, 2014.

## **APPENDIX**

Table I: NSCM mix design

Table 1. Concrete Mix Design Form (BRE method)

Job title: NSCM

stage	item	Reference or calculation	Values
1	1.1	Characteristic strength	Specified { .....37.....N/mm <sup>2</sup> at.....28.....days Proportion defective .....10.....%
	1.2	Standard deviation	Fig. 3 .....8..... N/mm <sup>2</sup> or no data ..... N/mm <sup>2</sup>
	1.3	Margin	C1 (k=.....) .....1.28 x 8 = .....10.24.....N/mm <sup>2</sup>
	1.4	Target mean strength	Specified .....//..... N/mm <sup>2</sup>
	1.5	Cement strength class	C2 .....37..... + .....10.3..... = .....47.3..... N/mm <sup>2</sup>
	1.6	Aggregate type: coarse	Specified 42.5/ <del>50</del>
	1.6	Aggregate type: fine	Crushed/ <del>Crushed</del>
	1.7	Free-water/cement ratio	Table 2, Fig. 4 .....0.52.....
1.8	Max. Free water/cement ratio	Specified .....//..... } Use the lower value ...0.52.....	
2	2.1	Slump or VeBe time	Specified Slump ...60-180.....mm or VeBe time.....//.....s
	2.2	Max. Aggregate size	Specified .....//.....mm
	2.3	Free-water content	Table 3 .....250.....kg/m <sup>3</sup>
3	3.1	Cement content	C3 .....250..... / .....0.52..... = .....480.80..... kg/m <sup>3</sup>
	3.2	Maximum Cement content	Specified .....//.....kg/m <sup>3</sup>
	3.3	Minimum Cement content	Specified .....//.....kg/m <sup>3</sup>
	3.4	Modified free-water/cement ratio	Do not use less than 3.3 or more than 3.2 .....480.80..... kg/m <sup>3</sup>
4	4.1	Relative density of aggregate (SSD)	.....2.75.....known/assumed
	4.2	Concrete density	Fig. 5 .....2400..... kg/m <sup>3</sup>
	4.3	Total aggregate content	C4 .....2400..... - .....480.80..... - .....250..... = .....1669.20kg/m <sup>3</sup>
5	5.1	Grading of fine aggregate	Percentage passing 600 micron sieve .....//.....%
	5.2	Proportion of fine aggregate	Fig. 6 .....//.....%
	5.3	Fine aggregate content	C5 .....//..... x .....//..... = .....//.....kg/m <sup>3</sup>
	5.4	Coarse aggregate content	

Quantities	Cement (kg)	water (kg or lt)	Fine aggregate (kg)	Coarse aggregate (kg)		
				10 mm	20 mm	40 mm
Per m <sup>3</sup> (to nearest 5 kg)	480.80	250	1669.20	//	//	
Per trial mix of ..... m <sup>3</sup>						

Table II: HSCM mix design

**Table 1. Concrete Mix Design Form (BRE method)**

**Job title: HSCM**

stage	item	Reference or calculation	Values
1	1.1	Characteristic strength	Specified { .....67.....N/mm <sup>2</sup> at.....28.....days Proportion defective .....10.....%
	1.2	Standard deviation	Fig. 3 .....8..... N/mm <sup>2</sup> or no data ..... N/mm <sup>2</sup>
	1.3	Margin	C1 (k=.....) .....1.28..... x .....8..... = .....10.24.....N/mm <sup>2</sup> Specified .....//..... N/mm <sup>2</sup>
	1.4	Target mean strength	C2 .....67..... + .....10.30..... = .....77.30.....N/mm <sup>2</sup>
	1.5	Cement strength class	Specified 42.5/ <del>52.5</del>
	1.6	Aggregate type: coarse	Crushed/ <del>Un-crushed</del>
		Aggregate type: fine	Crushed/ <del>Un-crushed</del>
	1.7	Free-water/cement ratio	Table 2, Fig. 4 .....0.38.....
1.8	Max. Free water/cement ratio	Specified .....//..... } Use the lower value .....0.38...	
2	2.1	Slump or VeBe time	Specified Slump .....60 - 180.....mm or VeBe time.....//.....s
	2.2	Max. Aggregate size	Specified .....//.....mm
	2.3	Free-water content	Table 3 .....250.....kg/m <sup>3</sup>
3	3.1	Cement content	C3 .....250..... / .....0.38..... = .....657.9..... kg/m <sup>3</sup>
	3.2	Maximum Cement content	Specified .....//.....kg/m <sup>3</sup>
	3.3	Minimum Cement content	Specified .....//.....kg/m <sup>3</sup> Do not use less than 3.3 or more than 3.2 .....658..... kg/m <sup>3</sup>
	3.4	Modified free-water/cement ratio	.....//.....
4	4.1	Relative density of aggregate (SSD)	.....2.75.....known/assumed
	4.2	Concrete density	Fig. 5 .....2400..... kg/m <sup>3</sup>
	4.3	Total aggregate content	C4 .....2400 - 658 - 250 = 1492 kg/m <sup>3</sup>
5	5.1	Grading of fine aggregate	Percentage passing 600 micron sieve .....//.....%
	5.2	Proportion of fine aggregate	Fig. 6 .....//.....%
	5.3	Fine aggregate content	C5 } .....//..... x .....//..... = .....//.....kg/m <sup>3</sup> .....//..... - .....//..... = .....//.....kg/m <sup>3</sup>
	5.4	Coarse aggregate content	

Quantities	Cement (kg)	water (kg or lt)	Fine aggregate (kg)	Coarse aggregate (kg)		
				10 mm	20 mm	40 mm
Per m <sup>3</sup> (to nearest 5 kg)	658	250	1492	//	//	//
Per trial mix of ..... m <sup>3</sup>						